Weierstrass Fractal Drums -I – A Glimpse of Complex Dimensions

Claire David, Michel Lapidus

Weierstrass Fractal Drums - I
–
A Glimpse of Complex Dimensions

Claire David [1] and Michel L. Lapidus [2] *

June 12, 2023

[1] Sorbonne Université
CNRS, UMR 7598, Laboratoire Jacques-Louis Lions, 4, place Jussieu 75005, Paris, France

[2] University of California, Riverside, Department of Mathematics,
Skye Hall, 900 University Ave., Riverside, CA 92521-0135, USA

Abstract

We establish *fractal tube formulae* for the sequence of prefractal graphs which converge to the Weierstrass Curve, called *Weierstrass Iterated Fractal Drums* (in short, Weierstrass IFDs), and which give, for a suitable (and geometrically meaningful) sequence of values of the parameter ϵ tending to zero, explicit expressions for the volume of the associated ϵ–neighborhoods. For this purpose, we prove new geometric properties of the Curve and of the associated function, in relation with its local Hölder and reverse Hölder continuity, with explicit estimates that had not been obtained before. We also show that the Codimension $2 - D_{\mathcal{W}}$ is the optimal Hölder exponent for the Weierstrass function $\mathcal{W}$, from which it follows that, as is well known, $\mathcal{W}$ is nowhere differentiable. Then, the formula, that yields the expression of the ϵ–neighborhood, consists of a fractal power series in ϵ, with underlying exponents the Complex Codimensions of the sequence of prefractal graphs. This enables us to obtain the associated (local and global, effective) *tube and distance fractal zeta functions*, whose poles yield the corresponding set of Complex Dimensions. We prove that the Complex Dimensions – apart from 0 and -2 – are periodically distributed along countably many vertical lines, with the same oscillatory period. By considering the lower and upper (effective) Minkowski contents of the m^{th} prefractal approximation to the Weierstrass Curve, which we prove to be strictly positive, we then show that the Weierstrass IFD is Minkowski nondegenerate, as well as not Minkowski measurable, but admits a nontrivial average Minkowski content – and that, as expected, the Minkowski dimension (or box dimension) $D_{\mathcal{W}}$ is the Complex Dimension with maximal real part, and zero imaginary part. An interesting (and likely general) new phenomenon arising in our investigation is that, for all sufficiently large positive integers m, the Complex Dimensions of the m^{th} prefractal approximation to the Weierstrass Curve are the same and coincide with the Complex Dimensions of the Weierstrass IFD.

MSC Classification: 11M41, 28A12, 28A75, 28A80.

*The research of M. L. L. was supported by the Burton Jones Endowed Chair in Pure Mathematics, as well as by grants from the U. S. National Science Foundation.

Keywords: Weierstrass Curve, prefractal approximations, best Hölder exponent, iterated fractal drum (IFD), Complex Dimensions of an IFD, box–counting (or Minkowski) dimension, fractal tube formula, effective local and global tube zeta function, effective local and global distance zeta function, (upper, lower and average) Minkowski contents, Minkowski non-measurability, Minkowski nondegeneracy, nowhere differentiability.

Contents

1 Introduction **2**

2 Geometric Framework **7**

3 Iterated Fractal Drums and Tubular Neighborhoods **35**

4 Prefractal Tube Formulas, Complex Dimensions and Average Minkowski Content **61**
4.1 Preliminaries 61
4.2 Prefractal Tube Formulas and Prefractal Effective Zeta Functions 65
4.3 Complex Dimensions 75
4.3.1 Main Results 75
4.3.2 Exceptional Cases 83
4.3.3 Possible Interpretation 85
4.3.4 Analogy with the General Theory of Complex Dimensions 87
4.4 Minkowski Dimension, Minkowski Nondegeneracy, and Average Minkowski Content . . 88
4.5 The Noninteger Case 94

5 Concluding Comments **95**

1 Introduction

Among the so-called "pathological objects" that appeared in the XIX$^{\text{th}}$ century, the Weierstrass Curve ($\mathcal{W}$-Curve) stands as one of the most fascinating and intriguing ones. At first, it was simply designed and thought of in order to be continuous everywhere, while being nowhere differentiable. Given $\lambda \in]0,1[$, and b such that $\lambda\, b > 1 + \dfrac{3\,\pi}{2}$, the associated function is defined as the sum of the uniformly convergent trigonometric series

$$x \in \mathbb{R} \mapsto \sum_{n=0}^{\infty} \lambda^n \cos\left(\pi\, b^n\, x\right) \cdot$$

The original proof, by K. Weierstrass [Wei75], in the case where b is an odd positive integer, can also be found in [Tit39] (pages 351-353). It has been completed by the one, now classical, given by G. H. Hardy [Har16], in the more general case, where b is any real number such that $\lambda\, b > 1$.

As is discussed in [Dav22], the introduction of this function challenged all the existing theories that went back to André-Marie Ampère, and has led to the emergence of many new functions possessing the same type of properties.

History then left it aside for a while, before new discovered properties brought it back once again to the forefront. It happened, in particular, that, in addition to its nowhere differentiability, the function – and the associated Curve – have self–similarity properties. After the works of A. S. Besicovitch and H. D. Ursell [BU37], Benoît Mandelbrot [Man77], [Man83], particularly highlighted the fractal

properties of the Weierstrass Curve. He also conjectured that the Hausdorff dimension of the graph is given by $D_{\mathcal{W}} = 2 + \dfrac{\ln \lambda}{\ln b} = 2 - \ln_b \dfrac{1}{\lambda}$.

Interesting discussions and results in relation to this question may be found in the book of K. Falconer [Fal86]. As for the box dimension, a first series of results have been obtained by J.-L. Kaplan, J. Mallet-Paret and J. A. Yorke [KMPY84], where the authors show that it is equal to the Lyapunov dimension of the equivalent attracting torus. Then, the problem was tackled by F. Przytycki and M. Urbański [PU89], as well as by T.-Y. Hu and K.-S. Lau [HL93].

As for the Hausdorff dimension, the first key result was obtained by F. Ledrappier [Led92], where the Curve is considered as "the repeller for some expanding self-mapping on $[0,1] \times \mathbb{R}$", in the case where b is an integer, an assumption that is of importance, in so far as a Markov partition for the mapping $x \mapsto b\,x \mod 1$ is involved. The resulting dynamics thus obeys the Markov property, a fact that has naturally led the author of [Led92] to using such notions as topological – metric entropies, explored in his earlier joint work with L. S. Young [LY85]. An interesting and useful connection was therefore established between Lyapunov exponents and dimensions, in this context. Another result was then obtained by B. Hunt [Hun98] in 1998 in the case where arbitrary phases are included in each cosinusoidal term of the summation. Later, in 2014, K. Barański, B. Bárány and J. Romanowska [BBR14] showed that, for any value of the real number b, there is a threshold value λ_b belonging to the interval $\left]\dfrac{1}{b}, 1\right[$ such that the Hausdorff dimension is equal to $D_{\mathcal{W}}$, for every b in $]\lambda_b, 1[$. The results obtained by W. Shen in [She18] went further than the main result of [BBR14] and, in fact, showed that the Hausdorff dimension of the Weierstrass Curve is equal to $D_{\mathcal{W}}$, for any (allowed) values of the parameters. Furthermore, in [Kel17], G. Keller proposed a very original and much simpler proof of the main results of [BBR14].

In [Dav18], the first author proved – in the case when $b = N_b$ is an integer, and in contrast to the then existing work – that the Minkowski dimension (or box–counting dimension) of the Weierstrass Curve could be obtained in a simple way, without requiring any theoretical background in dynamical systems theory. The proof relies on the use of prefractal approximations; that is, here, a suitable sequence of finite graphs which converges towards the Weierstrass Curve. They are obtained by means of a suitable nonlinear iterated function system (IFS) [Dav19], where, as in the case of the horseshoe attractor introduced by Stephen Smale, the nonlinear maps involved are not contractions, but possess what can be viewed as an equivalent property, since, at each step of the iterative process, they reduce the values of the two-dimensional Lebesgue measures of a given sequence of rectangles covering the Curve. As expected, the Weierstrass Curve is invariant with respect to the family of those maps, which provides us in this context with a result equivalent to the one that can be found in [BD85].

Interestingly, the intrinsic properties of the intriguing maps which constitute the nonlinear IFS can be directly linked to the computation of the box dimension of the Weierstrass Curve, and to a new proof of the nowhere differentiability of the Weierstrass function, as shown in [Dav22].

Yet, thus far, no connection has been established with the theory of Complex Dimensions. Therefore, the following questions arise naturally in this setting: Can one prove that the Minkowski (or box) dimension of the Weierstrass Curve is, also, a Complex Dimension? Can we also determine all of the (possible) Complex Dimensions of this Curve, as well as obtain an associated fractal tube formula, in the form of a fractal power series involving the underlying Complex Dimensions? (See [LRŽ17b], Problem 6.2.24, page 560.)

The foundations of the theory of **Complex Dimensions** were laid by M. L. Lapidus and his collaborators in [Lap91], [Lap92], [Lap93], [LP93], [LM95], [LvF00], [LP06], [Lap08], [LPW11], [ELMR15], [LvF06], [LRŽ17a], [LRŽ18], [Lap19], [HL21] and [Lap22], in particular. The theory provides a very

natural and intuitive way to characterize *fractal strings* or *drums*, in relation with their intrinsic vibrational properties. Geometrically, in the latter case, this means studying the oscillations of a small neighborhood of the boundary, i.e., of a tubular neighborhood, where points are located within an epsilon distance from any edge. As is explained in [Lap19], a fractal may be viewed "as a musical instrument tuned to play certain notes with frequencies (respectively, amplitudes) essentially equal to the real parts (respectively, the imaginary parts) of the underlying complex dimensions". One can also imagine a "*geometric wave* propagating through the fractal" [Lap19].

The one–dimensional theory of Complex Dimensions (i.e., that of fractal strings) was developed, in particular, in the books by the second author and M. van Frankenhuisjen [LvF00], [LvF06], where general explicit formulas and fractal tube formulas were obtained for fractal strings (see [LvF06], Chapters 5 and 8). Later, in the book [LRŽ17b] – as well as in a series of accompagnying papers, including [LRŽ17a], [LRŽ17c] and [LRŽ18] – the higher–dimensional theory of Complex Dimensions was developed by the second author, G. Radunovic and D. Žubrinić, in the general case of bounded subsets of Euclidean space $\mathbb{R}^N$ and of relative fractal drums of $\mathbb{R}^N$, with $N \geqslant 1$ being an arbitrary integer. General fractal tube formulas were also obtained in this context and applicable to a large variety of examples; see [LRŽ17b], Chapter 5, and [LRŽ18]. In short, Complex Dimensions are defined as the poles of the meromorphic continuation of suitable geometric or fractal zeta functions, associated with the fractal under study. A geometric object is then said to be *fractal* if it admits at least one *nonreal Complex Dimension*, thereby giving rise to geometric oscillations via the corresponding fractal tube formula. For example, in agreement with one's intuition, the Devil's Staircase (i.e., the graph of the Cantor–Lebesgue function) is shown to be fractal, in this sense, whereas it is not fractal according to Benoît B. Mandelbrot's definition in [Man83], because its topological and Hausdorff dimensions coincide.

Under a mild assumption, the (upper) Minkowski dimension of the geometric object under study is equal to the abscissa of convergence of the geometric, distance or tube, fractal zeta functions, and is the only Complex Dimension located on the real axis and with maximal real part, therefore giving rise, via the corresponding fractal tube formula, to geometric, spectral, or dynamical oscillations with the largest amplitudes. We note that fractal tube formulas express the volume of (small) ε-neighborhoods of the fractal as a fractal power series, with exponents the underlying Complex Codimensions.

Building on the work on multifractal zeta functions and Complex Dimensions of multifractals strings developed in [LR09], [LLVR09], [ELMR15], along with the work on Complex Dimensions and fractal tube formulas in [LvF00], [LvF06]. L. O. R. Olsen [Ols13a], [Ols13b], also obtained a suitable multifractal analog of fractal tube formulas in this context.

A clear summary of the theory of Complex Dimensions for fractal strings can be found in [Ols01], while a long survey of the theory of Complex Dimensions, both for fractal strings and in higher dimensions, is given in [Lap19].

A question which naturally arises in this context is that of differential operators on such structures. In the case of fractal strings, as an echo to noncommutative geometry, where *spectral triples* are involved, a *geometric zeta function* provides the set of complex modes, while the dimensions stand as its nonreal poles. The occurrence of the zeta function can be understood very intuitively, in so far as it simply represents the trace of the differential operator at a complex order s. Thus, the poles are nothing but the maximal orders of differentiation. Hence, dimensions.

The notion of *a fractal drum* extends that of *a fractal string* to higher–dimensional Euclidean spaces, and involves an open subset with a fractal boundary. In the Euclidean plane, this boundary is a curve. The word "drum" calls for vibrations: intuitively, one understands that they occur in a small neighborhood of the boundary, a tubular neighborhood, the Lebesgue measure of which is associated

to a *tube zeta function* which, similarly, enables one to obtain the Complex Dimensions, which stand as characteristic numbers that account for specific geometric properties of the fractal boundary, here, the underlying curve.

For the Koch Snowflake Curve, a *fractal tube formula* was obtained by M. L. Lapidus and E. P. J. Pearse in [LP06]. As was pointed out in [LRŽ17b] (see Problem 6.2.24, page 560), the case of **the Weierstrass Curve** remained a *difficult open problem*, which we propose to solve in this paper. It is directly associated to our previous work [Dav18], in so far as precise estimates are required for the elementary heights of the sequence of natural prefractal approximations tending towards the Curve. As is often the case in such a situation, we significantly improve these estimates, which also enable us to obtain the exact values of the local extrema, and to determine the optimal Hölder exponent of $\mathcal{W}$. Those extrema – which form a dense subset of the Weierstrass Curve – directly depend on the choice of an initial set of points, which happen to be here the fixed points of the nonlinear iterated function system involved in the construction of the Curve; see [Dav19] for further details. Moreover, we introduce *the concept of* ***self–shape similarity***, a more general one than the standard notion of *self-similarity*.

The first novelty of our approach is that we define the Complex Dimensions of the Weierstrass Curve as the set of the Complex Dimensions of the sequence of m^{th} prefractal graphs which converge to the Curve – *Weierstrass Iterated Fractal Drum* (in short, Weierstrass IFD), or, equivalently in our context, of the sequence of m^{th} prefractal approximations which converge to the Curve. More specifically, we show that the set of (possible) Complex Dimensions is independent of the positive integer m sufficiently large. For this IFD, our tubular neighborhoods are located on both sides of the involved prefractals, which seems natural, because vibrations may occur on either side of the underlying fractal drum. However, when it comes to computing the associated fractal tube zeta function, classical methods, as in [LP06] and [LPW11] (see also [LvF00], §10.3, and [LvF06], §12.4), cannot be directly applied, since our fractal tube formulas can only be obtained for a sequence of characteristic lengths – the *cohomology infinitesimals*. More precisely, we only dispose of discrete values (but geometrically natural) for the fractal tube formulas, instead of an explicit expression of the tube formula on an interval of the form $[0, \epsilon_0]$, where $\epsilon_0 > 0$ stands for a small parameter. The second novelty of our work is that we bypass this difficulty, by means of Riemann sums, insofar as, when one passes to the limit, we can obtain the desired integral formula, which gives the fractal tube zeta function. Once the fractal tube formula has been obtained, we deduce from it the explicit form of the local and global fractal (tube and distance) zeta functions, along with the Complex Dimensions of the IFD, which are the same at any step of the process, for all prefractal approximations sufficiently close to the Weierstrass Curve. Note that the later results obtained in [DL23b] corroborate and further justify our approach. Indeed, not only the Complex Dimensions of the IFD are the same as the Complex Dimensions of the fractal involved, as is proved in [DL23b], but, also, the determination of the Complex Dimensions of the IFD is a compulsory step in order to know the Complex Dimensions of the limiting object – in our case, the Weierstrass Curve. In the process, we introduce the new notions of *effective tubular neighborhood*, as well as of *effective local and global fractal zeta functions*.

The main results obtained in this paper, where we consider the case $b = N_b$ being an integer, can be found in the following places:

i. In Corollary 2.12, on page 24, and Theorem 2.13, on page 26, along with Corollary 2.14, on page 27, where we prove the sharp local Hölder continuity, and a sharp discrete version of reverse Hölder continuity, with optimal Hölder exponent, for the Weierstrass function $\mathcal{W}$, equal to the (Minkowski) Codimension $2 - D_{\mathcal{W}} = \ln_{N_b} \frac{1}{\lambda}$. It follows, in particular, that $\mathcal{W}$ is nowhere differentiable – as is well known, although our method of proof is completely different from the usual ones.

ii. In Theorem 4.7, on page 72 and Theorem 4.11, on page 83, wich yield, for specific (and geo-

metrically significant) values of the positive parameter ϵ, the expression of the area of the ϵ–neighborhood of each m^{th} prefractal graph approximation, for all sufficiently large positive integers m – a Weierstrass Fractal Tube Formula, which (apart from two terms associated with the Complex Dimensions 0 and -2) consists of an expansion of the form

$$\sum_{\alpha \,\text{real part of a Complex Dimension}} \epsilon^{2-\alpha}\, G_\alpha\left(\ln_{N_b}\left(\frac{1}{\epsilon}\right)\right), \qquad (\star)$$

where, for any real part α of a Complex Dimension, G_α denotes a continuous and one–periodic function. Furthermore, for $\alpha = \alpha_{max} = D_{\mathcal{W}}$, the Minkowski dimension of the Curve – i.e., for α being equal to the maximal real part of the Complex Dimensions of the Weierstrass IFD – the periodic function $G_{\alpha_{max}}$ is nonconstant, as well as bounded away from zero and infinity. As is the case in the general theory of fractal tube formulas (see [LvF06], [LRŽ17b], Chapter 8 and Chapter 5, respectively), the resulting fractal power series has for exponents the Complex Codimensions of the Weierstrass Curve. Observe that each nonconstant periodic function in $(\star)$ gives rise to multiplicatively periodic (or log–periodic) oscillations in the scaling variable ϵ.

iii. In Theorem 4.10, on page 81, where we exhibit the possible Complex Dimensions of the Weierstrass IFD, as the poles of the associated (local and global) Tube Zeta Functions, themselves obtained in Theorem 4.8, on page 76. Equivalently, in the light of [LRŽ17a], [LRŽ17b], since $D_{\mathcal{W}} < 2$, the Complex Dimensions are also the poles of the associated distance zeta functions. In particular, we show that the Complex Dimensions (other than 0 and -2) are all simple and periodically distributed (with the same period $\mathbf{p} = \dfrac{2\,\pi}{\ln N_b}$, the natural oscillatory period of the Weierstrass Curve) along countably many vertical lines, with abscissae $D_{\mathcal{W}} - k\,(2 - D_{\mathcal{W}})$ and $1 - 2\,k$, where k in $\mathbb{N} = \{0, 1, 2, \cdots\}$ is arbitrary. In addition, -2 and 0 are also Complex Dimensions, and they are simple.

iv. In Theorem 4.12, on page 90 and Corollary 4.13, on page 92, where we prove the nondegeneracy of the Weierstrass IFD, in the Minkowski sense (see [LRŽ17b]), coming from the fact that, for all sufficiently large positive integers m, the upper and lower (effective) Minkowski contents of the m^{th} prefractal polygonal approximation to the Curve are respectively positive and finite. As a result, the Minkowski dimension (or box–counting dimension) $D_{\mathcal{W}}$ of the Weierstrass IFD exists; i.e., the lower and upper Minkowski dimensions of the IFD coincide. Also, since the periodic function $G_{D_{\mathcal{W}}}$ is not constant, it follows that the Weierstrass IFD is not Minkowski measurable. Moreover, we show that the (effective) average Minkowski content of the Weierstrass IFD exists, is positive and finite, as well as coincides with the average value of the periodic function $G_{D_{\mathcal{W}}}$.

v. As a corollary of Theorem 4.12 (page 90), the fact that the number $D_{\mathcal{W}}$ is both the Minkowski Dimension and a Complex Dimension of the Weierstrass IFD; see Corollary 4.13, on page 92.

vi. The *fractality* of the Weierstrass IFD, in the sense of [LvF06], [LRŽ17b], [Lap19]; i.e., the existence of *nonreal* Complex Dimensions (with real part $D_{\mathcal{W}}$) giving rise to geometric oscillations, in the Fractal Tube Formula obtained in this paper (Theorem 4.7, on page 72 and Theorem 4.11, on page 83), as described in *ii.* above. In fact, in the terminology of [LvF06] and [LRŽ17b], the Weierstrass IFD is fractal in countably many dimensions d_k, with $d_k \to -\infty$, as $k \to \infty$.

The Minkowski dimension (or box dimension) of the Weierstrass Curve, $D_{\mathcal{W}}$, coincides with the maximum value of the real parts of the Complex Dimensions of the IFD. By considering the lower

Minkowski content, which we prove to be strictly positive, we show that $D_{\mathcal{W}}$ is, as expected, a Complex Dimension of the IFD. In fact, it is natural to expect that this is also true for the Complex Dimensions themselves, which will be shown in [DL23b] to be the same for the Weierstrass IFD and for the Weierstrass Curve.

We also briefly discuss, in Subsection 4.5, on page 94, the noninteger case, i.e., when b is any positive real number satisfying $\lambda\, b > 1$. This case will be studied in detail in a future work.

Now, the determination of those dimensions, as important as it may be, is not an end in itself. In fact, the Complex Dimensions directly echo the fractal cohomological properties of the Curve, which is the subject of our second paper, [DL22c]. The results of this paper and of [DL22c] are announced in the survey article [DL22a], where their main results are presented in a summarized form.

2 Geometric Framework

Henceforth, we place ourselves in the Euclidean plane, equipped with a direct orthonormal frame. The usual Cartesian coordinates are denoted by (x, y). The horizontal and vertical axes will be respectively referred to as $(x'x)$ and $(y'y)$.

Notation 1 (**Set of all Natural Numbers and Intervals**)**.**

As in Bourbaki [Bou04] (Appendix E. 143), we denote by $\mathbb{N} = \{0,\, 1,\, 2,\, \cdots\}$ the set of all natural numbers, and set $\mathbb{N}^\star = \mathbb{N} \setminus \{0\}$.

Given a, b with $-\infty \leqslant a \leqslant b \leqslant \infty$, $]a, b[\, = (a, b)$ denotes an open interval, while, for example, $]a, b] = (a, b]$ denotes a half–open, half–closed interval.

Notation 2 (**Wave Inequality Symbol (see [Tao06], Preface, page xiv)**)**.**

Given two positive numbers a and b, we will use the notation $a \lesssim b$, when there exists a strictly positive constant C such that $a \leqslant C\, b$, which is equivalent to $a = \mathcal{O}(b)$. Note that in our forthcoming context, we will often use $\mathcal{O}(1)$ to denote terms which depend on $m \in \mathbb{N}$, but are bounded away from 0 and ∞; more precisely, those terms will always satisfy bounds of the following form

$$0 < \text{Constant}_{inf} \leqslant \mathcal{O}(1) \leqslant \text{Constant}_{sup} < \infty\,, \tag{$\mathcal{R}\,1$}$$

where Constant_{inf} and Constant_{sup} denote strictly positive and finite constants.

Notation 3 (**Weierstrass Parameters**)**.**

In the sequel, λ and N_b are two real numbers such that

$$< \lambda < 1 \quad , \quad N_b \in \mathbb{N}^\star \quad \text{and} \quad \lambda\, N_b > 1\,. \qquad (\clubsuit) \tag{$\mathcal{R}\,2$}$$

As explained in [Dav19], we deliberately made the choice to introduce the notation N_b which replaces the initial b, in so far as, in Hardy's paper [Har16] (in contrast to Weierstrass's original

article [Wei75]), b is any positive real number satisfying $\lambda\, b > 1$, whereas we deal here with the specific case of a natural integer, which accounts for the natural notation N_b; see, however, Section 4.5.

Definition 2.1 (**Weierstrass Function, Weierstrass Curve**).

We consider the *Weierstrass function* $\mathcal{W}$, defined, for any real number x, by

$$\mathcal{W}(x) = \sum_{n=0}^{\infty} \lambda^n \cos\left(2\,\pi\, N_b^n\, x\right) \cdot \tag{$\mathcal{R}\,3$}$$

We call the associated graph the *Weierstrass Curve*.

Due to the one–periodicity of the $\mathcal{W}$–function, from now on, and without loss of generality, we restrict our study to the interval $[0, 1[= [0, 1)$.

Notation 4 (**Logarithm**).

Given $y > 0$, $\ln y$ denotes the natural logarithm of y, while, given $a > 0$, $a \neq 1$, $\ln_a y = \dfrac{\ln y}{\ln a}$ denotes the logarithm of y in base a; so that, in particular, $\ln = \ln_e$.

Notation 5. For the parameters λ and N_b satisfying condition $(\clubsuit)$ (see Notation 3, on page 7), we denote by

$$D_{\mathcal{W}} = 2 + \frac{\ln \lambda}{\ln N_b} = 2 - \ln_{N_b} \frac{1}{\lambda} \in\ ]1, 2[\tag{$\mathcal{R}\,4$}$$

the box–counting dimension (or Minkowski dimension) of the Weierstrass Curve $\Gamma_{\mathcal{W}}$, which happens to be equal to its Hausdorff dimension [KMPY84], [BBR14], [She18], [Kel17]. As was mentioned earlier, our results in this paper will also provide a direct geometric proof of the fact that $D_{\mathcal{W}}$, the Minkowski dimension (or box–counting dimension) of $\Gamma_{\mathcal{W}}$, exists and takes the above value.

Remark 2.1. As can be found, for instance, in [Fal86], we recall that the *box–counting dimension* (or *box dimension*, in short), of $\Gamma_{\mathcal{W}}$, is given by

$$D_{\mathcal{W}} = -\lim_{\delta \to 0^+} \frac{\ln N_\delta\left(\Gamma_{\mathcal{W}}\right)}{\ln \delta}\,, \quad (\diamond)$$

where $N_\delta\left(\Gamma_{\mathcal{W}}\right)$ stands for any of the following quantities:

i. the smallest number of sets of diameter at most δ that cover $\Gamma_{\mathcal{W}}$ on $[0, 1[$;

ii. the smallest number of closed balls of radius δ that cover $\Gamma_{\mathcal{W}}$ on $[0, 1[$;

iii. the smallest number of cubes of side δ that cover $\Gamma_{\mathcal{W}}$ on $[0, 1[$;

iv. the number of δ–mesh cubes that intersect $\Gamma_{\mathcal{W}}$ on $[0, 1[$;

v. the largest number of disjoint balls of radius δ with centers in $\Gamma_{\mathcal{W}}$ on $[0, 1[$.

Furthermore, for the Weierstrass Curve $\Gamma_{\mathcal{W}}$, as, more generally, for any bounded subset of Euclidean space – the box–counting dimension coincides with the Minkowski dimension.

We stress that our results will imply that the Minkowski (or box–counting) dimension of the Weierstrass Curve exists; more specifically, the above limit exists and is equal to $D_{\mathcal{W}} = 2 + \dfrac{\ln \lambda}{\ln N_b}$.

Convention (**The Weierstrass Curve as a Cyclic Curve**).

In the sequel, we identify the points $(0, \mathcal{W}(0))$ and $(1, \mathcal{W}(1)) = (1, \mathcal{W}(0))$. This is justified by the fact that the Weierstrass function $\mathcal{W}$ is 1–periodic, since N_b is an integer.

Remark 2.2. The above convention makes sense, because the points $(0, \mathcal{W}(0))$ and $(1, \mathcal{W}(1))$ have the same vertical coordinate, in addition to the periodic properties of the $\mathcal{W}$–function.

Property 2.1. $\left(\textbf{\textit{Symmetry with Respect to the Vertical Line }} x = \dfrac{1}{2}\right)$

Since, for any $x \in [0, 1]$,

$$\mathcal{W}(1 - x) = \sum_{n=0}^{\infty} \lambda^n \cos\left(2\,\pi\, N_b^n - 2\,\pi\, N_b^n\, x\right) = \mathcal{W}(x)\,,$$

the Weierstrass Curve is symmetric with respect to the vertical straight line $x = \dfrac{1}{2}$.

Proposition 2.2 (**Nonlinear and Noncontractive Iterated Function System (IFS)**).

Following our previous work [Dav18]*, we approximate the restriction* $\Gamma_{\mathcal{W}}$ *to* $[0, 1[\times \mathbb{R}$*, of the Weierstrass Curve, by a sequence of graphs, built via an iterative process. For this purpose, we use the nonlinear iterated function system (IFS) of the family of* C^{∞} *maps from* $\mathbb{R}^2$ *to* $\mathbb{R}^2$ *denoted by*

$$\mathcal{T}_{\mathcal{W}} = \left\{T_0, \cdots, T_{N_b - 1}\right\}\,,$$

where, for any integer i *belonging to* $\{0, \cdots, N_b - 1\}$ *and any point* (x, y) *of* $\mathbb{R}^2$,

$$T_i(x, y) = \left(\frac{x + i}{N_b}, \lambda\, y + \cos\left(2\,\pi\,\left(\frac{x + i}{N_b}\right)\right)\right)\,.$$

Remark 2.3. As is explained in [Dav19], it happens that the maps T_i, with $i = 0, \cdots, N_b - 1$, comprising the IFS $\mathcal{T}_{\mathcal{W}}$ in the statement of Proposition 2.2, on page 9 just above – are not contractions, *in the classical sense*. As a result, the nonlinearity of the IFS, $\mathcal{T}_{\mathcal{W}} = \{T_i\}_{i=0}^{N_b - 1}$, does not enable one to resort to the probabilistic approach of M. F. Barnsley and S. Demko [BD85], or to the earlier work of J. E. Hutchinson [Hut81], which is applicable in the case of standard fractals such as the Sierpiński Gasket and the Koch Curve. Interestingly, even if they are not contractions, our maps possess what can be viewed as satisfying an equivalent property, since, at each step of the iterative process, they reduce the two-dimensional Lebesgue measures of a given sequence of rectangles covering the Curve.

This is due to the fact that they correspond, in a sense, to the composition of a contraction of ratio r_x in the horizontal direction, and a dilatation of factor r_y in the vertical direction, with $r_x\, r_y < 1$. Such maps are considered, for example, in the book of Robert L. Devaney [Dev03], where they play a part in the first step of the horseshoe map process introduced by Stephen Smale.

Property 2.3 (**Attractor of the IFS**).

The Weierstrass Curve is the attractor of the IFS $\mathcal{T}_{\mathcal{W}}$*:* $\Gamma_{\mathcal{W}} = \bigcup_{i=0}^{N_b-1} T_i(\Gamma_{\mathcal{W}})$.

Proof. We refer to our works [Dav18], [Dav19].

□

Notation 6 (**Fixed Points**).

For any integer i belonging to $\{0, \cdots, N_b - 1\}$, we denote by

$$P_i = (x_i, y_i) = \left(\frac{i}{N_b - 1}, \frac{1}{1-\lambda} \cos\left(\frac{2\,\pi\, i}{N_b - 1} \right) \right)$$

the unique fixed point of the map T_i (see [Dav19]).

Definition 2.2 (**Sets of Vertices, Prefractals**).

We denote by V_0 the ordered set (according to increasing abscissae), of the points

$$\left\{ P_0, \cdots, P_{N_b-1} \right\} .$$

The set of points V_0 – where, for any i of $\{0, \cdots, N_b - 2\}$, the point P_i is linked to the point P_{i+1} – constitutes an oriented finite graph, ordered according to increasing abscissa, which we will denote by $\Gamma_{\mathcal{W}_0}$. Then, V_0 is called *the set of vertices* of the graph $\Gamma_{\mathcal{W}_0}$.

For any natural integer m, i.e., $m \in \mathbb{N}$, we set $V_m = \bigcup_{i=0}^{N_b-1} T_i\,(V_{m-1})$.

The set of points V_m, where two consecutive points are linked, is an oriented finite graph, ordered according to increasing abscissa, which we will call the $\boldsymbol{m^{th}}$**–order** $\boldsymbol{\mathcal{W}}$**–prefractal**. Then, V_m is called *the set of vertices* of the prefractal $\Gamma_{\mathcal{W}_m}$; see Figures 1, 2, 3 on pages 11, 12, and 13.

Definition 2.3 (**Adjacent Vertices, Edge Relation**).

For any natural integer m, the prefractal graph $\Gamma_{\mathcal{W}_m}$ is equipped with an edge relation $\underset{m}{\sim}$, as follows: two vertices X and Y of $\Gamma_{\mathcal{W}_m}$, i.e. two points belonging to V_m, will be said to be *adjacent* (i.e., neighboring or junction points) if and only if the line segment $[X, Y]$ is an edge of $\Gamma_{\mathcal{W}_m}$; we then

write $X \underset{m}{\sim} Y$. Note that this edge relation depends on m, which means that points adjacent in V_m might not remain adjacent in V_{m+1}.

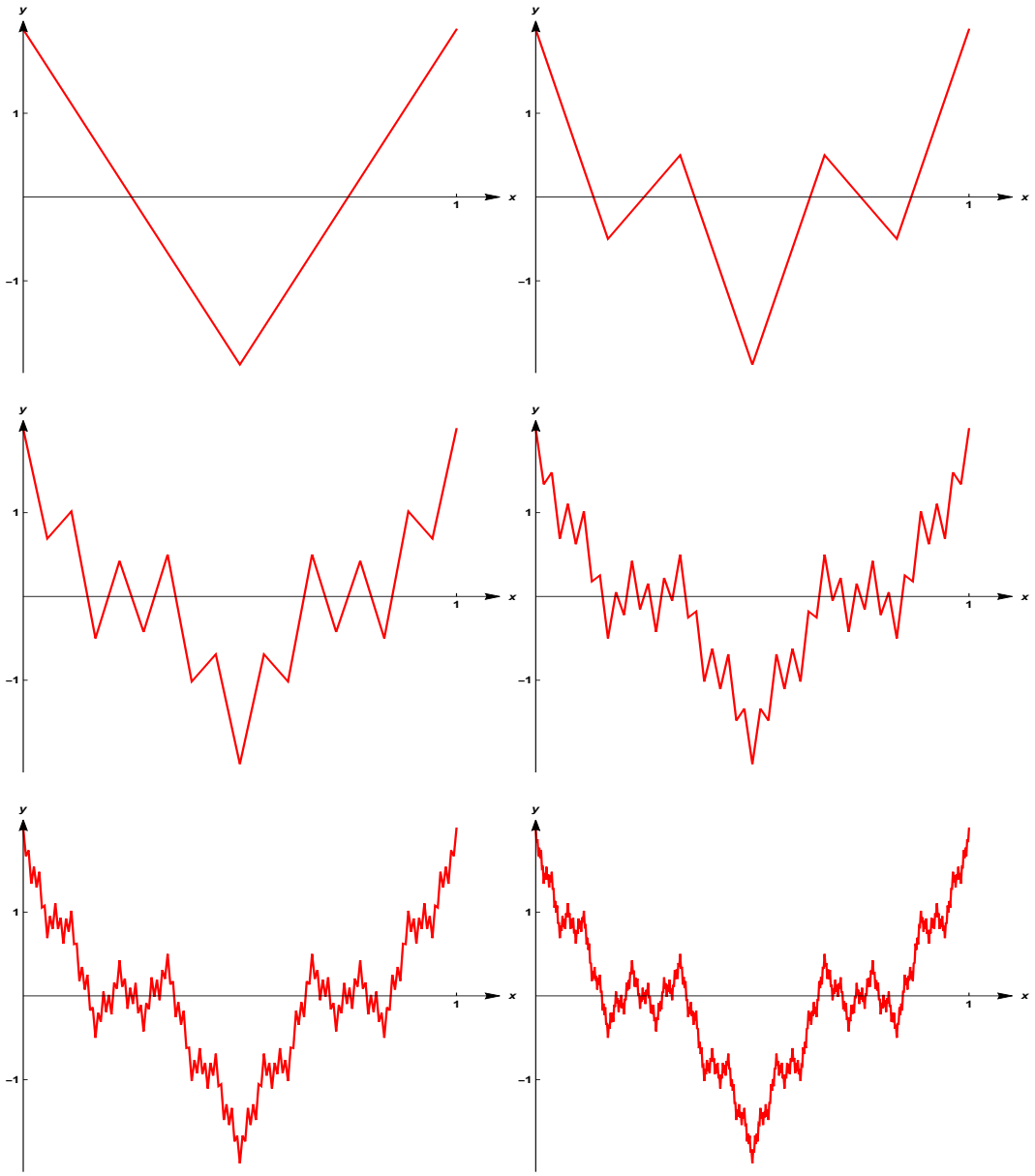

Figure 1: **The prefractal graphs $\Gamma_{\mathcal{W}_0}$, $\Gamma_{\mathcal{W}_1}$, $\Gamma_{\mathcal{W}_2}$, $\Gamma_{\mathcal{W}_3}$, $\Gamma_{\mathcal{W}_4}$, $\Gamma_{\mathcal{W}_5}$, in the case where $\lambda = \frac{1}{2}$, and $N_b = 3$. For example, $\Gamma_{\mathcal{W}_1}$ is on the right side of the top row, while $\Gamma_{\mathcal{W}_4}$ is on the left side of the bottom row.**

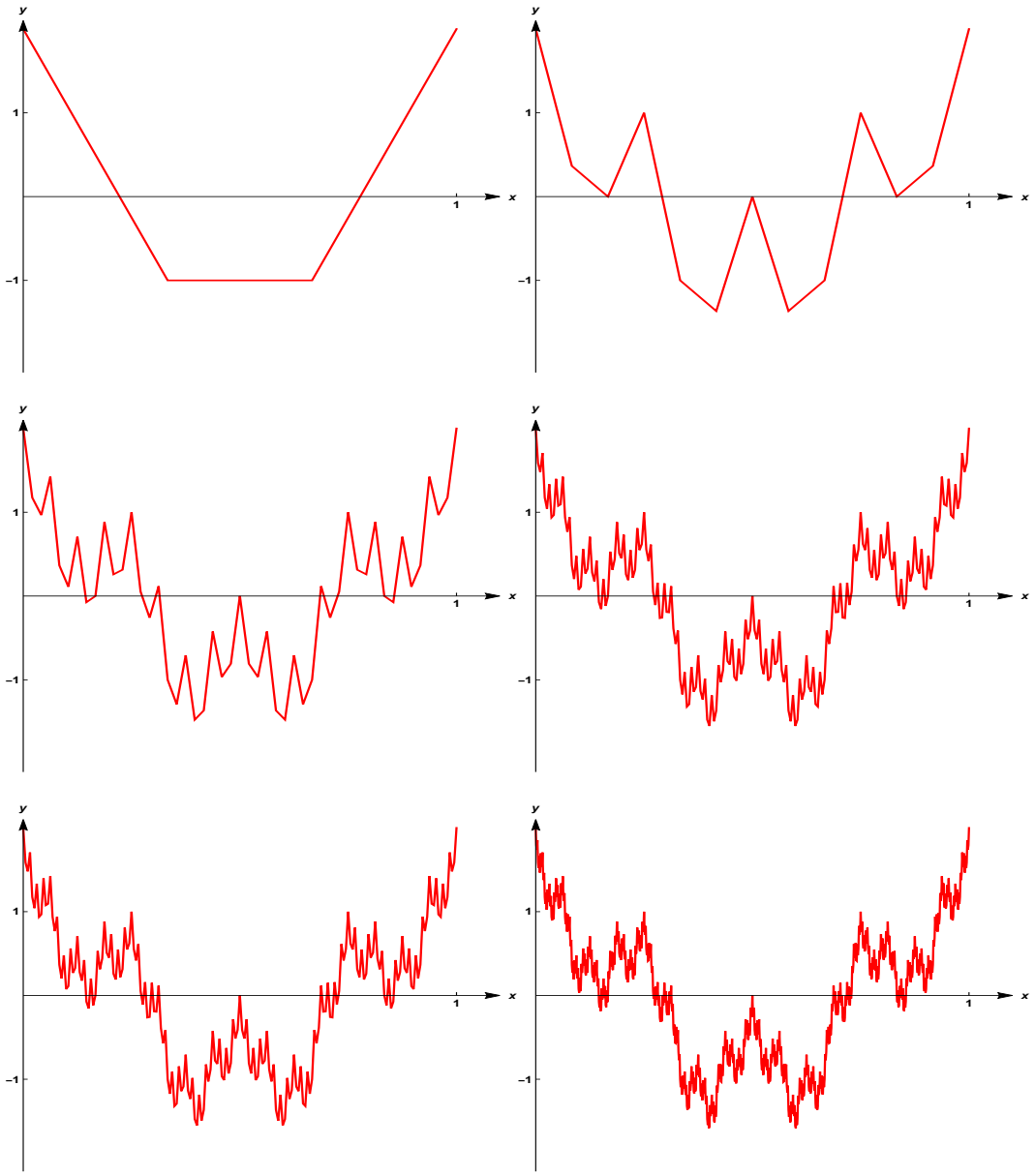

Figure 2: **The prefractal graphs $\Gamma_{\mathcal{W}_0}$, $\Gamma_{\mathcal{W}_1}$, $\Gamma_{\mathcal{W}_2}$, $\Gamma_{\mathcal{W}_3}$, $\Gamma_{\mathcal{W}_4}$, $\Gamma_{\mathcal{W}_5}$, in the case where $\lambda = \frac{1}{2}$ and $N_b = 4$.**

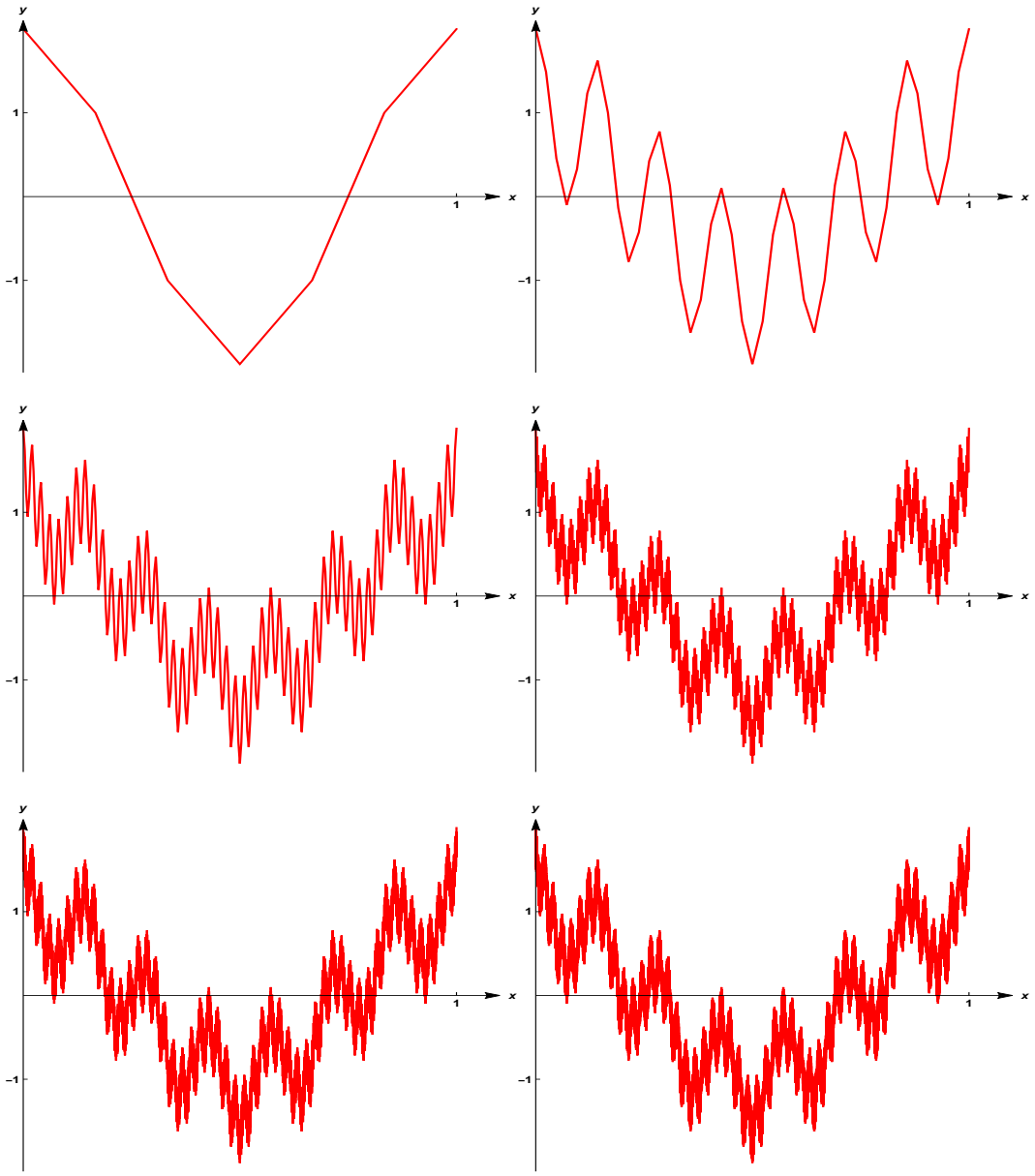

Figure 3: **The prefractal graphs $\Gamma_{\mathcal{W}_0}$, $\Gamma_{\mathcal{W}_1}$, $\Gamma_{\mathcal{W}_2}$, $\Gamma_{\mathcal{W}_3}$, $\Gamma_{\mathcal{W}_4}$, $\Gamma_{\mathcal{W}_5}$, in the case where $\lambda = \frac{1}{2}$ and $N_b = 7$.**

Property 2.4. [Dav18]
For any $m \in \mathbb{N}$, the following statements hold:

i. $V_m \subset V_{m+1}$.

ii. $\#V_m = (N_b - 1)\, N_b^m + 1$, *where* $\#V_m$ *denotes the number of elements in the finite set* V_m.

iii. *The prefractal graph* $\Gamma_{\mathcal{W}_m}$ *has exactly* $(N_b - 1)\, N_b^m$ *edges.*

iv. *The consecutive vertices of the prefractal graph* $\Gamma_{\mathcal{W}_m}$ *are the vertices of* N_b^m *simple nonregular polygons* $\mathcal{P}_{m,k}$ *with* N_b *sides. For any strictly positive integer* m, *the junction point between two consecutive polygons is the point*

$$\left(\frac{(N_b - 1)\, k}{(N_b - 1)\, N_b^m}, \mathcal{W}\left(\frac{(N_b - 1)\, k}{(N_b - 1)\, N_b^m} \right) \right) \quad , \quad 1 \leqslant k \leqslant N_b^m - 1 \,.$$

Hence, the total number of junction points is $N_b^m - 1$. *For instance, in the case* $N_b = 3$, *the polygons are all triangles; see Figure 4, on page 14.*

In the sequel, we will denote by $\mathcal{P}_0$ ***the initial polygon***, *whose vertices are the fixed points of the maps* T_i, $0 \leqslant i \leqslant N_b - 1$, *introduced in Definition 2.2, on page 10, i.e.,* $\{P_0, \cdots, P_{N_b - 1}\}$.

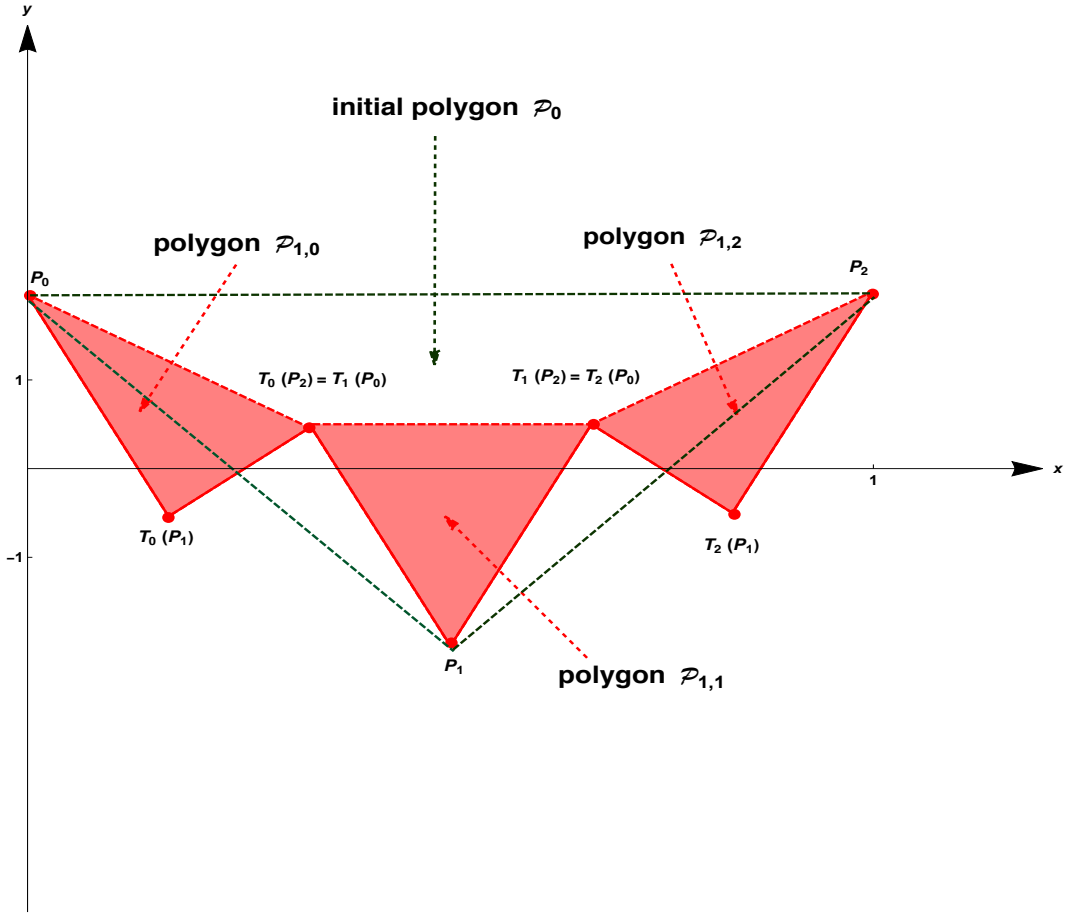

Figure 4: **The initial polygon $\mathcal{P}_0$, and the polygons $\mathcal{P}_{0,1}$, $\mathcal{P}_{1,1}$, $\mathcal{P}_{1,2}$, in the case where $\lambda = \frac{1}{2}$ and $N_b = 3$.**

Definition 2.4 (**Vertices of the Prefractals, Elementary Lengths, Heights and Angles**).

Given a strictly positive integer m, we denote by $\left(\boldsymbol{M_{j,m}}\right)_{\boldsymbol{0 \leqslant j \leqslant (N_b-1)\, N_b^m-1}}$ **the set of vertices** of the prefractal graph $\Gamma_{\mathcal{W}_m}$. One thus has, for any integer j in $\left\{0, \cdots, (N_b-1)\, N_b^m - 1\right\}$,

$$M_{j,m} = \left(\frac{j}{(N_b-1)\, N_b^m}, \mathcal{W}\left(\frac{j}{(N_b-1)\, N_b^m} \right) \right) .$$

We also introduce, for any integer j in $\left\{0, \cdots, (N_b-1)\, N_b^m - 2\right\}$, the following quantities:

i. the elementary horizontal lengths:

$$L_m = \frac{j}{(N_b-1)\, N_b^m} ;$$

ii. the elementary lengths:

$$\ell_{j,j+1,m} = d\left(M_{j,m}, M_{j+1,m}\right) = \sqrt{L_m^2 + h_{j,j+1,m}^2} ,$$

where $h_{j,j+1,m}$ is defined in *iii.* just below.

iii. the elementary heights:

$$h_{j,j+1,m} = \left| \mathcal{W}\left(\frac{j+1}{(N_b-1)\, N_b^m} \right) - \mathcal{W}\left(\frac{j}{(N_b-1)\, N_b^m} \right) \right| ;$$

iv. the minimal height:

$$h_m^{inf} = \inf_{0 \leqslant j \leqslant (N_b-1)\, N_b^m - 1} h_{j,j+1,m} , \tag{$\mathcal{R}$ 5}$$

along with the the maximal height:

$$h_m = \sup_{0 \leqslant j \leqslant (N_b-1)\, N_b^m - 1} h_{j,j+1,m} , \tag{$\mathcal{R}$ 6}$$

v. the geometric angles:

$$\theta_{j,j+1,m} = \left((y'y), \left(\widehat{M_{j,m}M_{j+1,m}}\right)\right),$$

which yield **the value of the geometric angle between consecutive edges** $\left[M_{j-1,m}\,M_{j,m}, M_{j,m}\,M_{j+1,m}\right]$:

$$\theta_{j-1,j,m} + \theta_{j,j+1,m} = \arctan\frac{L_m}{\left|h_{j-1,j,m}\right|} + \arctan\frac{L_m}{\left|h_{j,j+1,m}\right|}\cdot$$

Property 2.5. *For the geometric angle* $\theta_{j-1,j,m}$*, with* $0 \leqslant j \leqslant (N_b-1)\,N_b^m - 1$ *and* $m \in \mathbb{N}$*, we have the following relation:*

$$\tan\theta_{j-1,j,m} = \frac{h_{j-1,j,m}}{L_m}\cdot$$

One now requires, at a given step $m \in \mathbb{N}^\star$, the exact coordinates of the vertices of the prefractal graph $\Gamma_{\mathcal{W}_m}$, i.e. of the following set of points:

$$\left(\frac{j}{(N_b-1)\,N_b^m}, \mathcal{W}\left(\frac{j}{(N_b-1)\,N_b^m}\right)\right) \quad , \quad 0 \leqslant j \leqslant \#V_m\,.$$

Thus far, they could not be found in the existing literature on the subject.

For this purpose, it is interesting to use the scaling properties of the Weierstrass function.

Property 2.6 (**Scaling Properties of the Weierstrass Function, and Consequences**)**.**

Since, for any real number x, $\mathcal{W}(x) = \displaystyle\sum_{n=0}^{\infty}\lambda^n\cos\left(2\,\pi\,N_b^n\,x\right)$*, one also has*

$$\mathcal{W}(N_b\,x) = \sum_{n=0}^{\infty}\lambda^n\cos\left(2\,\pi\,N_b^{n+1}\,x\right) = \frac{1}{\lambda}\sum_{n=1}^{\infty}\lambda^n\cos\left(2\,\pi\,N_b^n\,x\right) = \frac{1}{\lambda}\left(\mathcal{W}(x) - \cos\left(2\,\pi\,x\right)\right),$$

which yields, for any strictly positive integer m *and any* j *in* $\{0,\cdots,\#V_m\}$*,*

$$\mathcal{W}\left(\frac{j}{(N_b-1)\,N_b^m}\right) = \lambda\,\mathcal{W}\left(\frac{j}{(N_b-1)\,N_b^{m-1}}\right) + \cos\left(\frac{2\,\pi\,j}{(N_b-1)\,N_b^m}\right)\cdot$$

By induction, one then obtains that

$$\mathcal{W}\left(\frac{j}{(N_b-1)\,N_b^m}\right) = \lambda^m\,\mathcal{W}\left(\frac{j}{N_b-1}\right) + \sum_{k=0}^{m-1}\lambda^k\cos\left(\frac{2\,\pi\,N_b^k\,j}{(N_b-1)\,N_b^m}\right)\cdot$$

Property 2.7 (A Consequence of the Symmetry with Respect to the Vertical Line $x = \frac{1}{2}$).

For any strictly positive integer m and any j in $\{0, \cdots, \#V_m\}$, we have that

$$\mathcal{W}\left(\frac{j}{(N_b-1)\,N_b^m}\right) = \mathcal{W}\left(\frac{(N_b-1)\,N_b^m - j}{(N_b-1)\,N_b^m}\right),$$

which means that the points

$$\left(\frac{(N_b-1)\,N_b^m - j}{(N_b-1)\,N_b^m}, \mathcal{W}\left(\frac{(N_b-1)\,N_b^m - j}{(N_b-1)\,N_b^m}\right)\right) \quad \textit{and} \quad \left(\frac{j}{(N_b-1)\,N_b^m}, \mathcal{W}\left(\frac{j}{(N_b-1)\,N_b^m}\right)\right)$$

are symmetric with respect to the vertical line $x = \frac{1}{2}$.

Definition 2.5 (Left-Side and Right-Side Vertices).

Given natural integers m, k such that $0 \leqslant k \leqslant N_b^m - 1$, and a polygon $\mathcal{P}_{m,k}$, we define:

i. The set of its *left-side vertices* as the set of the first $\left[\frac{N_b-1}{2}\right]$ vertices, where $[y]$ denotes the integer part of the real number y.

ii. The set of its *right-side vertices* as the set of the last $\left[\frac{N_b-1}{2}\right]$ vertices.

When the integer N_b is odd, we define the bottom vertex as the $\left(\frac{N_b-1}{2}\right)^{th}$ one; see Figure 6, on page 18.

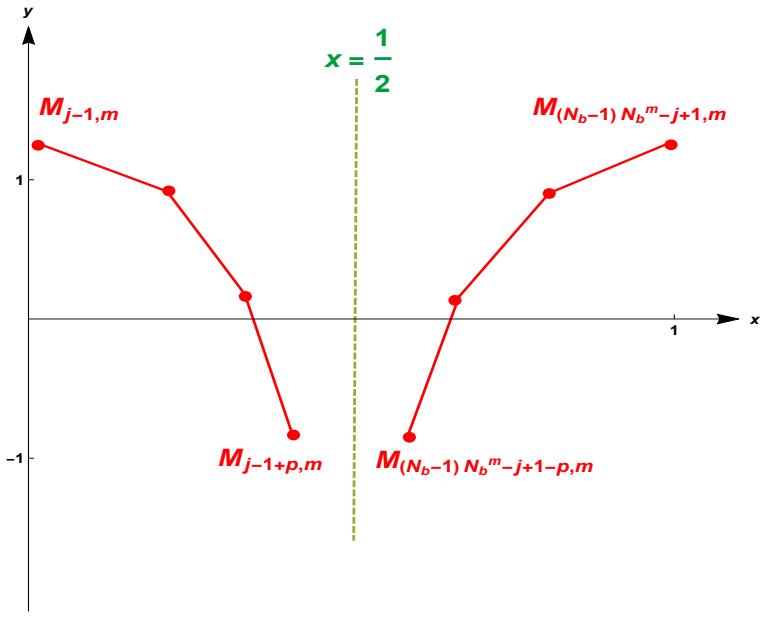

Figure 5: **Symmetric points with respect to the vertical line $x = \frac{1}{2}$.**

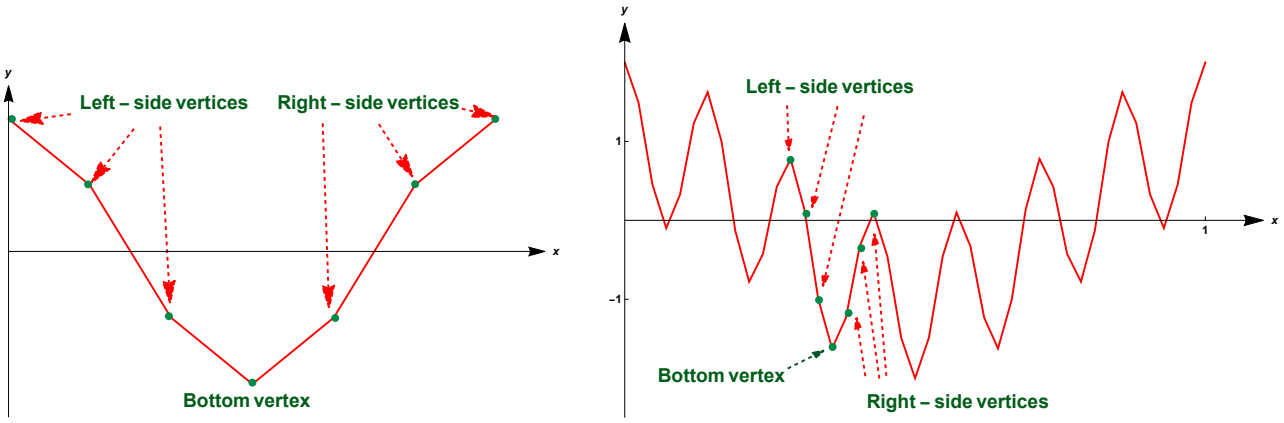

Figure 6: **The left-side and right-side vertices.**

Property 2.8. *Since, for any natural integer n,*

$$N_b^n = (1 + N_b - 1)^n = \sum_{k=0}^{n} \binom{n}{k} (N_b - 1)^k \equiv 1 \quad mod\ N_b - 1\,,$$

one obtains, for any integer j in $\{0, \cdots, N_b - 1\}$:

$$\mathcal{W}\left(\frac{j}{N_b - 1}\right) = \sum_{n=0}^{\infty} \lambda^n \cos\left(2\,\pi\, N_b^n\, \frac{j}{(N_b - 1)}\right) = \sum_{n=0}^{\infty} \lambda^n \cos\left(\frac{2\,\pi\, j}{N_b - 1}\right) = \frac{1}{1 - \lambda} \cos\left(\frac{2\,\pi\, j}{N_b - 1}\right).$$

We observe that the point

$$\left(\frac{j}{N_b - 1}, \mathcal{W}\left(\frac{j}{N_b - 1}\right)\right) = \left(\frac{j}{N_b - 1}, \frac{1}{1 - \lambda} \cos\left(\frac{2\,\pi\, j}{N_b - 1}\right)\right)$$

*is also **the fixed point** of the map T_j introduced in Proposition 2.2 page 9.*

Property 2.9.

For $0 \leqslant j \leqslant \dfrac{(N_b - 1)}{2}$ (resp., for $\dfrac{(N_b - 1)}{2} \leqslant j \leqslant N_b - 1$), we have that

$$\mathcal{W}\left(\frac{j+1}{N_b - 1}\right) - \mathcal{W}\left(\frac{j}{N_b - 1}\right) \leqslant 0 \quad \left(resp.,\ \mathcal{W}\left(\frac{j+1}{N_b - 1}\right) - \mathcal{W}\left(\frac{j}{N_b - 1}\right) \geqslant 0\right).$$

Proof. For any integer j in $\{0, \cdots, N_b - 1\}$,

$$\mathcal{W}\left(\frac{j+1}{N_b - 1}\right) - \mathcal{W}\left(\frac{j}{N_b - 1}\right) = \frac{1}{1 - \lambda}\left(\cos\left(\frac{2\,\pi\,(j+1)}{N_b - 1}\right) - \cos\left(\frac{2\,\pi\, j}{N_b - 1}\right)\right).$$

i. For $0 \leqslant j \leqslant \dfrac{N_b - 1}{2}$:

$$0 \leqslant \frac{2\,\pi\, j}{N_b - 1} \leqslant \pi \quad , \quad 0 \leqslant \frac{2\,\pi\,(j+1)}{N_b - 1} \leqslant \pi\left(1 + \frac{2}{N_b - 1}\right).$$

The limit case

$$\frac{2\,\pi\,(j+1)}{N_b-1} = \pi\left(1+\frac{2}{N_b-1}\right)$$

only occurs when the integer N_b is odd, for the value $j = \dfrac{N_b-1}{2}$, and corresponds to the bottom vertex of the initial polygon $\mathcal{P}_0$. In this case, one has

$$\mathcal{W}\left(\frac{N_b-1}{2}\right) = -\frac{1}{1-\lambda}\cdot$$

This case can thus be left aside.

One may therefore only consider the cases when $0 \leqslant \dfrac{2\,\pi\,j}{N_b-1} \leqslant \dfrac{2\,\pi\,(j+1)}{N_b-1} \leqslant \pi$.

The cosine function being nonincreasing on $[0,\pi]$, one obtains the expected result:

$$\mathcal{W}\left(\frac{j+1}{N_b-1}\right) - \mathcal{W}\left(\frac{j}{N_b-1}\right) \leqslant 0\cdot$$

ii. For $\dfrac{(N_b-1)}{2} \leqslant j \leqslant N_b-1$:

$$\pi \leqslant \frac{2\,\pi\,j}{N_b-1} \leqslant 2\,\pi \quad , \quad \pi\left(1+\frac{2}{N_b-1}\right) \leqslant \frac{2\,\pi\,(j+1)}{N_b-1} \leqslant \frac{2\,\pi\,N_b}{N_b-1}\cdot$$

As previously, the limit case

$$\frac{2\,\pi\,(j+1)}{N_b-1} = \pi\left(1+\frac{2}{N_b-1}\right)$$

can be left aside. The increasing property of the cosine function on $[\pi, 2\,\pi]$ then yields the expected result:

$$\mathcal{W}\left(\frac{j+1}{N_b-1}\right) - \mathcal{W}\left(\frac{j}{N_b-1}\right) \geqslant 0\cdot$$

□

Notation 7 (**Signum Function**).

The *signum function* of a real number x is defined by

$$\operatorname{sgn}(x) = \begin{cases} -1, & \text{if} \quad x < 0, \\ 0, & \text{if} \quad x = 0, \\ +1, & \text{if} \quad x > 0\cdot \end{cases}$$

Property 2.10. *Given any strictly positive integer m, we have the following properties:*

i. For any j in $\{0, \cdots, \#V_m\}$, the point

$$\left(\frac{j}{(N_b - 1)\, N_b^m}, \mathcal{W}\left(\frac{j}{(N_b - 1)\, N_b^m} \right) \right)$$

is the image of the point

$$\left(\frac{j}{(N_b - 1)\, N_b^{m-1}} - i, \mathcal{W}\left(\frac{j}{(N_b - 1)\, N_b^{m-1}} - i \right) \right) = \left(\frac{j - i\,(N_b - 1)\, N_b^{m-1}}{(N_b - 1)\, N_b^{m-1}}, \mathcal{W}\left(\frac{j - i\,(N_b - 1)\, N_b^{m-1}}{(N_b - 1)\, N_b^{m-1}} \right) \right)$$

under the map T_i, $0 \leqslant i \leqslant N_b - 1$.

*Consequently, for $0 \leqslant j \leqslant N_b - 1$, **the j^{th} vertex of the polygon** $\mathcal{P}_{m,k}$, $0 \leqslant k \leqslant N_b^m - 1$, i.e., the point*

$$\left(\frac{(N_b - 1)\, k + j}{(N_b - 1)\, N_b^m}, \mathcal{W}\left(\frac{(N_b - 1)\, k + j}{(N_b - 1)\, N_b^m} \right) \right)$$

is the image of the point

$$\left(\frac{(N_b - 1)\, \left(k - i\,(N_b - 1)\, N_b^{m-1} \right) + j}{(N_b - 1)\, N_b^{m-1}}, \mathcal{W}\left(\frac{(N_b - 1)\, \left(k - i\,(N_b - 1)\, N_b^{m-1} \right) + j}{(N_b - 1)\, N_b^{m-1}} \right) \right);$$

*it is also **the j^{th} vertex of the polygon** $\mathcal{P}_{m-1,k-i\,(N_b-1)\,N_b^{m-1}}$. Therefore, there is an exact correspondance between vertices of the polygons at consecutive steps $m-1$, m.*

ii. Given j in $\{0, \cdots, N_b - 2\}$ and k in $\left\{0, \cdots, N_b^m - 1\right\}$, we have that

$$sgn\left(\mathcal{W}\left(\frac{k\,(N_b - 1) + j + 1}{(N_b - 1)\, N_b^m} \right) - \mathcal{W}\left(\frac{k\,(N_b - 1) + j}{(N_b - 1)\, N_b^m} \right) \right) = sgn\left(\mathcal{W}\left(\frac{j+1}{N_b - 1} \right) - \mathcal{W}\left(\frac{j}{N_b - 1} \right) \right).$$

Proof.

i. One simply applies Proposition 2.3, on page 10, in conjunction with Property 2.8, on page 18.

For i in $\{0, \cdots, N_b - 1\}$, we have that

$$T_i\left(\frac{j - i\,(N_b-1)\,N_b^{m-1}}{(N_b-1)\,N_b^{m-1}}, \mathcal{W}\left(\frac{j - i\,(N_b-1)\,N_b^{m-1}}{(N_b-1)\,N_b^{m-1}}\right)\right)$$

$$||$$

$$\left(\frac{j - i\,(N_b-1)\,N_b^{m-1}}{(N_b-1)\,N_b^{m}} + \frac{i}{N_b}, \lambda\,\mathcal{W}\left(\frac{j - i\,(N_b-1)\,N_b^{m-1}}{(N_b-1)\,N_b^{m-1}}\right) + \cos\left(2\,\pi\,\left(\frac{j - i\,(N_b-1)\,N_b^{m-1}}{(N_b-1)\,N_b^{m}} + \frac{i}{N_b}\right)\right)\right)$$

$$= \left(\frac{j}{(N_b-1)\,N_b^{m}}, \mathcal{W}\left(\frac{j}{(N_b-1)\,N_b^{m-1}} - i\right) + \cos\left(2\,\pi\,\frac{j}{(N_b-1)\,N_b^{m}}\right)\right)$$

$$= \left(\frac{j}{(N_b-1)\,N_b^{m}}, \mathcal{W}\left(\frac{j}{(N_b-1)\,N_b^{m-1}} - i\right) + \cos\left(2\,\pi\,\frac{j-i}{(N_b-1)\,N_b^{m}} + \frac{i}{N_b}\right)\right)$$

$$= \left(\frac{j}{(N_b-1)\,N_b^{m}}, \lambda\,\mathcal{W}\left(\frac{j}{(N_b-1)\,N_b^{m-1}}\right) + \cos\left(2\,\pi\,\frac{j-i}{(N_b-1)\,N_b^{m}}\right)\right)$$

$$= \left(\frac{j}{(N_b-1)\,N_b^{m}}, \mathcal{W}\left(\frac{j}{(N_b-1)\,N_b^{m}}\right)\right).$$

ii. We prove the result by induction on m. Accordingly, let us consider j in $\{0, \cdots, N_b - 2\}$.

The result at *the initial step* $m = 1$ is satisfied, in so far as, for any integer k in $\{0, \cdots, N_b - 1\}$:

$$\begin{aligned}
\mathcal{W}\left(\frac{k\,(N_b-1)+j+1}{(N_b-1)\,N_b}\right) - \mathcal{W}\left(\frac{k\,(N_b-1)+j}{(N_b-1)\,N_b}\right) &= \lambda\left(\mathcal{W}\left(\frac{k\,(N_b-1)+j+1}{N_b-1}\right) - \mathcal{W}\left(\frac{k\,(N_b-1)+j}{N_b-1}\right)\right) \\
&\quad + \cos\left(\frac{2\,\pi\,(k\,(N_b-1)+j+1)}{N_b-1}\right) - \cos\left(\frac{2\,\pi\,(k\,(N_b-1)+j)}{N_b-1}\right) \\
&= \lambda\left(\mathcal{W}\left(k + \frac{j+1}{(N_b-1)}\right) - \mathcal{W}\left(k + \frac{j}{(N_b-1)}\right)\right) \\
&\quad + \cos\left(\frac{2\,\pi\,(j+1)}{(N_b-1)}\right) - \cos\left(\frac{2\,\pi\,j}{N_b-1}\right) \\
&= \lambda\left(\mathcal{W}\left(\frac{j+1}{N_b-1}\right) - \mathcal{W}\left(\frac{j}{N_b-1}\right)\right) \\
&\quad + \mathcal{W}\left(\frac{j+1}{N_b-1}\right) - \mathcal{W}\left(\frac{j}{N_b-1}\right) \\
&= (1+\lambda)\left(\mathcal{W}\left(\frac{j+1}{N_b-1}\right) - \mathcal{W}\left(\frac{j}{N_b-1}\right)\right).
\end{aligned}$$

Let us now assume that, for any integer k in $\left\{0, \cdots, N_b^{m-1} - 1\right\}$,

$$\operatorname{sgn}\left(\mathcal{W}\left(\frac{k\,(N_b-1)+j+1}{(N_b-1)\,N_b^{m}}\right) - \mathcal{W}\left(\frac{k\,(N_b-1)j}{(N_b-1)\,N_b^{m}}\right)\right) = \operatorname{sgn}\left(\mathcal{W}\left(\frac{j+1}{N_b-1}\right) - \mathcal{W}\left(\frac{j}{N_b-1}\right)\right).$$

Henceforth, we want to prove that, for any integer k in $\left\{0, \cdots, N_b^{m-1} - 1\right\}$,

$$\operatorname{sgn}\left(\mathcal{W}\left(\frac{k\,(N_b-1)+j+1}{(N_b-1)\,N_b^m}\right) - \mathcal{W}\left(\frac{k\,(N_b-1)j}{(N_b-1)\,N_b^m}\right)\right) = \operatorname{sgn}\left(\mathcal{W}\left(\frac{j+1}{N_b-1}\right) - \mathcal{W}\left(\frac{j}{N_b-1}\right)\right) \cdot$$

The induction hypothesis will be used in so far as any k in $\left\{0, \cdots, N_b^{m-1} - 1\right\}$ can also be expressed in the following form:

$$k = \widetilde{k} + i\,N_b^{m-1} \quad , \quad 0 \leqslant \widetilde{k} \leqslant N_b^{m-1} - 1 \quad , \quad 0 \leqslant i \leqslant N_b - 1 \cdot$$

This will be useful because of *the one–periodicity of the $\mathcal{W}$–function*, since, for any real number x and any integer i, we have that

$$\mathcal{W}(x+i) = \mathcal{W}(x) \cdot$$

Due to the symmetry with respect to the vertical line $x = \dfrac{1}{2}$ (see Property 2.1, on page 9), given a natural integer m, one can, in addition, restrict oneself to the cases when

$$0 \leqslant (N_b-1)\,k + j < (N_b-1)\,k + j + 1 \leqslant \left[\frac{(N_b-1)\,N_b^m + 1}{2}\right] = \frac{(N_b-1)\,N_b^m}{2}\,,$$

which yields

$$0 \leqslant \frac{(2\,(N_b-1)\,k + 2\,j - 1)\;\pi}{2\,(N_b-1)\,N_b^m} < \frac{(2\,(N_b-1)\,k + 2\,j + 1)\;\pi}{(N_b-1)\,N_b^m} \leqslant \pi \cdot$$

Thus, we only have to consider the cases when

$$\sin\left(\frac{(2\,(N_b-1)\,k + 2\,j - 1)\;\pi}{(N_b-1)\,N_b^m}\right) \geqslant 0 \quad \text{and} \quad \sin\left(\frac{(2\,(N_b-1)\,k + 2\,j + 1)\;\pi}{(N_b-1)\,N_b^m}\right) \geqslant 0 \cdot$$

The remaining ones, namely, the cases when

$$\sin\left(\frac{(2\,(N_b-1)\,k + 2\,j - 1)\;\pi}{(N_b-1)\,N_b^m}\right) \leqslant 0 \quad \text{and} \quad \sin\left(\frac{(2\,(N_b-1)\,k + 2\,j + 1)\;\pi}{(N_b-1)\,N_b^m}\right) \leqslant 0\,,$$

are then obtained by symmetry.

Hence,

$$\begin{array}{c} \mathcal{W}\left(\dfrac{k\,(N_b-1)+j+1}{(N_b-1)\,N_b^m}\right) - \mathcal{W}\left(\dfrac{j}{(N_b-1)\,N_b^m}\right) \\ || \end{array}$$

$$
\begin{aligned}
= \quad & \lambda\left(\mathcal{W}\left(\frac{k\,(N_b-1)+j+1}{(N_b-1)\,N_b^{m-1}}\right)-\mathcal{W}\left(\frac{k\,(N_b-1)+j}{(N_b-1)\,N_b^{m-1}}\right)\right)\\
& +\cos\left(\frac{2\,\pi\;(k\,(N_b-1)+j+1)}{(N_b-1)\,N_b^{m-1}}\right)-\cos\left(\frac{2\,\pi\;(k\,(N_b-1)+j)}{(N_b-1)\,N_b^{m-1}}\right)\\
= \quad & \lambda\left(\mathcal{W}\left(\frac{k\,(N_b-1)+j+1}{(N_b-1)\,N_b^{m-1}}\right)-\mathcal{W}\left(\frac{k\,(N_b-1)+j}{(N_b-1)\,N_b^{m-1}}\right)\right)\\
& -2\,\sin\left(\frac{\pi}{(N_b-1)\,N_b^{m-1}}\right)\sin\left(\frac{(2\,(N_b-1)\,k+2\,j+1)\;\pi}{(N_b-1)\,N_b^{m-1}}\right)\\
= \quad & \lambda\left(\mathcal{W}\left(\frac{\widetilde{k}\,(N_b-1)+i\;(N_b-1)\,N_b^{m-1}+j+1}{(N_b-1)\,N_b^{m-1}}\right)-\mathcal{W}\left(\frac{\widetilde{k}\,(N_b-1)+i\;(N_b-1)\,N_b^{m-1}+j}{(N_b-1)\,N_b^{m-1}}\right)\right)\\
& -2\,\sin\left(\frac{\pi}{(N_b-1)\,N_b^{m-1}}\right)\sin\left(\frac{(2\,(N_b-1)\,k+2\,j+1)\;\pi}{(N_b-1)\,N_b^{m-1}}\right)\\
= \quad & \lambda\left(\mathcal{W}\left(i+\frac{\widetilde{k}\,(N_b-1)+j+1}{(N_b-1)\,N_b^{m-1}}\right)-\mathcal{W}\left(i+\frac{\widetilde{k}\,(N_b-1)+j}{(N_b-1)\,N_b^{m-1}}\right)\right)\\
& -2\,\sin\left(\frac{\pi}{(N_b-1)\,N_b^{m-1}}\right)\sin\left(\frac{(2\,(N_b-1)\,k+2\,j+1)\;\pi}{(N_b-1)\,N_b^{m-1}}\right)\\
= \quad & \lambda\left(\mathcal{W}\left(\frac{\widetilde{k}\,(N_b-1)+j+1}{(N_b-1)\,N_b^{m-1}}\right)-\mathcal{W}\left(\frac{\widetilde{k}\,(N_b-1)+j}{(N_b-1)\,N_b^{m-1}}\right)\right)\\
& -2\,\sin\left(\frac{\pi}{(N_b-1)\,N_b^{m-1}}\right)\sin\left(\frac{(2\,(N_b-1)\,k+2\,j+1)\;\pi}{(N_b-1)\,N_b^{m-1}}\right).
\end{aligned}
$$

In the case when

$$
0\leqslant(N_b-1)\,k+j+1\leqslant\left[\frac{(N_b-1)\,N_b^m+1}{2}\right]=\frac{(N_b-1)\,N_b^m}{2}\,,
$$

one thus has

$$
-2\,\sin\left(\frac{\pi}{(N_b-1)\,N_b^{m-1}}\right)\sin\left(\frac{(2\,(N_b-1)\,k+2\,j-1)\;\pi}{(N_b-1)\,N_b^{m-1}}\right)\leqslant 0\,.
$$

The configuration of the initial polygon ensures, for $0\leqslant j\leqslant\dfrac{N_b-1}{2}$, that

$$
\mathcal{W}\left(\frac{j+1}{N_b-1}\right)-\mathcal{W}\left(\frac{j}{N_b-1}\right)\leqslant 0
$$

and therefore, thanks to the induction hypothesis,

$$
\mathcal{W}\left(\frac{\widetilde{k}\,(N_b-1)+j+1}{(N_b-1)\,N_b^{m-1}}\right)-\mathcal{W}\left(\frac{\widetilde{k}\,(N_b-1)+j}{(N_b-1)\,N_b^{m-1}}\right)\leqslant 0\,.
$$

By induction, one thus obtains, for any natural integer m, any k in $\left\{0, \cdots, N_b^m - 1\right\}$, and any j in $\left\{0, \cdots, \dfrac{N_b - 3}{2}\right\}$, that

$$\mathcal{W}\left(\frac{(N_b-1)\,k+j+1}{(N_b-1)\,N_b^m}\right) - \mathcal{W}\left(\frac{(N_b-1)\,k+j}{(N_b-1)\,N_b^m}\right) \leqslant 0\,,$$

as required. □

Corollary 2.11 (**Lower Bound for the Elementary Heights** (**Coming from Property** 2.10, on page 20))**.**

For any strictly positive integer m, and any j in $\left\{0, \cdots, (N_b-1)\,N_b^m\right\}$, we have that

$$\left|\mathcal{W}\left(\frac{j+1}{(N_b-1)\,N_b^m}\right) - \mathcal{W}\left(\frac{j}{(N_b-1)\,N_b^m}\right)\right| \geqslant \lambda \left|\mathcal{W}\left(\frac{j+1}{(N_b-1)\,N_b^{m-1}}\right) - \mathcal{W}\left(\frac{j}{(N_b-1)\,N_b^{m-1}}\right)\right|,$$

which yields, by induction,

$$\left|\mathcal{W}\left(\frac{j+1}{(N_b-1)\,N_b^m}\right) - \mathcal{W}\left(\frac{j}{(N_b-1)\,N_b^m}\right)\right| \geqslant \underbrace{\lambda^m}_{N_b^{m\,(D_{\mathcal{W}}-2)}} \left|\mathcal{W}\left(\frac{j+1}{N_b-1}\right) - \mathcal{W}\left(\frac{j}{N_b-1}\right)\right|.$$

This improves our previous result in [Dav18].

Corollary 2.12 (**Upper Bound for the Elementary Heights** (**Coming from Property** 2.10, on page 20))**.**

For any strictly positive integer m, and any j in $\left\{0, \cdots, (N_b-1)\,N_b^m\right\}$, we have that

$$\begin{aligned}\left|\mathcal{W}\left(\frac{j+1}{(N_b-1)\,N_b^m}\right) - \mathcal{W}\left(\frac{j}{(N_b-1)\,N_b^m}\right)\right| &\leqslant \lambda^m \left(\left|\mathcal{W}\left(\frac{j+1}{N_b-1}\right) - \mathcal{W}\left(\frac{j}{N_b-1}\right)\right| + \frac{2\,\pi}{(N_b-1)\,(\lambda\,N_b-1)}\right)\\ &\leqslant \underbrace{\lambda^m}_{N_b^{m\,(D_{\mathcal{W}}-2)}} \left(\left|\mathcal{W}\left(\frac{j+1}{N_b-1}\right) - \mathcal{W}\left(\frac{j}{N_b-1}\right)\right| + \frac{2\,\pi}{(N_b-1)\,(\lambda\,N_b-1)}\right),\end{aligned}$$

which also improves our previous result in [Dav18].

Proof. For any strictly positive integer m and any j in $\left\{0, \cdots, (N_b - 1)\, N_b^m\right\}$, we have the following estimates:

$$\begin{aligned}
\left|\mathcal{W}\left(\frac{j+1}{(N_b-1)\,N_b^m}\right) - \mathcal{W}\left(\frac{j}{(N_b-1)\,N_b^m}\right)\right| &\leqslant \lambda \left|\mathcal{W}\left(\frac{j+1}{(N_b-1)\,N_b^{m-1}}\right) - \mathcal{W}\left(\frac{j}{(N_b-1)\,N_b^{m-1}}\right)\right| \\
&\quad + \left|\cos\left(\frac{2\,\pi\,(j+1)}{(N_b-1)\,N_b^{m-1}}\right) - \cos\left(\frac{2\,\pi\,j}{(N_b-1)\,N_b^{m-1}}\right)\right| \\
&\leqslant \lambda \left|\mathcal{W}\left(\frac{j+1}{(N_b-1)\,N_b^{m-1}}\right) - \mathcal{W}\left(\frac{j}{(N_b-1)\,N_b^{m-1}}\right)\right| \\
&\quad + \frac{2\,\pi}{(N_b-1)\,N_b^{m-1}}\,,
\end{aligned}$$

which yields, by induction,

$$\begin{aligned}
\left|\mathcal{W}\left(\frac{j+1}{(N_b-1)\,N_b^m}\right) - \mathcal{W}\left(\frac{j}{(N_b-1)\,N_b^m}\right)\right| &\leqslant \lambda^m \left|\mathcal{W}\left(\frac{j+1}{N_b-1}\right) - \mathcal{W}\left(\frac{j}{N_b-1}\right)\right| + \sum_{k=0}^{m-1} \lambda^k\, \frac{2\,\pi\,N_b^k}{(N_b-1)\,N_b^m} \\
&\leqslant \lambda^m \left|\mathcal{W}\left(\frac{j+1}{N_b-1}\right) - \mathcal{W}\left(\frac{j}{N_b-1}\right)\right| + \frac{2\,\pi\,\lambda^m\,N_b^m}{(N_b-1)\,N_b^m\,(\lambda\,N_b-1)} \\
&= \lambda^m \left(\left|\mathcal{W}\left(\frac{j+1}{N_b-1}\right) - \mathcal{W}\left(\frac{j}{N_b-1}\right)\right| + \frac{2\,\pi}{(N_b-1)\,(\lambda\,N_b-1)}\right),
\end{aligned}$$

as desired. □

Remark 2.4. Corollaries 2.11 (page 24) and 2.12 (page 24) are important, because they enable one to obtain exact and more accurate values of the bounding constants C_{inf} and C_{sup} involved in the following inequality:

$$C_{inf}\, L_m^{2-D_{\mathcal{W}}} \leqslant \underbrace{\left|\mathcal{W}\left((j+1)\,L_m\right) - \mathcal{W}\left(j\,L_m\right)\right|}_{h_{j,j+1,m}} \leqslant C_{sup}\, L_m^{2-D_{\mathcal{W}}} \quad , \quad m \in \mathbb{N},\, 0 \leqslant j \leqslant (N_b-1)\,N_b^m, \quad (\maltese) \tag{$\mathcal{R}\,7$}$$

where

$$C_{inf} = (N_b-1)^{2-D_{\mathcal{W}}} \min_{0 \leqslant j \leqslant N_b-1} \left|\mathcal{W}\left(\frac{j+1}{N_b-1}\right) - \mathcal{W}\left(\frac{j}{N_b-1}\right)\right|$$

and

$$C_{sup} = (N_b-1)^{2-D_{\mathcal{W}}} \left(\max_{0 \leqslant j \leqslant N_b-1} \left|\mathcal{W}\left(\frac{j+1}{N_b-1}\right) - \mathcal{W}\left(\frac{j}{N_b-1}\right)\right| + \frac{2\,\pi}{(N_b-1)\,(\lambda\,N_b-1)}\right).$$

One should note, in addition, that *these constants depend on the initial polygon* $\mathcal{P}_0$.

Theorem 2.13 (**Sharp Local Discrete Reverse Hölder Properties of the Weierstrass Function (Coming from Corollary 2.11, on page 24)**).

For any natural integer m, let us consider a pair of real numbers (x, x') such that

$$x = \frac{(N_b - 1)\, k + j}{(N_b - 1)\, N_b^m} = ((N_b - 1)\, k + j)\; L_m \quad , \quad x' = \frac{(N_b - 1)\, k + j + \ell}{(N_b - 1)\, N_b^m} = ((N_b - 1)\, k + j + \ell)\; L_m \,,$$

where $0 \leqslant k \leqslant N_b - 1^m - 1$, *and*

i. if the integer N_b is odd,

$$0 \leqslant j < \frac{N_b - 1}{2} \quad \textit{and} \quad 0 < j + \ell \leqslant \frac{N_b - 1}{2}$$

or

$$\frac{N_b - 1}{2} \leqslant j < N_b - 1 \quad \textit{and} \quad \frac{N_b - 1}{2} < j + \ell \leqslant N_b - 1\,;$$

ii. if the integer N_b is even,

$$0 \leqslant j < \frac{N_b}{2} \quad \textit{and} \quad 0 < j + \ell \leqslant \frac{N_b}{2}$$

or

$$\frac{N_b}{2} + 1 \leqslant j < N_b - 1 \quad \textit{and} \quad \frac{N_b}{2} + 1 < j + \ell \leqslant N_b - 1\,\cdot$$

This means that the points $(x, \mathcal{W}(x))$ and $\left(x', \mathcal{W}(x')\right)$ are vertices of the polygon $\mathcal{P}_{m,k}$ (see Property 2.4, on page 14 above), both located on the left-side of the polygon, or both located on the right-side; see Figure 6, on page 18.

Then, one has the following (discrete, local) reverse–Hölder inequality*, with sharp Hölder exponent* $-\dfrac{\ln \lambda}{\ln N_b} = 2 - D_{\mathcal{W}}$,

$$C_{inf}\, |x' - x|^{2 - D_{\mathcal{W}}} \leqslant \left|\mathcal{W}(x') - \mathcal{W}(x)\right| \,\cdot$$

Proof. In the light of Property 2.9, on page 18, one can restrict oneself to the case when

$$0 \leqslant j < \frac{N_b - 1}{2} \quad \text{and} \quad 0 < j + \ell \leqslant \frac{N_b - 1}{2}\,\cdot$$

The expected result in the remaining case can easily be proved in a similar way. Since

$$\mathcal{W}\left(((N_b - 1)\, k + j + \ell)\; L_m\right) \leqslant \cdots \leqslant \mathcal{W}\left(((N_b - 1)\, k + j + 1)\; L_m\right) \leqslant \mathcal{W}\left(((N_b - 1)\, k + j)\; L_m\right)$$

then, by applying the results of Remark 2.4, on page 25, we have the following ℓ inequalities:

$$C_{inf}\, L_m^{2 - D_{\mathcal{W}}} \leqslant -\mathcal{W}\left(((N_b - 1)\, k + j + 1)\; L_m\right) + \mathcal{W}\left((N_b - 1)\, k + j)\; L_m\right)$$

$$C_{inf}\, L_m^{2 - D_{\mathcal{W}}} \leqslant -\mathcal{W}\left(((N_b - 1)\, k + j + 2)\; L_m\right) + \mathcal{W}\left(((N_b - 1)\, k + j + 1)\; L_m\right)$$

.....

$$C_{inf}\, L_m^{2-D_{\mathcal{W}}} \leqslant -\mathcal{W}\left(\left(\left(N_b-1\right)k+j+\ell\right)\, L_m\right)+\mathcal{W}\left(\left(\left(N_b-1\right)k+\ell-1\right)\, L_m\right)\,\cdot$$

Thus, upon summation, we obtain that

$$\ell\, C_{inf}\, L_m^{2-D_{\mathcal{W}}} \leqslant -\mathcal{W}\left(\left(\left(N_b-1\right)k+j+\ell\right)\, L_m\right)+\mathcal{W}\left(\left(\left(N_b-1\right)k+j\right)\, L_m\right)\,\cdot$$

Since $\ell \geqslant \ell^{2-D_{\mathcal{W}}}$ and $|x'-x| = \ell\, L_m$, one deduces the desired result.

□

Remark 2.5. Thus far, no such *reverse Hölder estimates* had been obtained for the Weierstrass function. The fact that they are discrete ones is natural, since the Weierstrass Curve is approximated by a sequence of polygonal prefractal finite graphs. Recall that the countable set of vertices of all of these graphs is dense in the whole Weierstrass Curve.

Corollary 2.14 (**Optimal Hölder Exponent for the Weierstrass Function**)**.**

The local reverse Hölder property of Theorem 2.13, on page 26 – in conjunction with the Hölder condition satisfied by the Weierstrass function (see also [Zyg02], Chapter II, Theorem 4.9, page 47) – shows that the Codimension $2-D_{\mathcal{W}} = -\dfrac{\ln\lambda}{\ln N_b} \in \left]0,1\right[$ *is the best (i.e., optimal) Hölder exponent for the Weierstrass function (as was originally shown, by a completely different method, by G. H. Hardy in [Har16]).*

Note that, as a consequence, since the Hölder exponent is strictly smaller than one, the Weierstrass function $\mathcal{W}$ *is nowhere differentiable.*

Remark 2.6. Indeed, if $\mathcal{W}$ were differentiable at some point $x_0 \in [0,1]$, then it would have to be locally Lipschitz at x_0, and hence, its Hölder exponent at x_0 would be equal to 1, which is impossible.

Corollary 2.15 (**Coming from Property** 2.10, on page 20)**.**

Thanks to Remark 2.4, on page 25, one may now write, for any strictly positive integer m *and any integer* j *in* $\left\{0,\cdots,\left(N_b-1\right)N_b^m-1\right\}$*:*

i. *for the elementary heights:*

$$h_{j-1,j,m} = L_m^{2-D_{\mathcal{W}}}\,\mathcal{O}\left(1\right)\,; \tag{$\mathcal{R}$ 8}$$

ii. *for the elementary quotients:*

$$\frac{h_{j-1,j,m}}{L_m} = L_m^{1-D_{\mathcal{W}}}\,\mathcal{O}\left(1\right)\ , \tag{$\mathcal{R}$ 9}$$

as follows from Remark 2.4, on page 25 above, and where

$$0 < C_{inf} \leqslant \mathcal{O}\left(1\right) \leqslant C_{sup}\,\cdot$$

Corollary 2.16 (**Nonincreasing Sequence of Geometric Angles** (**Coming from Property** 2.10))**.**

For the ***geometric angles*** $\theta_{j-1,j,m}$, $0 \leqslant j \leqslant (N_b - 1)\, N_b^m - 1$, $m \in \mathbb{N}$, *we have the following result:*

$$\tan\theta_{j-1,j,m} = \frac{L_m}{h_{j-1,j,m}}(N_b - 1) > \tan\theta_{j-1,j,m+1}\,,$$

which yields

$$\theta_{j-1,j,m} > \theta_{j-1,j,m+1} \quad \textit{and} \quad \theta_{j-1,j,m+1} \lesssim L_m^{D_{\mathcal{W}}-1}\,.$$

Proof.

i. One simply writes, successively:

$$\begin{aligned}
\tan\theta_{j-1,j,m} &= \frac{L_m}{\left|\mathcal{W}\left(\dfrac{j}{(N_b-1)\,N_b^m}\right) - \mathcal{W}\left(\dfrac{j-1}{(N_b-1)\,N_b^m}\right)\right|} \\
&\geqslant \frac{\lambda\, L_m}{\left|\mathcal{W}\left(\dfrac{j}{(N_b-1)\,N_b^{m+1}}\right) - \mathcal{W}\left(\dfrac{j-1}{(N_b-1)\,N_b^{m+1}}\right)\right|} \\
&= \frac{\lambda\,(N_b-1)\,N_b\, L_{m+1}}{\left|\mathcal{W}\left(\dfrac{j}{(N_b-1)\,N_b^{m+1}}\right) - \mathcal{W}\left(\dfrac{j-1}{(N_b-1)\,N_b^{m+1}}\right)\right|} \\
&= \lambda\,(N_b-1)\,N_b\,\tan\theta_{j-1,j,m+1} \\
&> (N_b-1)\,\tan\theta_{j-1,j,m+1}
\end{aligned}$$

since $\lambda\, N_b > 1$. Then, *i.* holds.

ii. One also has

$$\theta_{j-1,j,m+1} < \arctan\frac{(N_b-1)\,L_m}{h_{j-1,j,m}}\,,$$

where

$$h_{j-1,j,m} = L_m^{2-D_{\mathcal{W}}}\,\mathcal{O}(1) \quad \text{and} \quad C_{inf} \leqslant \mathcal{O}(1) \leqslant C_{sup}\,.$$

This yields

$$\frac{(N_b-1)\,L_m}{h_{j-1,j,m}} = L_m^{D_{\mathcal{W}}-1}\,\mathcal{O}(1) \quad \text{and} \quad (N_b-1)\,C_{inf} \leqslant \mathcal{O}(1) \leqslant (N_b-1)\,C_{sup}\,.$$

Consequently, $\theta_{j-1,j,m+1} \lesssim L_m^{D_{\mathcal{W}}-1}$, as claimed.

□

Corollary 2.17 (**Local Extrema of the Weierstrass Function** (**Coming from Property** 2.10, on page 20))**.**

i. The set of local maxima of the Weierstrass function on the interval $[0,1]$ *is given by*

$$\left\{\left(\frac{(N_b-1)\,k}{N_b^m}, \mathcal{W}\left(\frac{(N_b-1)\,k}{N_b^m}\right)\right) : 0 \leqslant k \leqslant N_b^m - 1,\, m \in \mathbb{N}\right\},$$

and corresponds to the extreme vertices of the polygons at a given step m *(vertices connecting consecutive polygons).*

ii. For odd values of N_b*, the set of local minima of the Weierstrass function on the interval* $[0,1]$ *is given by*

$$\left\{\left(\frac{(N_b-1)\,k+\frac{N_b-1}{2}}{(N_b-1)\,N_b^m}, \mathcal{W}\left(\frac{(N_b-1)\,k+\frac{N_b-1}{2}}{(N_b-1)\,N_b^m}\right)\right) : 0 \leqslant k \leqslant N_b^m - 1,\, m \in \mathbb{N}\right\},$$

and corresponds to the bottom vertices of the polygons at a given step m*.*

Property 2.18 (**Existence of Reentrant Angles**)**.**

i. The initial polygon $\mathcal{P}_0$*, admits* ***reentrant interior angles****, at a vertex* P_j*, with* $0 < j \leqslant N_b - 1$*, in the sense that, with the right-hand rule, according to which angles are measured in a counter-clockwise direction* $\left(\widehat{(P_jP_{j+1}),(P_jP_{j-1})}\right) > \pi$*, in the case when*

$$0 < j \leqslant \frac{N_b-3}{4} \quad or \quad \frac{3\,N_b-1}{4} \leqslant j < N_b - 1$$

(see Figure 7, on page 30), which does not occur for values of $N_b < 7$*.*

The number of reentrant angles is then equal to $2\left[\frac{N_b-3}{4}\right]$*.*

ii. At a given step $m \in \mathbb{N}^\star$*, with the above convention, a polygon* $\mathcal{P}_{m,k}$ *admits reentrant interior angles in the sole cases when* $N_b \geqslant 7$*, at vertices* M_{k+j}*,* $1 \leqslant k \leqslant N_b^m$*,* $0 < j \leqslant N_b - 1$*, as well as in the case when*

$$0 < j \leqslant \frac{N_b-3}{4} \quad or \quad \frac{3\,N_b-1}{4} \leqslant j < N_b - 1\,.$$

The number of reentrant angles is then equal to $2\,N_b^m\left[\frac{N_b-3}{4}\right]$*.*

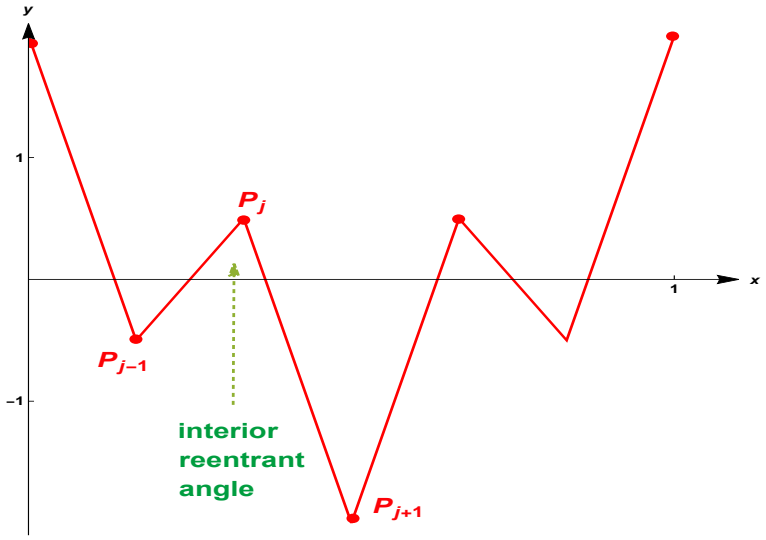

Figure 7: **An interior reentrant angle. Here, $N_b = 7$ and $\lambda = \frac{1}{2}$.**

Proof.

i. Due to the symmetry with respect to the vertical line $x = \frac{1}{2}$ (see Property 2.1, on page 9), one can restrict oneself to the vertices P_j, with $0 < j < \frac{N_b - 1}{2}$.

The initial polygon $\mathcal{P}_0$, admits reentrant interior angles at a vertex P_j, with $j + 1 < \frac{N_b - 1}{2}$, in the case when

$$\left((y'y), \widehat{(P_{j-1}P_j)}\right) > \left((y'y), \widehat{(P_jP_{j+1})}\right) \qquad (\spadesuit) \tag{$\mathcal{R}$ 10}$$

Since

$$P_j = (x_j, y_j) = \left(\frac{j}{N_b - 1}, \mathcal{W}\left(\frac{j}{N_b - 1}\right)\right) = \left(\frac{j}{N_b - 1}, \frac{1}{1 - \lambda} \cos\left(\frac{2\,\pi\, j}{N_b - 1}\right)\right),$$

one has

$$\tan\left((y'y), \widehat{(P_{j-1}P_j)}\right) = \frac{L_0}{\left|\mathcal{W}\left(\frac{j}{N_b - 1}\right) - \mathcal{W}\left(\frac{j-1)}{N_b - 1}\right)\right|}$$

and

$$\tan\left((y'y), \widehat{(P_jP_{j+1})}\right) = \frac{L_0}{\left|\mathcal{W}\left(\frac{j+1}{N_b - 1}\right) - \mathcal{W}\left(\frac{j}{N_b - 1}\right)\right|},$$

where $L_0 = \frac{1}{N_b - 1}$.

Therefore, condition ($\mathcal{R}$10) – ($\spadesuit$) above corresponds to the case when

$$\left|\mathcal{W}\left(\frac{j+1}{N_b - 1}\right) - \mathcal{W}\left(\frac{j}{N_b - 1}\right)\right| > \left|\mathcal{W}\left(\frac{j}{N_b - 1}\right) - \mathcal{W}\left(\frac{j-1}{N_b - 1}\right)\right|,$$

i.e.,

$$\left|\cos\left(\frac{2\,\pi\,(j+1)}{N_b-1}\right)-\cos\left(\frac{2\,\pi\,j}{N_b-1}\right)\right| > \left|\cos\left(\frac{2\,\pi\,j}{N_b-1}\right)-\cos\left(\frac{2\,\pi\,(j-1)}{N_b-1}\right)\right|,$$

or, equivalently,

$$\left|2\,\sin\frac{\pi}{N_b-1}\,\sin\left(\frac{\pi\,(2\,j+1)}{N_b-1}\right)\right| > \left|2\,\sin\frac{\pi}{N_b-1}\,\sin\left(\frac{\pi\,(2\,j-1)}{N_b-1}\right)\right|,$$

and thus happens if

$$\left|\sin\left(\frac{\pi\,(2\,j+1)}{N_b-1}\right)\right| > \left|\sin\left(\frac{\pi\,(2\,j-1)}{N_b-1}\right)\right|.$$

Since

$$0 < \frac{\pi\,(2\,j-1)}{N_b-1} < \frac{\pi\,(2\,j+1)}{N_b-1} < \pi\,,$$

we conclude that condition ($\mathcal{R}10$) – (♠), on page 30, occurs if

$$0 < \pi\,(2\,j-1)N_b - 1 < \frac{\pi\,(2\,j+1)}{N_b-1} \leqslant \frac{\pi}{2}\,,$$

i.e., if $0 < j \leqslant \dfrac{N_b-3}{4}$.

For vertices P_j, with $\dfrac{N_b+1}{2} < j < N_b-1$, the result is obtained thanks to the aforementioned symmetry. The initial polygon $\mathcal{P}_0$, admits **reentrant interior angles** at a vertex P_j in the case when $\dfrac{3\,N_b-1}{4} \leqslant j < N_b-1$.

ii. The result is obtained by strong induction on the integer m. We restrict ourselves to the values $N_b \geqslant 7$, and consider j in $\left\{0,\cdots,\left[\dfrac{N_b-3}{4}\right]\right\}$.

We claim that the result is satisfied at *the initial step* $m = 1$. Indeed, as was already encountered in the proof of Property 2.10, on page 20, for any integer k in $\{0,\cdots,N_b-1\}$, we have that

$$\left|\mathcal{W}\left(\frac{k\,(N_b-1)+j+1}{(N_b-1)\,N_b}\right)-\mathcal{W}\left(\frac{j}{(N_b-1)\,N_b}\right)\right| = \left|(1+\lambda)\left\{\mathcal{W}\left(\frac{j+1}{N_b-1}\right)-\mathcal{W}\left(\frac{j}{N_b-1}\right)\right\}\right|$$

and

$$\left|\mathcal{W}\left(\frac{k\,(N_b-1)+j}{(N_b-1)\,N_b}\right)-\mathcal{W}\left(\frac{j-1}{(N_b-1)\,N_b}\right)\right| = \left|(1+\lambda)\left\{\mathcal{W}\left(\frac{j}{N_b-1}\right)-\mathcal{W}\left(\frac{j-1}{N_b-1}\right)\right\}\right|.$$

Thus,

$$\frac{\tan\theta_{k\,(N_b-1)+j-1,k\,(N_b-1)+j,1}}{\tan\theta_{k\,(N_b-1)+j,k\,(N_b-1)+j+1,1}} = \frac{\left|\mathcal{W}\left(\frac{k\,(N_b-1)+j+1}{(N_b-1)\,N_b}\right)-\mathcal{W}\left(\frac{k\,(N_b-1)+j}{(N_b-1)\,N_b}\right)\right|}{\left|\mathcal{W}\left(\frac{k\,(N_b-1)+j}{(N_b-1)\,N_b}\right)-\mathcal{W}\left(\frac{k\,(N_b-1)+j-1}{(N_b-1)\,N_b}\right)\right|}$$

$$= \frac{\left|\mathcal{W}\left(\frac{j+1}{N_b-1}\right)-\mathcal{W}\left(\frac{j-1}{N_b-1}\right)\right|}{\left|\mathcal{W}\left(\frac{j}{N_b-1}\right)-\mathcal{W}\left(\frac{j-1}{N_b-1}\right)\right|} > 1\,,$$

which implies that

$$\theta_{k\,(N_b-1)+j-1,k\,(N_b-1)+j,1} > \theta_{k\,(N_b-1)+j,k\,(N_b-1)+j+1,1}$$

and yields the existence of an interior reentrant angle at the vertex

$$\left(\frac{k\,(N_b-1)+j}{(N_b-1)\,N_b},\mathcal{W}\left(\frac{k\,(N_b-1)+j}{(N_b-1)\,N_b}\right)\right).$$

Let us now assume that, up to a given step $m \geqslant 1$, there is a reentrant interior angle at any vertex

$$\left(\frac{k\,(N_b-1)+j}{(N_b-1)\,N_b^{m-1}},\mathcal{W}\left(\frac{k\,(N_b-1)+j}{(N_b-1)\,N_b^{m-1}}\right)\right) \quad , \quad \text{with } 0 \leqslant k \leqslant N_b^{m-1}-1\,.$$

We then want to prove that there is a reentrant interior angle at any vertex

$$\left(\frac{k\,(N_b-1)+j}{(N_b-1)\,N_b^{m}},\mathcal{W}\left(\frac{k\,(N_b-1)+j}{(N_b-1)\,N_b^{m}}\right)\right) \quad , \quad \text{with } 0 \leqslant k \leqslant N_b^{m}-1\,.$$

As was the case in the proof of Property 2.10 (page 20), in order to be able to use the induction hypothesis, we express any integer k in $\{0,\cdots,N_b^m-1\}$ in the following form:

$$k = \tilde{k} + i\,N_b^{m-1} \quad , \quad 0 \leqslant \tilde{k} \leqslant N_b^{m-1}-1 \quad , \quad 0 \leqslant i \leqslant N_b-1\,. \tag{$\mathcal{R}$ 11}$$

Thus,

$$\mathcal{W}\left(\frac{k\,(N_b-1)+j+1}{(N_b-1)\,N_b^m}\right)-\mathcal{W}\left(\frac{j}{(N_b-1)\,N_b^m}\right) = \lambda\left(\mathcal{W}\left(\frac{\tilde{k}\,(N_b-1)+j+1}{(N_b-1)\,N_b^{m-1}}\right)-\mathcal{W}\left(\frac{\tilde{k}\,(N_b-1)+j}{(N_b-1)\,N_b^{m-1}}\right)\right)$$
$$-2\,\sin\left(\frac{\pi}{(N_b-1)\,N_b^{m-1}}\right)\sin\left(\frac{\left(2\,(N_b-1)\,\tilde{k}+2\,j+1\right)\pi}{(N_b-1)\,N_b^{m-1}}\right), \tag{$\mathcal{R}$ 12}$$

and

$$\mathcal{W}\left(\frac{k\,(N_b-1)+j}{(N_b-1)\,N_b^m}\right)-\mathcal{W}\left(\frac{j-1}{(N_b-1)\,N_b^m}\right) = \lambda\left(\mathcal{W}\left(\frac{\tilde{k}\,(N_b-1)+j}{(N_b-1)\,N_b^{m-1}}\right)-\mathcal{W}\left(\frac{\tilde{k}\,(N_b-1)+j-1}{(N_b-1)\,N_b^{m-1}}\right)\right)$$
$$-2\,\sin\left(\frac{\pi}{(N_b-1)\,N_b^{m-1}}\right)\sin\left(\frac{\left(2\,(N_b-1)\,\tilde{k}+2\,j-1\right)\pi}{(N_b-1)\,N_b^{m-1}}\right). \tag{$\mathcal{R}$ 13}$$

In light of Property 2.10, on page 20, given such an integer k - and hence also, $\tilde{k}$ and j – and since

$$0 \leqslant j \leqslant \left[\frac{N_b-3}{4}\right] \leqslant \frac{N_b-1}{2}\,,$$

the only configuration to be considered corresponds to the case when

$$\theta_{\tilde{k}\,(N_b-1)+j-1,\tilde{k}\,(N_b-1)+j,m-1} > \theta_{\tilde{k}\,(N_b-1)+j,\tilde{k}\,(N_b-1)+j+1,m-1}$$

and

$$\mathcal{W}\left(\frac{\tilde{k}\,(N_b-1)+j-1}{(N_b-1)\,N_b^{m-1}}\right)-\mathcal{W}\left(\frac{j}{(N_b-1)\,N_b^{m-1}}\right)>0 \quad , \quad \mathcal{W}\left(\frac{\tilde{k}\,(N_b-1)+j}{(N_b-1)\,N_b^{m-1}}\right)-\mathcal{W}\left(\frac{\tilde{k}\,(N_b-1)+j+1}{(N_b-1)\,N_b^{m-1}}\right)>0\,\cdot$$

Then,

$$\tan\theta_{\tilde{k}\,(N_b-1)+j-1,\tilde{k}\,(N_b-1)+j,m-1} > \tan\theta_{\tilde{k}\,(N_b-1)+j,\tilde{k}\,(N_b-1)+j+1,m-1}\,;$$

i.e.,

$$\frac{L_{m-1}}{\left|\mathcal{W}\left(\frac{\tilde{k}\,(N_b-1)+j}{(N_b-1)\,N_b^{m-1}}\right)-\mathcal{W}\left(\frac{\tilde{k}\,(N_b-1)+j-1}{(N_b-1)\,N_b^{m-1}}\right)\right|} > \frac{L_{m-1}}{\left|\mathcal{W}\left(\frac{\tilde{k}\,(N_b-1)+j+1}{(N_b-1)\,N_b^{m-1}}\right)-\mathcal{W}\left(\frac{\tilde{k}\,(N_b-1)+j}{(N_b-1)\,N_b^{m-1}}\right)\right|}\,,$$

which yields

$$\left|\mathcal{W}\left(\frac{\tilde{k}\,(N_b-1)+j+1}{(N_b-1)\,N_b^{m-1}}\right)-\mathcal{W}\left(\frac{\tilde{k}\,(N_b-1)+j}{(N_b-1)\,N_b^{m-1}}\right)\right| > \left|\mathcal{W}\left(\frac{\tilde{k}\,(N_b-1)+j}{(N_b-1)\,N_b^{m-1}}\right)-\mathcal{W}\left(\frac{\tilde{k}\,(N_b-1)+j-1}{(N_b-1)\,N_b^{m-1}}\right)\right|\,,$$

or, equivalently,

$$\mathcal{W}\left(\frac{\tilde{k}\,(N_b-1)+j}{(N_b-1)\,N_b^{m-1}}\right)-\mathcal{W}\left(\frac{\tilde{k}\,(N_b-1)+j+1}{(N_b-1)\,N_b^{m-1}}\right) > \mathcal{W}\left(\frac{\tilde{k}\,(N_b-1)+j-1}{(N_b-1)\,N_b^{m-1}}\right)-\mathcal{W}\left(\frac{\tilde{k}\,(N_b-1)+j}{(N_b-1)\,N_b^{m-1}}\right)\,.$$

The *strong induction hypothesis*, which ensures the existence of a reentrant interior angle at the vertex

$$\left(\frac{(N_b-1)\,\tilde{k}+j}{(N_b-1)\,N_b^{m-2}}, \mathcal{W}\left(\frac{(N_b-1)\,\tilde{k}+j}{(N_b-1)\,N_b^{m-2}}\right)\right)\,,$$

requires, in conjunction with

$$\mathcal{W}\left(\frac{\tilde{k}\,(N_b-1)+j}{(N_b-1)\,N_b^{m-2}}\right)-\mathcal{W}\left(\frac{\tilde{k}\,(N_b-1)+j+1}{(N_b-1)\,N_b^{m-2}}\right) > \mathcal{W}\left(\frac{\tilde{k}\,(N_b-1)+j-1}{(N_b-1)\,N_b^{m-2}}\right)-\mathcal{W}\left(\frac{\tilde{k}\,(N_b-1)+j}{(N_b-1)\,N_b^{m-2}}\right)\,,$$

that

$$\sin\left(\frac{\pi\,(2\,\tilde{k}\,(N_b-1)+2\,j+1)}{(N_b-1)\,N_b^{m-2}}\right) > \sin\left(\frac{\pi\,(2\,\tilde{k}\,(N_b-1)+2\,j-1)}{(N_b-1)\,N_b^{m-2}}\right),$$

which corresponds to

$$0 < \frac{\pi\,(2\,\tilde{k}\,(N_b-1)+2\,j+1)}{(N_b-1)\,N_b^{m-2}} < \frac{\pi\,(2\,\tilde{k}\,(N_b-1)+2\,j-1)}{(N_b-1)\,N_b^{m-2}} \leqslant \frac{\pi}{2}$$

and, as a matter of fact, ensures that

$$0 < \frac{\pi\,(2\,\tilde{k}\,(N_b-1)+2\,j+1)}{(N_b-1)\,N_b^{m-1}} < \frac{\pi\,(2\,\tilde{k}\,(N_b-1)+2\,j-1)}{(N_b-1)\,N_b^{m-21}} \leqslant \frac{\pi}{2\,N_b} < \frac{\pi}{2}\,.$$

One then has the following inequality:

$$\lambda\left(\mathcal{W}\left(\frac{\tilde{k}\,(N_b-1)+j}{(N_b-1)\,N_b^{m-1}}\right)-\mathcal{W}\left(\frac{\tilde{k}\,(N_b-1)+j+1}{(N_b-1)\,N_b^{m-1}}\right)\right)+2\,\sin\left(\frac{\pi}{(N_b-1)\,N_b^{m-1}}\right)\sin\left(\frac{\pi\,(2\,\tilde{k}\,(N_b-1)+2\,j+1)}{(N_b-1)\,N_b^{m-1}}\right)$$

$$> \lambda\left(\mathcal{W}\left(\frac{\tilde{k}\,(N_b-1)+j-1}{(N_b-1)\,N_b^{m-1}}\right)-\mathcal{W}\left(\frac{\tilde{k}\,(N_b-1)+j}{(N_b-1)\,N_b^{m-1}}\right)\right)+2\,\sin\left(\frac{\pi}{(N_b-1)\,N_b^{m-1}}\right)\sin\left(\frac{\pi\,(2\,\tilde{k}\,(N_b-1)+2\,j-1)}{(N_b-1)\,N_b^{m-1}}\right).$$

Hence,

$$\tan\theta_{\tilde{k}\,(N_b-1)+j-1,\tilde{k}\,(N_b-1)+j,m}$$

$$||$$

$$\frac{L_m}{\left|\mathcal{W}\left(\frac{\tilde{k}\,(N_b-1)+j}{(N_b-1)\,N_b^{m}}\right)-\mathcal{W}\left(\frac{\tilde{k}\,(N_b-1)+j-1}{(N_b-1)\,N_b^{m}}\right)\right|}$$

$$= \frac{L_m}{\left|\lambda\left(\mathcal{W}\left(\frac{\tilde{k}\,(N_b-1)+j}{(N_b-1)\,N_b^{m}}\right)-\mathcal{W}\left(\frac{\tilde{k}\,(N_b-1)+j-1}{(N_b-1)\,N_b^{m}}\right)\right)-2\,\sin\left(\frac{\pi}{(N_b-1)\,N_b^{m-1}}\right)\sin\left(\frac{\pi\,(2\,\tilde{k}\,(N_b-1)+2\,j-1)}{(N_b-1)\,N_b^{m-1}}\right)\right|}$$

$$= \frac{L_m}{\lambda\left(\mathcal{W}\left(\frac{\tilde{k}\,(N_b-1)+j-1}{(N_b-1)\,N_b^{m}}\right)-\mathcal{W}\left(\frac{j}{(N_b-1)\,N_b^{m}}\right)\right)+2\,\sin\left(\frac{\pi}{(N_b-1)\,N_b^{m-1}}\right)\sin\left(\frac{\pi\,(2\,\tilde{k}\,(N_b-1)+2\,j-1)}{(N_b-1)\,N_b^{m-1}}\right)}$$

$$> \frac{L_m}{\lambda\left(\mathcal{W}\left(\frac{\tilde{k}\,(N_b-1)+j}{(N_b-1)\,N_b^{m}}\right)-\mathcal{W}\left(\frac{\tilde{k}\,(N_b-1)+j+1}{(N_b-1)\,N_b^{m}}\right)\right)+2\,\sin\left(\frac{\pi}{(N_b-1)\,N_b^{m-1}}\right)\sin\left(\frac{\pi\,(2\,\tilde{k}\,(N_b-1)+2\,j+1)}{(N_b-1)\,N_b^{m-1}}\right)}$$

$$= \tan\theta_{\tilde{k}\,(N_b-1)+j,\tilde{k}\,(N_b-1)+j+1,m}\,,$$

which yields the expected result. Namely,

$$\theta_{\tilde{k}\,(N_b-1)+j-1,\tilde{k}\,(N_b-1)+j,m} > \theta_{\tilde{k}\,(N_b-1)+j,k\,(N_b-1)+j+1,m}\,;$$

i.e., the presence of a reentrant angle at the j^{th} vertex of the polygon $\mathcal{P}_{m,k}$.

The result in the remaining case $\dfrac{3\,N_b-1}{4} \leqslant j < N_b-1$ can be obtained in an entirely similar way. It corresponds to the cases when

$$\theta_{k\,(N_b-1)+j-1,\tilde{k}\,(N_b-1)+j,mc} < \theta_{k\,(N_b-1)+j,\tilde{k}\,(N_b-1)+j+1,m}$$

and

$$\mathcal{W}\left(\frac{k\,(N_b-1)+j-1}{(N_b-1)\,N_b^m}\right)-\mathcal{W}\left(\frac{k\,(N_b-1)+j}{(N_b-1)\,N_b^m}\right)<0 \quad , \quad \mathcal{W}\left(\frac{k\,(N_b-1)+j}{(N_b-1)\,N_b^m}\right)-\mathcal{W}\left(\frac{k\,(N_b-1)+j+1}{(N_b-1)\,N_b^m}\right)<0\,.$$

Therefore, the shape of the initial polygon $\mathcal{P}_0$ governs the shape of any polygon $\mathcal{P}_{m,k}$, $0 \leqslant k \leqslant N_b^m$, which, if $N_b \geqslant 7$, admits reentrant interior angles at vertices $M_{(N_b-1)\,k+j}$, $0 \leqslant k \leqslant N_b^m - 1$, $0 < j \leqslant N_b - 1$, in the case when

$$0 < j \leqslant \frac{N_b-3}{4} \quad \text{or} \quad \frac{3\,N_b-1}{4} \leqslant j < N_b - 1\,.$$

This concludes the proof of Property 2.18 given on page 29.

□

Definition 2.6 (**Self–Shape Similarity of the Weierstrass Curve**).

We will say that the Weierstrass Curve – as the two-dimensional Hausdorff and uniform limit curve of a sequence of polygonal prefractals, which satisfy Property 2.10, on page 20 and Property 2.18, on page 29 – has *self–shape similarity*, in the sense that the shape of the initial polygon $\mathcal{P}_0$ governs the shape of all the polygons $\mathcal{P}_{m,k}$, with $0 \leqslant k \leqslant N_b^m$, at any step m of the prefractal approximation process. This *self–shape similarity property* is apparent in Figure 1, on page 11, Figure 2, on page 12, and Figure 3, on page 13. As for the existence of reentrant angles, it can be observed on the first two graphs of Figure 3, on page 13, in the case when $N_b = 7$.

3 Iterated Fractal Drums and Tubular Neighborhoods

In the case of classical fractals, and when the associated geometry allows it, the values of the Complex Dimensions are obtained by studying the oscillations of a small neighborhood of the boundary, i.e., of a tubular neighborhood of the fractal, where points are located within an epsilon distance from any edge; see, e.g., [LRŽ17a], [LRŽ17b], [LRŽ18]. In the case of our fractal Weierstrass Curve $\Gamma_{\mathcal{W}}$, which is, also, the limit of the sequence of (polygonal) prefractal graphs $(\Gamma_{\mathcal{W}})_{m\,\in\,\mathbb{N}}$, it is natural – and consistent with the result of Property 3.9, on page 59 below – to envision the tubular neighborhood of $\Gamma_{\mathcal{W}}$ as the limit of the (obviously convergent) sequence $\left(\mathcal{D}\left(\Gamma_{\mathcal{W}_m},\varepsilon_m^m\right)\right)_{m\,\in\,\mathbb{N}}$ of ε_m^m–neighborhoods of $\Gamma_{\mathcal{W}_m}$, where $\varepsilon = \left(\varepsilon_m^m\right)_{m\,\in\,\mathbb{N}}$ is a (suitable) *infinitesimal* – the *cohomology infinitesimal* – as introduced in Definition 3.1, on page 37 below. The cohomology infinitesimal is completely determined by the geometric characteristics of the fractal curve $\Gamma_{\mathcal{W}}$ (or of the associated iterated fractal drum).

We note that, in a sense, the above description amounts to using a sequence of what we call *Weierstrass Iterated Fractal Drums* (in short, Weierstrass IFDs), by analogy with the *Relative Fractal Drums* (RFDs), for instance, in the case of the Cantor Staircase, in [LRŽ17b], Section 5.5.4, as well as in [LRŽ17c] and in [LRŽ18]. In our present setting, the Weierstrass IFDs – i.e., the sets $\mathcal{D}\left(\Gamma_{\mathcal{W}_m},\varepsilon_m^m\right)$, for $m \in \mathbb{N}$ sufficiently large – contain the Weierstrass Curve $\Gamma_{\mathcal{W}}$, and are sufficiently close to $\Gamma_{\mathcal{W}}$, so that we can expect their Complex Dimensions to be the same.

For this purpose, one thus requires fractal tube formulas for the sequence of prefractal graphs which converge to the Weierstrass Curve; i.e., here, the area of a two–sided ε_m^m–neighborhood of each prefractal approximation (with $m \in \mathbb{N}^\star$ sufficiently large), which is expected to be of the following form, in the case of simple Complex Dimensions:

$$\sum_{\omega \text{ Complex Dimension}} c_\omega \left(\varepsilon_m^m\right)^{2-\omega} \quad , \quad c_\omega \in \mathbb{C}\,, \qquad (\star\star)$$

where, for any Complex Dimension ω, c_ω is directly expressed in terms of the residue at ω of the effective tube zeta function $\widetilde{\zeta}_\omega^e$ (or of the effective distance zeta function ζ_ω^e).

More specifically, consistent with the corresponding results in [LRŽ17a], [LRŽ17b] and [LRŽ18],

$$c_\omega = \operatorname{res}\left(\widetilde{\zeta}_\omega^e, \omega\right) = \frac{1}{2-\omega} \operatorname{res}\left(\zeta_\omega^e, \omega\right) .$$

We shall proceed as in [LP06], by the second author and E. P. J. Pearse, as well as in the later paper [LPW11], by the same authors and S. Winter (see also [LvF00], §10.3, or [LvF06], §12.1). Note that these two papers were written prior to the development of the higher–dimensional theory of Complex Dimensions and fractal tube formulas, by the second author, G. Radunovic and D. Zubrinic, in the book [LRŽ17b] and in a series of accompanying papers by the same authors, including [LRŽ17a], [LRŽ18].

The proper fractal zeta function to be used for this purpose, called the distance zeta function, was discovered by the second author in 2009, while the equivalent, and equally convenient, tube zeta function, depending on the problem at hand, was later introduced by the aforementioned authors in the above references. Both types of fractal zeta functions are connected via an explicit functional equation.

Consequently, once we have obtained the desired fractal tube formula for the Weierstrass IFD, we will be able to use extensions of the general results and methods of the higher–dimensional theory of Complex Dimensions in [LRŽ17a], [LRŽ17b] and [LRŽ18] in order to deduce the fractal zeta functions of the Weierstrass IFD: first, the so–called *effective* tube zeta function and then, via the aforementioned functional equation connecting those two zeta functions, the *effective distance zeta function*. We will then conclude from the expression of either fractal zeta function (since $D_{\mathcal{W}} < 2$, they yield the same result here) the values of the possible Complex Dimensions of the Weierstrass IFD. For many of those Complex Dimensions, including the principal ones, in the terminology of [LRŽ17b] (i.e., those with real parts equal to the maximal real part $D_{\mathcal{W}} < 2$), we will also be able to determine that they are *actual* (and simple) Complex Dimensions of the Weierstrass IFD – that is, simple poles of the tube zeta function, or, equivalently, of the distance zeta function.

We note that the only possible exceptions to the latter statement would be the potential Complex Dimensions with real part equal to 1 (except for 1 itself), some (or all) of which could have a vanishing residue; further theoretical or numerical work will be needed in order to deal with this last remaining issue.

Notation 8 (**Euclidean Distance**)**.**

In the sequel, we denote by d the Euclidean distance on $\mathbb{R}^2$.

Our results on fractal cohomology obtained in [DL22c] have highlighted the part played by specific threshold values for the number $\varepsilon > 0$ at any step $m \in \mathbb{N}$ of the prefractal graph approximation; namely, the m^{th} *cohomology infinitesimal* introduced in Definition 3.1, on page 37 just below.

Definition 3.1 (m^{th} Cohomology Infinitesimal).

From now on, given any $m \in \mathbb{N}$, we will call m^{th} *cohomology infinitesimal* the number $\varepsilon_m^m > 0$ which also corresponds to the elementary horizontal length introduced in part *i.* in Definition 2.4, on page 15; i.e., $\varepsilon_m^m = (\varepsilon_m)^m = \dfrac{1}{N_b - 1}\dfrac{1}{N_b^m}$.

Observe that, clearly, ε_m itself – and not just ε_m^m – depends on m.

In addition, since $N_b > 1$, ε_m^m satisfies the following asymptotic behavior,

$$\varepsilon_m^m \to 0\,, \text{ as } m \to \infty,$$

which, naturally, results in the fact that the larger m, the smaller ε_m^m. It is for this reason that we call ε_m^m – or rather, the *infinitesimal sequence* $\left(\varepsilon_m^m\right)_{m=0}^{\infty}$ of positive numbers tending to zero as $m \to \infty$, with $\varepsilon_m^m = (\varepsilon_m)^m$, for each $m \in \mathbb{N}$ – an *infinitesimal*. Note that this m^{th} cohomology infinitesimal is the one naturally associated to the scaling relation of Property 2.6, on page 16.

In the sequel, it is also useful to keep in mind that the sequence of positive numbers $(\varepsilon_m)_{m=0}^{\infty}$ itself satisfies

$$\varepsilon_m \sim \frac{1}{N_b}\,, \text{ as } m \to \infty \;;$$

i.e., $\varepsilon_m \to \dfrac{1}{N_b}$, as $m \to \infty$. In particular, $\varepsilon_m \not\to 0$, as $m \to \infty$, but, instead, ε_m tends to a strictly positive and finite limit.

Remark 3.1 (**Addressing Numerical Estimates**).

From a practical point of view, an important question is the value of the ratio

$$\frac{\text{Cohomology infinitesimal}}{\text{Maximal height}} = \frac{\varepsilon_m^m}{h_m} \;;$$

see relation ($\mathcal{R}6$), on page 15.

Thanks to the estimates given in relation ($\mathcal{R}9$), on page 27, we have that

$$\frac{\varepsilon_m^m}{h_m} = L_m^{1-D_{\mathcal{W}}}\,\mathcal{O}(1) = \varepsilon_m^{m(1-D_{\mathcal{W}})}\,\mathcal{O}(1)\;,$$

with

$$0 < C_{inf} \leqslant \mathcal{O}(1) \leqslant C_{sup}\,.$$

Given $q \in \mathbb{N}^{\star}$, we then have

$$\frac{1}{10^q}\, C_{inf} \leqslant \frac{\varepsilon_m^m}{h_m} \leqslant \frac{1}{10^q}\, C_{sup}$$

when

$$\frac{C_{inf}}{10^q} \leqslant e^{(1-D_{\mathcal{W}})\,\ln L_m} \leqslant \frac{C_{sup}}{10^q}\,,$$

or, equivalently, when

$$-\frac{1}{\ln N_b}\,\ln\left((N_b-1)\left(\frac{C_{sup}}{10^q}\right)^{\frac{1}{1-D_{\mathcal{W}}}}\right) \leqslant m \leqslant -\frac{1}{\ln N_b}\,\ln\left((N_b-1)\left(\frac{C_{inf}}{10^q}\right)^{\frac{1}{1-D_{\mathcal{W}}}}\right).$$

Numerical values for $N_b = 3$ and $\lambda = \dfrac{1}{2}$ yield:

i. For $q = 1$: $2 \leqslant m \leqslant 3$.

ii. For $q = 2$: $7 \leqslant m \leqslant 9$.

iii. For $q = 3$: $13 \leqslant m \leqslant 15$.

Hence, when m increases, the ratio decreases, and tends to 0. This numerical – but very practical and explicit argument – also applies to our forthcoming neighborhoods, of width equal to the cohomology infinitesimal.

Definition 3.2 (**Iterated Fractal Drums (IFDs)**).

Let us consider a fractal curve $\mathcal{F} \subset \mathbb{R}^2$, obtained by means of a suitable IFS $\mathcal{T}_{\mathcal{F}}$ (consisting, in particular, of a family of C^{∞} maps from $\mathbb{R}^2$ to $\mathbb{R}^2$). For each $m \in \mathbb{N}$, we denote by $\mathcal{F}_m$ the m^{th} prefractal approximation to the fractal $\mathcal{F}$. We restrict ourselves to the case when there exists a natural scaling relation associated to the sequence $\left(\Gamma_{\mathcal{F}_m}\right)_{m\in\mathbb{N}}$, involving a sequence of elementary lengths (or cohomology infinitesimals) $\left(\varepsilon_{m,\mathcal{F}}^m\right)_{m\in\mathbb{N}}$, and, as in Definition 3.1, on page 37 above.

We then call *Iterated Fractal Drum* (in short, *IFD*), and denote by $\mathcal{F}^{\mathcal{I}}$, the sequence of ordered pairs $\left(\mathcal{F}_m, \varepsilon_{m,\mathcal{F}}^m\right)_{m\in\mathbb{N}}$, where, for each $m \in \mathbb{N}$, $\mathcal{F}_m$ is the m^{th} prefractal (graph) approximation associated with the fractal $\mathcal{F}$.

Definition 3.3 (**Weierstrass Iterated Fractal Drum (Weierstrass IFD)**).

We call *Weierstrass Iterated Fractal Drum* (in short, *Weierstrass IFD*), and denote by $\Gamma_{\mathcal{W}}^{\mathcal{I}}$, the sequence of ordered pairs $\left(\Gamma_{\mathcal{W}_m}, \varepsilon_m^m\right)_{m\in\mathbb{N}}$ where, for each $m \in \mathbb{N}$, $\Gamma_{\mathcal{W}_m}$ is the m^{th} prefractal approximation to the Weierstrass Curve $\Gamma_{\mathcal{W}}$, as introduced in Definition 2.2, on page 10, and where ε_m^m is the m^{th} cohomology infinitesimal, as introduced in Definition 3.1, on page 37 above. Note that the m^{th} prefractal graph approximation (viewed as an oriented curve) determines the m^{th} prefractal curve (viewed as an oriented polygonal curve), and conversely. Indeed, the line segments of which the latter polygonal curve is comprised are nothing but the edges of the former prefractal graph.

In the sequel, $\left(\varepsilon_m^m\right)_{m\in\mathbb{N}}$ stands for the cohomology infinitesimal, as introduced in Definition 3.1, on page 37 above.

Definition 3.4 (**(m, ε_m^m)-Upper and Lower Neighborhoods**).

Given $m \in \mathbb{N}$, and a point $M \in \mathbb{R}^2$, we denote by $d\left(M, \Gamma_{\mathcal{W}_m}\right)$ the distance from M to $\Gamma_{\mathcal{W}_m}$. Then, for any sufficiently large m (so that ε_m^m be a sufficiently small positive number), we introduce:

i. The (m, ε_m^m)-Upper Neighborhood of the m^{th} prefractal approximation $\Gamma_{\mathcal{W}_m}$:

$$\mathcal{D}^+\left(\Gamma_{\mathcal{W}_m}, \varepsilon_m^m\right) = \left\{M = (x, y) \in \mathbb{R}^2, y \geqslant \mathcal{W}(x) \text{ and } d\left(M, \Gamma_{\mathcal{W}_m}\right) \leqslant \varepsilon_m^m\right\};$$

ii. The (m, ε_m^m)-Lower Neighborhood of the m^{th} prefractal approximation $\Gamma_{\mathcal{W}_m}$:

$$\mathcal{D}^-\left(\Gamma_{\mathcal{W}_m}, \varepsilon_m^m\right) = \left\{M = (x, y) \in \mathbb{R}^2, y \leqslant \mathcal{W}(x) \text{ and } d\left(M, \Gamma_{\mathcal{W}_m}\right) \leqslant \varepsilon_m^m\right\}.$$

Definition 3.5 (**(m, ε_m^m)–Neighborhood**).

Given $m \in \mathbb{N}$ sufficiently large (as in Definition 3.4, on page 39 just above), along with $\mathcal{D}^-\left(\Gamma_{\mathcal{W}_m}, \varepsilon_m^m\right)$ and $\mathcal{D}^+\left(\Gamma_{\mathcal{W}_m}, \varepsilon_m^m\right)$, we define the (m, ε_m^m)–Neighborhood as the union of the upper and lower ones, as follows:

$$\mathcal{D}\left(\Gamma_{\mathcal{W}_m}, \varepsilon_m^m\right) = \mathcal{D}^-\left(\Gamma_{\mathcal{W}_m}, \varepsilon_m^m\right) \cup \mathcal{D}^+\left(\Gamma_{\mathcal{W}_m}, \varepsilon_m^m\right).$$

Definition 3.6 (**Left–Side and Right–Side (m, ε_m^m)–Neighborhoods**).

Given $m \in \mathbb{N}$ sufficiently large, we introduce:

i. the Left–Side (m, ε_m^m)–Neighborhood of the m^{th} prefractal approximation $\Gamma_{\mathcal{W}_m}$ as

$$\mathcal{D}_{\text{Left}}\left(\Gamma_{\mathcal{W}_m}, \varepsilon_m^m\right) = \left\{M = (x, y) \in \left[0, \frac{1}{2}\right] \times \mathbb{R}, d\left(M, \Gamma_{\mathcal{W}_m}\right) \leqslant \varepsilon_m^m\right\};$$

ii. the Right–Side (m, ε_m^m)–Neighborhood of the m^{th} prefractal approximation $\Gamma_{\mathcal{W}_m}$ as

$$\mathcal{D}_{\text{Right}}\left(\Gamma_{\mathcal{W}_m}, \varepsilon_m^m\right) = \left\{M = (x, y) \in \left[\frac{1}{2}, 1\right] \times \mathbb{R}, d\left(M, \Gamma_{\mathcal{W}_m}\right) \leqslant \varepsilon_m^m\right\}.$$

Those neighborhoods are symmetric with respect to the vertical line $x = \dfrac{1}{2}$; see Figure 5, on page 17, and Figure 13, on page 46. They constitute, in a sense, a partition of the whole tubular neighborhood.

Notation 9 (**Integer to Cohomology Infinitesimal Map**).

We hereafter introduce the map

$$\varepsilon_m^m \mapsto m(\varepsilon_m^m) = \left[-\ln_{N_b}\left(\left(N_b - 1\right)\varepsilon_m^m\right)\right] = \left[m(\varepsilon_m^m)\right] + \left\{m(\varepsilon_m^m)\right\},$$

where $[\cdot]$ and $\{\cdot\}$ respectively denote the integer and fractional parts.

For notational simplicity, we temporarily set $x = m(\varepsilon_m^m) = -\ln_{N_b}\left((N_b-1)\,\varepsilon_m^m\right)$.

Previous works give a very unfriendly expression for the absolute value of the *elementary heights*, $\left|h_{j,m}\right|$, for $\dfrac{3\,N_b-1}{4} \leqslant j < N_b-1$, and $(i_1,\cdots,i_m) \in \{0,\cdots,N_b-1\}^m$, as

$$\left|h_{j,m}\right| = \left|\lambda^m\,\left(y_{j+1}-y_j\right) - 2\sum_{k=1}^{m}\lambda^{m-k}\,\sin\left(\frac{\pi}{N_b^{k+1}\,(N_b-1)}\right)\sin\left(\frac{\pi\,(2\,j+1)}{N_b^{k+1}\,(N_b-1)} + 2\,\pi\sum_{q=0}^{k}\frac{i_{m-q}}{N_b^{k-q}}\right)\right| \,.$$

Although it is sufficient to compute the Minkowski dimension of the Curve, one also requires, in the present work, an explicit expression for the elementary lengths L_m, $m \in \mathbb{N}^\star$.

Accordingly, one has

$$N_b^m = N_b^{[x]} = N_b^{x-\{x\}} \quad , \quad N_b^{-m} = N_b^{\{x\}-x}\,,$$

$$L_m = \frac{1}{(N_b-1)\,N_b^m} = \frac{1}{N_b-1}\,N_b^{\{x\}-x}\,,$$

$$-\left([x]+\{x\}\right)\,\ln N_b = \ln\left((N_b-1)\,\varepsilon_m^m\right) \quad , \quad e^{-([x]+\{x\})\,\ln N_b} = (N_b-1)\,\varepsilon_m^m \quad , \quad \varepsilon_m^m = \frac{1}{N_b-1}\,N_b^{-([x]+\{x\})}\,.$$

The (m,ε_m^m)-Upper and Lower Neighborhoods introduced in Definition 3.4, on page 39, are then obtained by means of rectangles and wedges, as depicted in Figures 8–14 (on pages 42–47).

Proposition 3.1 ((m,ε_m^m)-Upper Neighborhood).

According to Property 2.4, on page 14 (and Definition 2.4, on page 15), given a strictly positive integer m, the (m,ε_m^m)-upper neighborhood consists of:

i. $(N_b-1)\,N_b^m$ ***rectangles****, each of length $\ell_{j-1,j,m}$, for $1 \leqslant j \leqslant N_b^m-1$, and height ε_m^m.*

Those rectangles are also ***overlapping ones****, at least at their bottom. If we denote by $M_{j,m}$ the common vertex between two consecutive overlapping rectangles (see Figure 10, on page 44), the area that is thus counted twice corresponds to parallelograms, of height ε_m^m and basis $\varepsilon_m^m\,cotan\left(\pi-\theta_{j-1,j,m}-\theta_{j,j+1,m}\right)$; i.e., this area is equal to $\left(\varepsilon_m^m\right)^2\,cotan\left(\theta_{j-1,j,m}+\theta_{j,j+1,m}\right)$.*

Since one deals here with an upper neighborhood, one also has to substract the areas of the ***extra outer lower triangles****, i.e., $\dfrac{1}{2}\,\varepsilon_m^m\left(b_{j-1,j,m}+b_{j,j+1,m}\right)$.*

ii. $N_b^m\left(1+2\left[\dfrac{N_b-3}{4}\right]\right)-1$ ***upper wedges*** *(to be understood in the strict sense, which means that the extreme ones are not taken into account here). If we denote by $M_{j,m}$ the vertex from which is issued the wedge (see Figure 14, on page 47), the area of this latter wedge is given by*

$$\frac{1}{2}\left(\pi-\theta_{j-1,j,m}-\theta_{j,j+1,m}\right)\left(\varepsilon_m^m\right)^2 \quad , \quad \textit{for } 1\leqslant j\leqslant N_b^m-2\,\cdot$$

The number of wedges is determined by the shape of the initial polygon $\mathcal{P}_0$, as well by the existence of reentrant angles. This directly follows from Property 2.18, on page 29. For the sake of simplicity, we set

$$r_b^+ = 1+2\left[\frac{N_b-3}{4}\right]\cdot \tag{$\mathcal{R}$ 14}$$

iii. Two ***extreme wedges*** *(see Figure 15, on page 48), each of area equal to $\frac{1}{2}\pi\left(\varepsilon_m^m\right)^2$.*

Proposition 3.2 (**(m,ε_m^m)-Lower Neighborhood**)**.**

In the same way, given a strictly positive integer m, the (m,ε_m^m)-lower neighborhood consists of:

i. $(N_b-1)\,N_b^m$ ***rectangles****, each of length $\ell_{j-1,j,m}$, for $1\leqslant j\leqslant N_b^m-1$, and height ε_m^m.*

Those rectangles are also ***overlapping ones****, this time at least at their top. If we denote by $M_{j,m}$ the common vertex between two consecutive overlapping rectangles, the area that is thus counted twice again corresponds to parallelograms, of height ε_m^m and basis ε_m^m cotan $\left(\pi-\theta_{j-1,j,m}-\theta_{j,j+1,m}\right)$; i.e., this area is equal to $\left(\varepsilon_m^m\right)^2$ cotan $\left(\theta_{j-1,j,m}+\theta_{j,j+1,m}\right)$.*

Since one deals here with a lower neighborhood, one has this time to substract the areas of the ***extra outer upper triangles****, namely, amounting to $\frac{1}{2}\,\varepsilon_m^m\left(b_{j-1,j,m}+b_{j,j+1,m}\right)$.*

ii. $N_b^m\left(N_b-2\left[\frac{N_b-3}{4}\right]\right)-1$ ***lower wedges****. If we denote by $M_{j,m}$ the vertex from which is issued the wedge, the area of this latter wedge is obtained as previously, and is given by*

$$\frac{1}{2}\left(\pi-\theta_{j-1,j,m}-\theta_{j,j+1,m}\right)\left(\varepsilon_m^m\right)^2 \quad , \quad \textit{for } 1\leqslant j\leqslant N_b^m-2\,\cdot$$

The number of lower wedges is determined by the shape of the initial polygon $\mathcal{P}_0$, as well as by the existence of reentrant angles. This directly comes from Property 2.18, on page 29. For the sake of simplicity, we set

$$r_b^- = N_b-2\left[\frac{N_b-3}{4}\right]\cdot \tag{$\mathcal{R}$ 15}$$

Remark 3.2.

i. The number of upper overlapping rectangles is equal to the number of lower extra triangles, and also to the number of upper wedges.

ii. The number of lower overlapping rectangles is equal to the number of upper extra triangles, and also to the number of lower wedges.

iii. In light of *i.* and *ii.* just above, those numbers can be respectively calculated as being equal to

$$(r_b^+ - 1)\, N_b^m \quad \text{and} \quad (r_b^- - 1)\, N_b^m\,,$$

where the coefficients r_b^- and r_b^+ are respectively defined in formulas ($\mathcal{R}15$), page 41 and ($\mathcal{R}14$), page 41.

iv. Note that the small parameter ε_m^m has to be sufficiently small (say $0 < \varepsilon_m^m < \varepsilon_{m_0}^{m_0}$, for some $\varepsilon_{m_0}^{m_0} > 0$ which exists, but appears difficult to specify explicitly) in order to avoid more unfriendly overlaps than the parallelograms; see Figure 16, on page 49.

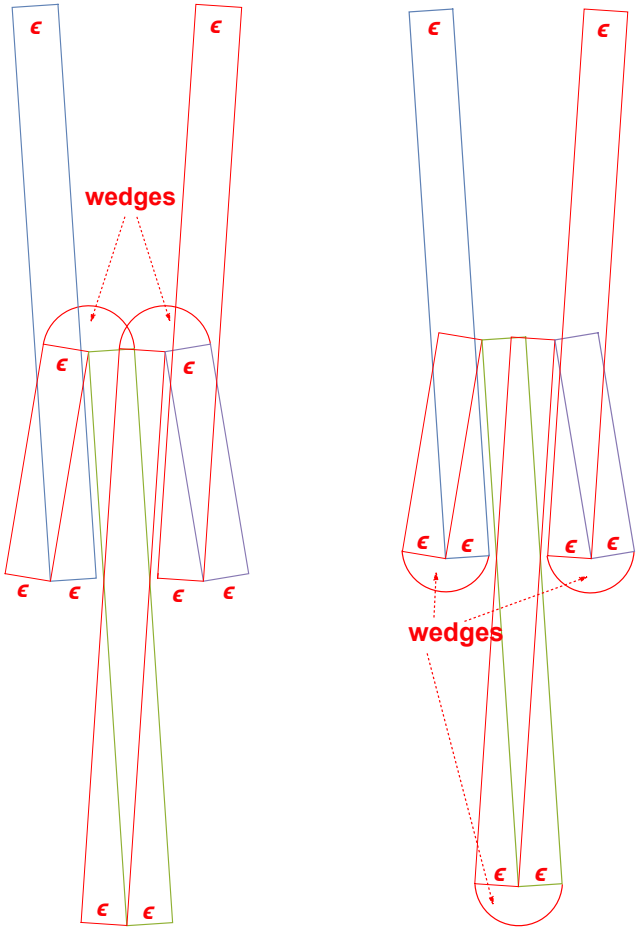

Figure 8: **The $(1, \varepsilon_1^1)$–Upper and Lower Neighborhoods, in the case when $\lambda = \frac{1}{2}$ and $N_b = 3$.**

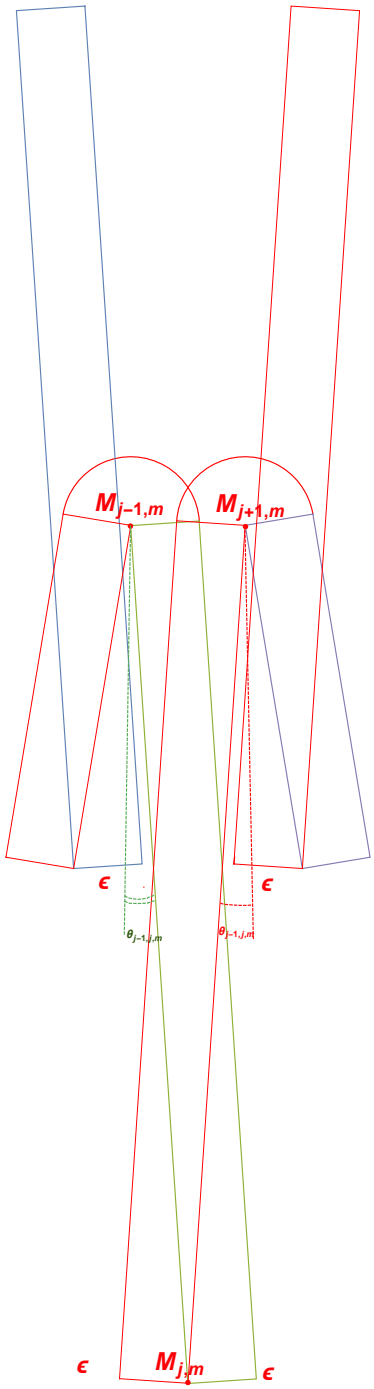

Figure 9: **The $(1, \varepsilon_1^1)$-Upper Neighborhood, in the case when $\lambda = \frac{1}{2}$ and $N_b = 3$.**

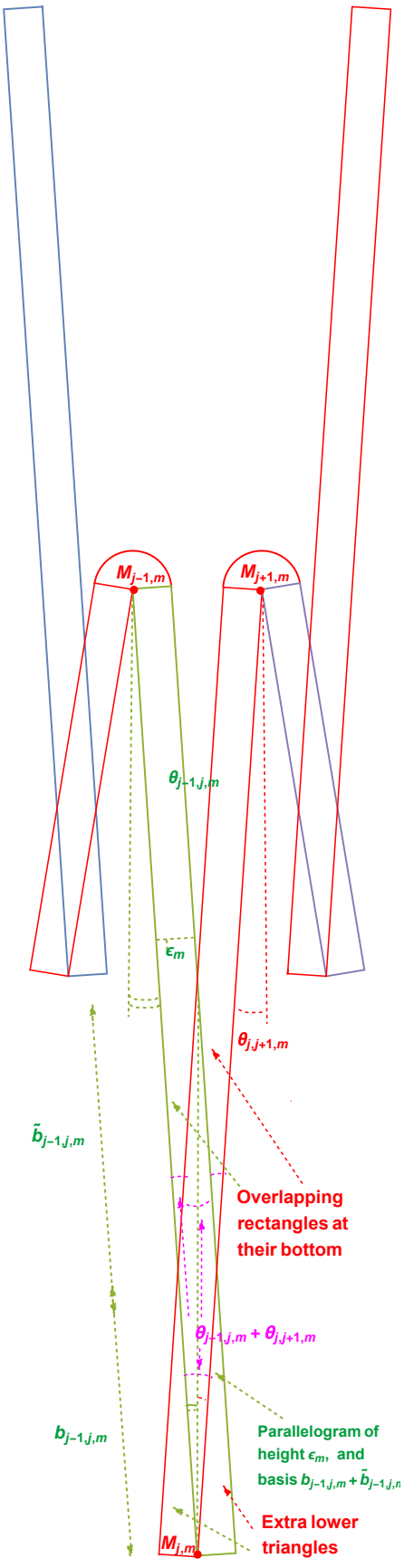

Figure 10: **Two overlapping rectangles, in the case when $\lambda = \frac{1}{2}$ and $N_b = 3$.**

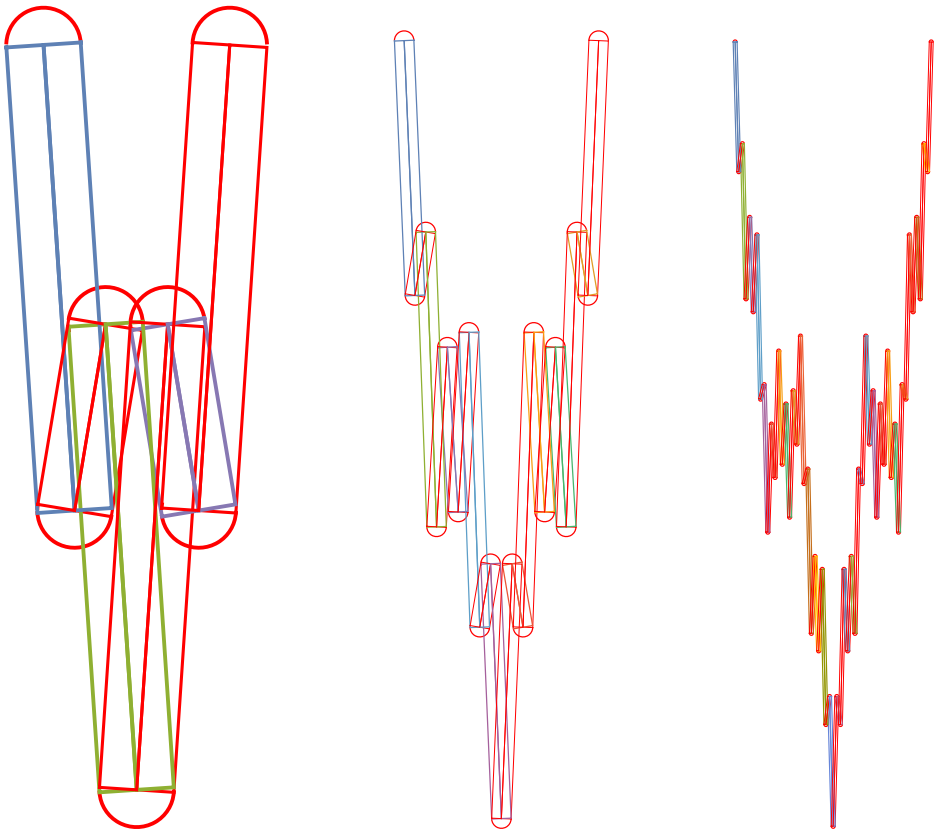

Figure 11: **The $(1, \varepsilon_1^1)$, $(2, \varepsilon_2^2 m)$ and $(3, \varepsilon_m^m)$–Neighborhoods, in the case when $\lambda = \frac{1}{2}$ and $N_b = 3$.**

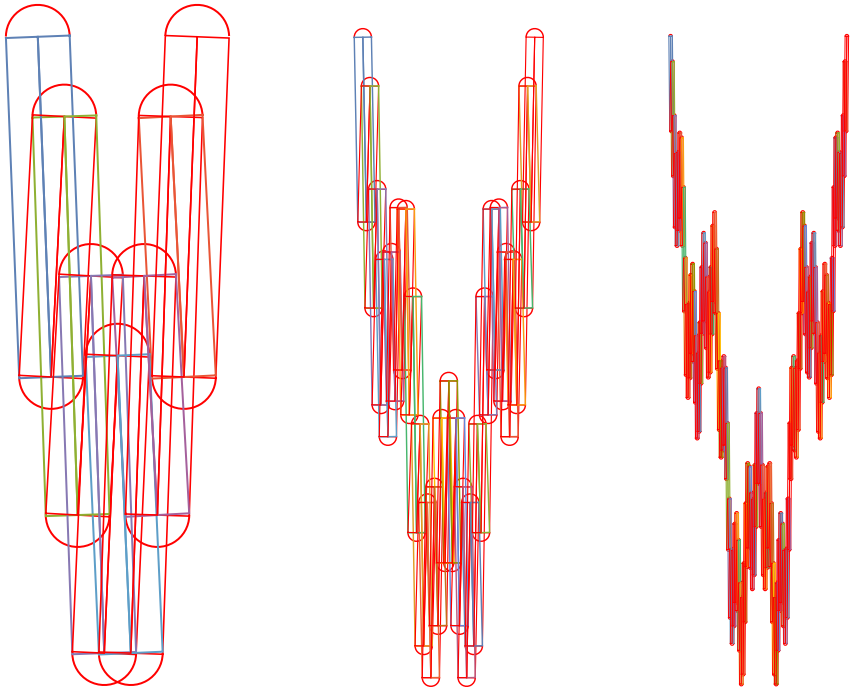

Figure 12: **The $(1, \varepsilon_1^1)$, $(2, \varepsilon_2^2)$ and $(3, \varepsilon_3^3)$–Upper Neighborhoods, in the case when $\lambda = \frac{1}{2}$ and $N_b = 4$.**

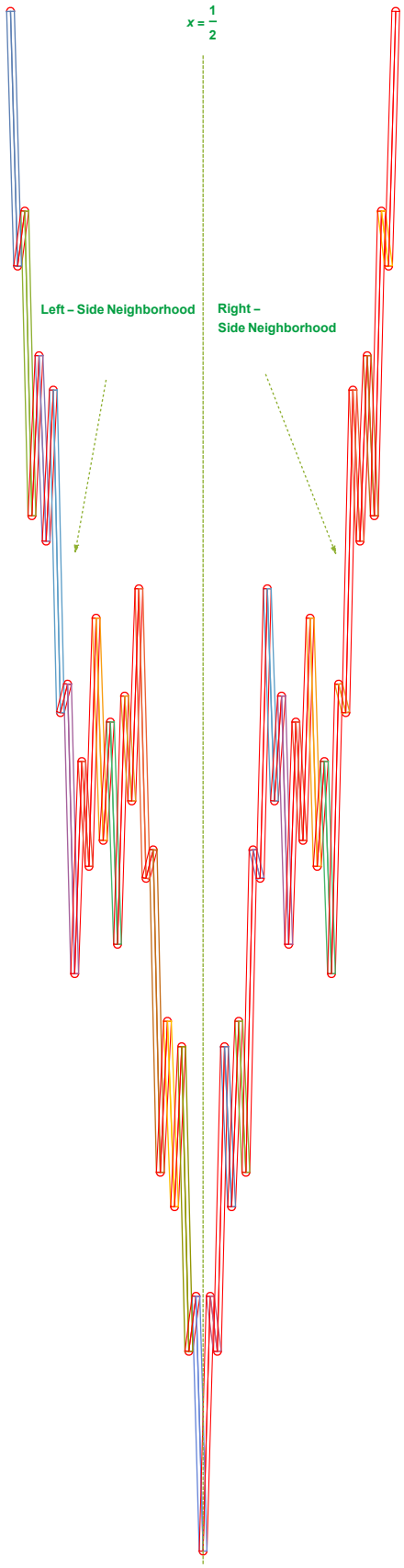

Figure 13: **The $(3, \varepsilon_3^3)$–Left and Right-Side Neighborhoods, in the case when $\lambda = \frac{1}{2}$ and $N_b = 3$.**

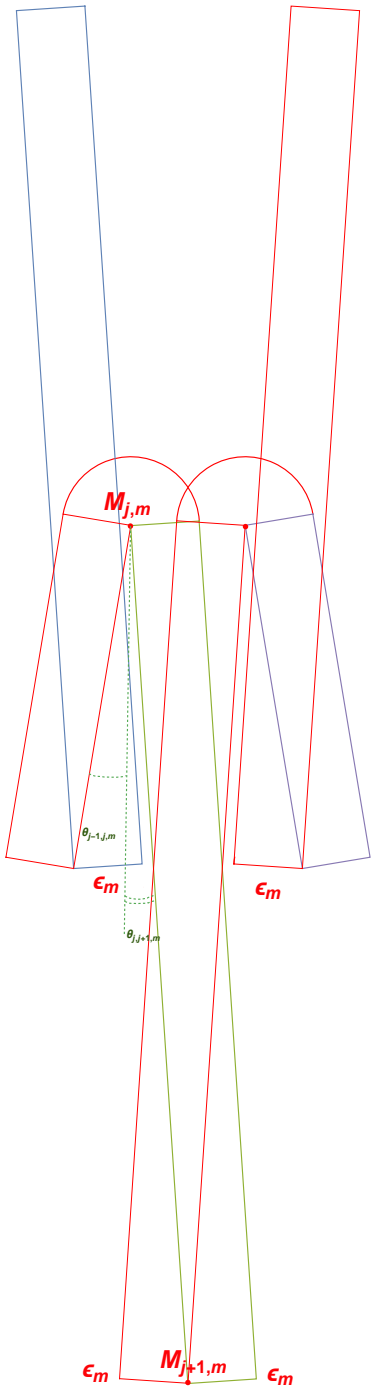

Figure 14: **An upper wedge.**

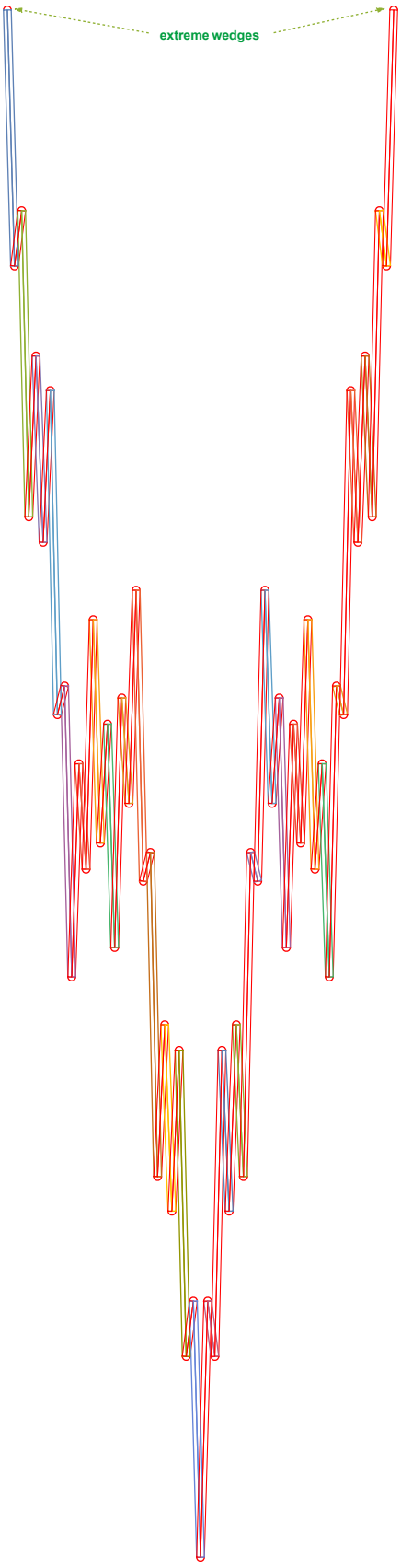

Figure 15: **The extreme wedges, in the case when $\lambda = \frac{1}{2}$ and $N_b = 3$.**

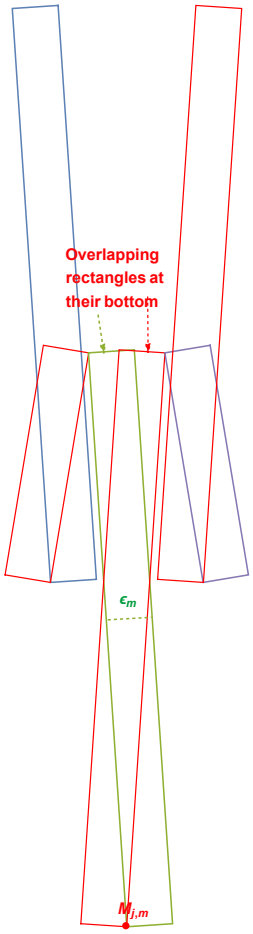

Figure 16: **Two overlapping rectangles, when the parameter ε_m^m is not sufficiently small: the overlap is a pentagon.**

In order to obtain, for the ε–tubular volume at a given level $m \in \mathbb{N}^\star$ (i.e., the area of the ε–neighborhood of $\Gamma_{\mathcal{W}_m}$, the m^{th} prefractal approximation) – not only a pleasant and understandable expression – but, also, an expression which takes into account the underlying fractality, we have to consider the case when $\varepsilon = \varepsilon_m^m$; i.e., the case when the infinitesimal is equal to the cohomoogy infinitesimal, as introduced in Definition 3.1, on page 37. Indeed, only the cohomoogy infinitesimal conveys the scaling relation associated with the Weierstrass IFD. This enables us to make use of the following relations, coming from Corollary 2.15, on page 27. Note that the associated tubular volume is, therefore, not a plain tubular volume associated with a plain polygonal graph. Since the cohomology infinitesimal is associated to the scaling relation obeyed by the Weierstrass function (see Property 2.6, on page 16), this tubular volume takes into account the fractality of the limit object of the sequence of prefractal graphs $\left(\Gamma_{\mathcal{W}_m}\right)_{m \in \mathbb{N}}$, i.e., the Weierstrass Curve $\Gamma_{\mathcal{W}}$.

Proposition 3.3.

i. *For the number of rectangles:* $N_b^m = N_b^{x-\{x\}}$.

Due to the fact that

$$\varepsilon_m^m = \frac{1}{N_b-1}\, N_b^{-([x]+\{x\})} = \frac{1}{N_b-1}\, N_b^{-x} \quad , \quad N_b^{-x} = (N_b-1)\,\varepsilon_m^m \quad , \quad N_b^x = \frac{1}{N_b-1}\,\left(\varepsilon_m^m\right)^{-1} ,$$

one thus also has

$$N_b^m\,\varepsilon_m^m = N_b^{x-\{x\}}\,\frac{1}{N_b-1}\,N_b^{-x} = \frac{1}{N_b-1}\,N_b^{-\{x\}}\,.$$

ii. *For the elementary horizontal lengths:*

$$L_m = \frac{1}{(N_b-1)\,N_b^m} = \frac{1}{N_b-1}\,N_b^{\{x\}-x} = N_b^{\{x\}}\,\varepsilon_m^m\,.$$

iii. *For the elementary vertical heigths:*

$$h_{j,j+1,m} = \mathcal{O}\left(L_m^{2-D_{\mathcal{W}}}\right) = \mathcal{O}\left(N_b^{(2-D_{\mathcal{W}})\,(\{x\}-x)}\right) = N_b^{(2-D_{\mathcal{W}})\,(\{x\}-x)}\,\mathcal{O}\,(1) \;\; , 1 \leqslant j \leqslant N_b^m - 2\,,$$

where, thanks to inequality ($\mathcal{R}7$*) given in Remark 25, page 25,* $\mathcal{O}\,(1)$ *may depend on* m*, but is bounded away from 0 and* ∞*; namely, there exist constants independent of* $m \in \mathbb{N}$ *such that*

$$0 < C_{inf} \leqslant \mathcal{O}\,(1) \leqslant C_{sup} < \infty\,.$$

iv. *For the elementary ratios,* $0 \leqslant j \leqslant N_b^m - 2$*:*

$$\frac{L_m}{h_{j,j+1,m}} = \mathcal{O}\left(L_m^{D_{\mathcal{W}}-1}\right) = \mathcal{O}\left(N_b^{(1-D_{\mathcal{W}})\,(\{x\}-x)}\right) = \mathcal{O}\left(N_b^{(1-D_{\mathcal{W}})\,\{x\}}\,\varepsilon_m^m\right) = N_b^{(1-D_{\mathcal{W}})\,\{x\}}\,\varepsilon_m^m\,\mathcal{O}\,(1)\;,$$

where, again thanks to inequality ($\mathcal{R}7$*) given in Remark 25, page 25,* $\mathcal{O}\,(1)$ *may depend on* m*, but is uniformly bounded away from 0 and* ∞ *(i.e, here and in the sequel, independently of* $m \in \mathbb{N}^\star$ *large enough); more specifically,*

$$0 < \frac{1}{C_{inf}} \leqslant \mathcal{O}\,(1) \leqslant \frac{1}{C_{sup}} < \infty\,.$$

Proposition 3.4 (**Basis of the Parallelograms in Common to Overlapping Rectangles**)**.**

Given $m \in \mathbb{N}^\star$*, and* j *in* $\left\{1, \cdots, (N_b-1)\,N_b^m - 1\right\}$*, the basis* $b_{j-1,j,m}$ *of the parallelogram in common to overlapping rectangles associated to the vertex* $M_{j,m}$ *is such that*

$$b_{j-1,j,m} = N_b^{(3\,D_{\mathcal{W}}-2)\,\{x\}}\,\left(\varepsilon_m^m\right)^2\,\mathcal{O}\,(1)\;,$$

where,

$$0 < C_{inf}^3 \leqslant \mathcal{O}\,(1) \leqslant C_{sup}^3 < \infty\,.$$

Proof. One has, according to Figure 10, on page 44,

$$\tan\theta_{j-1,j,m} = \frac{\varepsilon_m^m}{b_{j-1,j,m} + \widetilde{b}_{j-1,j,m}} ,$$

where $b_{j-1,j,m} + \widetilde{b}_{j-1,j,m}$ is the side–length of the parallelogram of basis ε_m^m

$$\tan\left(\theta_{j-1,j,m} + \theta_{j,j+1,m}\right) = \frac{\varepsilon_m^m}{\widetilde{b}_{j-1,j,m}} \cdot$$

Hence,

$$b_{j-1,j,m} + \widetilde{b}_{j-1,j,m} = \varepsilon_m^m \left|\operatorname{cotan}\theta_{j-1,j,m}\right| ,$$

which yields

$$b_{j-1,j,m} = \varepsilon_m^m \left|\operatorname{cotan}\theta_{j-1,j,m}\right| - \widetilde{b}_{j-1,j,m} = \varepsilon_m^m \left\{\left|\operatorname{cotan}\theta_{j-1,j,m}\right| - \left|\operatorname{cotan}\left(\theta_{j-1,j,m} + \theta_{j,j+1,m}\right)\right|\right\} ;$$

i.e.,

$$\begin{aligned} b_{j-1,j,m} &= \varepsilon_m^m \left(\frac{h_{j-1,j,m}}{L_m} - \left| \operatorname{cotan}\left(\arctan\frac{L_m}{h_{j-1,j,m}} + \arctan\frac{L_m}{h_{j,j+1,m}} \right) \right| \right) \\ &= \varepsilon_m^m \left(\frac{h_{j-1,j,m}}{L_m} - \left| \frac{\frac{L_m}{h_{j-1,j,m}}\,\frac{L_m}{h_{j,j+1,m}} - 1}{\frac{L_m}{h_{j-1,j,m}} + \frac{L_m}{h_{j,j+1,m}}} \right| \right) \qquad (\mathcal{R}\,16) \\ &= \varepsilon_m^m \left(\frac{h_{j-1,j,m}}{L_m} - \frac{1 - \frac{L_m}{h_{j-1,j,m}}\,\frac{L_m}{h_{j,j+1,m}}}{\frac{L_m}{h_{j-1,j,m}} + \frac{L_m}{h_{j,j+1,m}}} \right) . \end{aligned}$$

Thanks to Proposition 3.3, on page 50, we have that

$$\frac{h_{j-1,j,m}}{L_m} = N_b^{(D_{\mathcal{W}}-1)\{x\}}\, \varepsilon_m^m\, \mathcal{O}(1) \quad , \quad \text{with } 0 < C_{inf} \leqslant \mathcal{O}(1) \leqslant C_{sup} \cdot$$

In order to obtain the corresponding estimate for $b_{j-1,j,m}$, we need an asymptotic expansion for $b_{j-1,j,m}$. A slight difficulty occurs, coming from the term

$$\frac{1}{\frac{L_m}{h_{j-1,j,m}} + \frac{L_m}{h_{j,j+1,m}}} \cdot$$

The apparent problem is the following:

i. Either one uses, as previously, expressions of the form

$$\frac{1}{\frac{L_m}{h_{j-1,j,m}} + \frac{L_m}{h_{j,j+1,m}}} = N_b^{(D_{\mathcal{W}}-1)\{x\}}\, \mathcal{O}(1) ,$$

with nothing but a *black box* (which means, unknown terms) in factor of constants, that would yield Complex Dimensions with a real part equal to two, and would therefore lead to a contradiction because the Weierstrass Curve has box dimension $D_{\mathcal{W}} < 2$.

ii. Either, knowing that, which is not the more satisfactorily way of reasoning, from a mathematician's point of view, one copes with it and tries to find how to get rid of those terms.

Two configurations occur:

↝ If $h_{j-1,j,m} < h_{j,j+1,m}$, and, thus, $\dfrac{L_m}{h_{j-1,j,m}} > \dfrac{L_m}{h_{j,j+1,m}}$, in which case we have that

$$\begin{aligned}
\frac{h_{j-1,j,m}}{L_m} - \frac{1 - \frac{L_m}{h_{j-1,j,m}} \frac{L_m}{h_{j,j+1,m}}}{\frac{L_m}{h_{j-1,j,m}} + \frac{L_m}{h_{j,j+1,m}}} &= \frac{h_{j-1,j,m}}{L_m} - \frac{1 - \frac{L_m}{h_{j-1,j,m}} \frac{L_m}{h_{j,j+1,m}}}{\frac{L_m}{h_{j-1,j,m}} \left(1 + h_{j-1,j,m}\, h_{j,j+1,m}\right)} \\
&= \frac{h_{j-1,j,m}}{L_m} \\
&\quad - \frac{h_{j-1,j,m}}{L_m} \left(1 - \frac{L_m^2}{h_{j-1,j,m}\, h_{j,j+1,m}}\right) \left(1 - h_{j-1,j,m}\, h_{j,j+1,m} + \text{smaller order terms}\right) \\
&= \frac{h_{j-1,j,m}}{L_m} \\
&\quad - \frac{h_{j-1,j,m}}{L_m} \left(1 - h_{j-1,j,m}\, h_{j,j+1,m} - \frac{L_m^2}{h_{j-1,j,m}\, h_{j,j+1,m}} + L_m^2 + \text{smaller order terms}\right) \\
&= \frac{h_{j-1,j,m}^2\, h_{j,j+1,m}}{L_m} + \frac{L_m}{h_{j,j+1,m}} - L_m\, h_{j-1,j,m} \\
&\quad + \text{smaller order and negligeable terms.}
\end{aligned}$$

Since

$$\frac{h_{j-1,j,m}^2\, h_{j,j+1,m}}{L_m} = N_b^{2\,(2-D_{\mathcal{W}})\,\{x\}}\, \varepsilon_m^m\, N_b^{(D_{\mathcal{W}}-1)\,\{x\}}\, \mathcal{O}(1) = N_b^{(3-D_{\mathcal{W}})\,\{x\}}\, \varepsilon_m^m\, \mathcal{O}(1)\ ,$$

along with

$$L_m\, h_{j-1,j,m} = N_b^{(3-D_{\mathcal{W}})\,\{x\}}\, \left(\varepsilon_m^m\right)^2\, \mathcal{O}(1)\ ,$$

and

$$\frac{L_m}{h_{j,j+1,m}} = N_b^{(1-D_{\mathcal{W}})\,\{x\}}\, \left(\varepsilon_m^m\right)^2\, \mathcal{O}(1) << \frac{h_{j-1,j,m}^2\, h_{j,j+1,m}}{L_m}\ ,$$

the terms that have to be taken into account in relation ($\mathcal{R}16$), on page 51 above, are then

$$N_b^{(3-D_{\mathcal{W}})\,\{x\}}\, \left(\varepsilon_m^m\right)^2\, \mathcal{O}(1) = b_{j-1,j,m}\,\cdot$$

↝ If $h_{j-1,j,m} < h_{j,j+1,m}$, and, thus, $\dfrac{L_m}{h_{j-1,j,m}} < \dfrac{L_m}{h_{j,j+1,m}}$, in which case we have that

$$\frac{h_{j-1,j,m}}{L_m} - \frac{1}{\frac{L_m}{h_{j-1,j,m}} + \frac{L_m}{h_{j,j+1,m}}} = \frac{h_{j-1,j,m}}{L_m} - \frac{h_{j,j+1,m}}{L_m} + \text{smaller order and negligeable terms}\,\cdot$$

Fortunately, due to results obtained in the proof of Property 2.18, on page 29, this situation occurs only in the case of reentrant angles, when $N_b \geqslant 7$, twice, for respectively $\left[\dfrac{N_b - 3}{4}\right]$ consecutive vertices of polygons $\mathcal{P}_{m,k}$, $0 \leqslant k \leqslant N_b^m - 1$. Given a polygon $\mathcal{P}_{m,k}$, and as already encountered, one just has to reason on the associated first set of consecutive vertices. The annoying terms simplify two by two in a telescopic sum, from the first reentrant

vertex, to the penultimate one. There remains the term coming from the first vertex with an interior reentrant angle, that will be denoted $M_{j,m}$, and the term coming from the ultimate one, $M_{j+p-1,m}$: due to the symmetry with respect to the vertical line $x = \frac{1}{2}$ (see Property 2.1, on page 9), they are cancelled by those coming from the symmetric polygon, see Figure 17, on page 54). To summarize, one obtains a sum of the form

$$\frac{h_{j-1,j,m}}{L_m} \underbrace{- \frac{h_{j,j+1,m}}{L_m} + \frac{h_{j,j+1,m}}{L_m} - \frac{h_{j+1,j+2,m}}{L_m} + \frac{h_{j+1,j+2,m}}{L_m} \cdots}_{\text{telescoping sum}} - \frac{h_{j+p,j+p+1,m}}{L_m} \cdot$$

The remaining terms $\frac{h_{j-1,j,m}}{L_m}$ and $-\frac{h_{j+p,j+p+1,m}}{L_m}$ are the ones which will simplify with the exact opposites coming from the symmetric polygon with respect to the vertical line $x = \frac{1}{2}$ (see Figure 17, on page 54), since

$$\begin{aligned}
\frac{h_{j+p,j+p+1,m}}{L_m} &= \frac{1}{L_m} \left| \mathcal{W}\left(\frac{j+p+1}{(N_b-1)\, N_b^m} \right) - \mathcal{W}\left(\frac{j+p}{(N_b-1)\, N_b^m} \right) \right| \\
&= \frac{1}{L_m} \left| \mathcal{W}\left(\frac{(N_b-1)\, N_b^m - j - p - 1}{(N_b-1)\, N_b^m} \right) - \mathcal{W}\left(\frac{(N_b-1)\, N_b^m j - p}{(N_b-1)\, N_b^m} \right) \right| \\
&= \frac{h_{(N_b-1)\, N_b^m - j - p - 1, (N_b-1)\, N_b^m - j - p, m}}{L_m} \cdot
\end{aligned}$$

Thus, in the end, there is no problem.

In the light of the above results, one may now rewrite $b_{j-1,j,m}$ as follows:

$$b_{j-1,j,m} = N_b^{(3-D_{\mathcal{W}})\{x\}} \left(\varepsilon_m^m\right)^2 \mathcal{O}(1) \,, \tag{$\mathcal{R}$ 17}$$

where, thanks to inequality ($\mathcal{R}$7) given in Remark 25, on page 25,

$$0 < C_{inf}^3 \leqslant \mathcal{O}(1) \leqslant C_{sup}^3 < \infty \cdot$$

This concludes the proof of Proposition 3.4, stated on page 50.

□

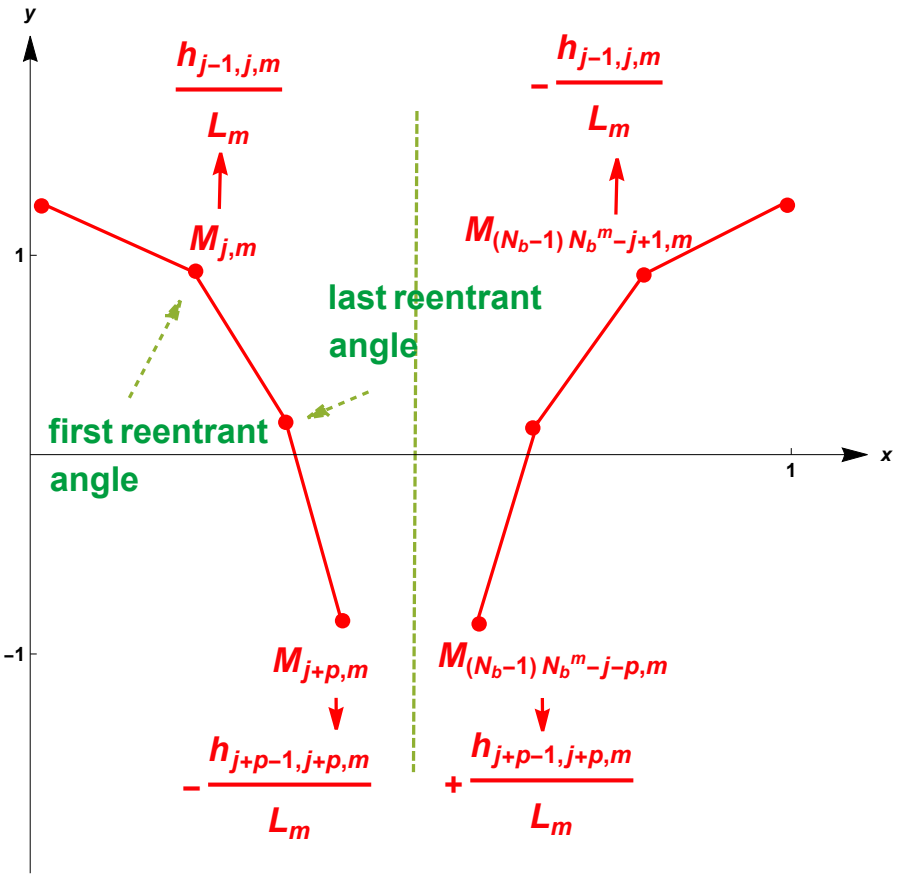

Figure 17: **The symmetric points with respect to the vertical line $x = \frac{1}{2}$, leading to terms that cancel each other out in the proof of Proposition 3.4.**

In the sequel, we will use the following two power series expansions:

i. $\forall\, z \in [0,1[: \quad \sqrt{1+z} = \sum_{k=0}^{\infty} \binom{\frac{1}{2}}{k} z^k,$

where, for any pair of natural integer k, $\binom{\frac{1}{2}}{k}$ is the generalized binomial coefficient

$$\binom{\frac{1}{2}}{k} = \frac{\frac{1}{2} \times \left(\frac{1}{2}-1\right) \times \left(\frac{1}{2}-2\right) \times \cdots \times \left(\frac{1}{2}-k+1\right)}{k\,!} = \frac{\left(\frac{1}{2}\right)_k}{k\,!}\,.$$

This expansion is thus valid for

$$z = \frac{L_m^2}{h_{j-1,j,m}^2} = \mathcal{O}\left(L_m^{2\,(D_{\mathcal{W}}-1)}\right) \ll 1\,.$$

ii. $\forall\, z \in [0,1[: \quad \tan^{-1} z = \arctan z = \sum_{k=0}^{\infty} \frac{(-1)^k\, z^{2\,k+1}}{2\,k+1}$, which is also valid for

$$z = \frac{L_m^2}{h_{j-1,j,m}^2} = \mathcal{O}\left(L_m^{2\,(D_{\mathcal{W}}-1)}\right) \ll 1\,.$$

Notation 10. In the sequel, for the sake of simplicity, we will use the following notation:

i. $\sum_{j \text{ rectangle}} \cdots$, to denote a sum involving all the upper and lower rectangles, which amounts to taking into accounts indices j such that $1 \leqslant j \leqslant (N_b - 1) N_b^m$.

ii. $\sum_{j \text{ lower wedge}} \cdots$, to denote a sum involving all the lower wedges, which amounts to taking into accounts indices j such that $N_b^m \left(N_b - 2 \left[\frac{N_b - 3}{4} \right] \right) - 1$.

iii. $\sum_{j \text{ upper wedge}} \cdots$, to denote ta sum involving all the upper wedges, which amounts to taking into accounts indices j such that $N_b^m \left(1 + 2 \left[\frac{N_b - 3}{4} \right] \right) - 1$.

And, similarly:

iv. $\sum_{j \text{ upper triangle}} \cdots$, to denote a sum involving all the extra outer upper triangles.

v. $\sum_{j \text{ lower triangle}} \cdots$, to denote a sum involving all the extra outer lower triangles.

vi. $\sum_{j \text{ lower parallelogram}} \cdots$, to denote a sum involving all the upper overlapping rectangles.

vii. $\sum_{j \text{ upper parallelogram}} \cdots$, to denote a sum involving all the lower overlapping rectangles.

Proposition 3.5 (Contribution of the Rectangles to the Tubular Volume).

*Given $m \in \mathbb{N}^\star$ sufficiently large, the contribution of the $(N_b - 1)\, N_b^m$ **rectangles** to the tubular volume is given by*

$$
\begin{aligned}
\mathcal{V}_{m,\Gamma_{\mathcal{W}_m},Rectangles}(\varepsilon_m^m) &= 2 \sum_{j\ rectangle} \varepsilon_m^m\, \ell_{j-1,j,m} \\
&= 2 \sum_{j\ rectangle} \varepsilon_m^m \sqrt{L_m^2 + h_{j-1,j,m}^2} \\
&= 2 \sum_{j\ rectangle} \varepsilon_m^m\, h_{j-1,j,m} \sqrt{1 + \frac{L_m^2}{h_{j-1,j,m}^2}} \\
&= 2 \sum_{j\ rectangle} \varepsilon_m^m\, h_{j-1,j,m} \sqrt{1 + \frac{L_m^2}{h_{j-1,j,m}^2}} \\
&= 2 \sum_{j\ rectangle} \varepsilon_m^m\, h_{j-1,j,m} \sum_{k=0}^{\infty} \binom{\frac{1}{2}}{k} \frac{L_m^{2k}}{h_{j-1,j,m}^{2k}} \\
&= 2 \sum_{j\ rectangle} \varepsilon_m^m\, h_{j-1,j,m} \sum_{k=0}^{\infty} \binom{\frac{1}{2}}{k} N_b^{k(2-D_{\mathcal{W}})\{x\}} \left(\varepsilon_m^m\right)^{k(2-D_{\mathcal{W}})} \mathcal{O}(1) \\
&= 2 \sum_{j\ rectangle} \varepsilon_m^m \left(\varepsilon_m^m\right)^{2-D_{\mathcal{W}}} \mathcal{O}(1) \sum_{k=0}^{\infty} \binom{\frac{1}{2}}{k} N_b^{k(2-D_{\mathcal{W}})\{x\}} \left(\varepsilon_m^m\right)^{k(2-D_{\mathcal{W}})} \mathcal{O}(1) \\
&= 2\, N_b^m \left(\varepsilon_m^m\right)^{2-D_{\mathcal{W}}} \mathcal{O}(1) \sum_{k=0}^{\infty} \binom{\frac{1}{2}}{k} N_b^{k(2-D_{\mathcal{W}})\{x\}} \left(\varepsilon_m^m\right)^{1+k(2-D_{\mathcal{W}})} \mathcal{O}(1) \\
&= 2\,(N_b - 1)\, N_b^m\, \varepsilon_m^m \left(\varepsilon_m^m\right)^{2-D_{\mathcal{W}}} \sum_{k=0}^{\infty} \binom{\frac{1}{2}}{k} N_b^{k(2-D_{\mathcal{W}})\{x\}} \left(\varepsilon_m^m\right)^{k(2-D_{\mathcal{W}})} \mathcal{O}(1) \\
&= 2\, N_b^{-\{x\}} \left(\varepsilon_m^m\right)^{2-D_{\mathcal{W}}} \sum_{k=0}^{\infty} \binom{\frac{1}{2}}{k} N_b^{k(2-D_{\mathcal{W}})\{x\}} \left(\varepsilon_m^m\right)^{k(2-D_{\mathcal{W}})} \mathcal{O}(1) \\
&= 2 \sum_{k=0}^{\infty} \binom{\frac{1}{2}}{k} N_b^{(k(2-D_{\mathcal{W}})-1)\{x\}} \left(\varepsilon_m^m\right)^{2-D_{\mathcal{W}}+k(2-D_{\mathcal{W}})} \mathcal{O}(1)\,,
\end{aligned}
\tag{$\mathcal{R}$ 18}
$$

where, for notational simplicity, we have used the estimates obtained in relation ($\mathcal{R}$9), given on page 27, for the elementary quotients $\dfrac{L_m}{h_{j-1,j,m}}$, in the form

$$
\frac{h_{j-1,j,m}}{L_m} = L_m^{1-D_{\mathcal{W}}}\, \mathcal{O}(1)\,,
$$

where $\mathcal{O}(1)$ may depend on m, but is uniformly bounded away from 0 and ∞; more specifically,

$$
0 < C_{inf} \leqslant \mathcal{O}(1) \leqslant C_{sup} < \infty\,.
$$

This ensures here that, for all $k \in \mathbb{N}$,

$$
2 \binom{\frac{1}{2}}{k} N_b^{(k(2-D_{\mathcal{W}})-1)\{x\}} \left(\varepsilon_m^m\right)^{2-D_{\mathcal{W}}+k(2-D_{\mathcal{W}})} \mathcal{O}(1) > 0\,. \tag{$\mathcal{R}$ 19}
$$

Note that the contribution of the rectangles to the tubular volume is, geometrically, the main one. For this reason, we have used the capital letter R, contrary to the other – and forthcoming – contributions.

Proposition 3.6 (**Contribution of the Extreme, Upper and Lower Wedges to the Tubular Volume**).

*i. Given $m \in \mathbb{N}^\star$ sufficiently large, the contribution of the **extreme wedges** to the tubular volume is given by*

$$\mathcal{V}_{m,\Gamma_{\mathcal{W}_m},extreme\ wedges}(\varepsilon_m^m) = \pi \left(\varepsilon_m^m\right)^2 \cdot$$

*ii. Given $m \in \mathbb{N}^\star$ sufficiently large, the contribution of the $r_b^+ N_b^m - 1$ **upper wedges** to the tubular volume is given by*

$$\begin{aligned}
\mathcal{V}_{m,\Gamma_{\mathcal{W}_m},upper\ wedges}(\varepsilon_m^m) &= \frac{1}{2} \sum_{j\ upper\ wedge} \left(\pi - \theta_{j-1,m} - \theta_{j,j+1,m}\right) \left(\varepsilon_m^m\right)^2 \\
&= \frac{1}{2} \sum_{j\ upper\ wedge} \left(\varepsilon_m^m\right)^2 \left(\pi - \arctan \frac{L_m}{h_{j-1,j,m}} - \arctan \frac{L_m}{h_{j,j+1,m}}\right) \\
&= \frac{\left(\varepsilon_m^m\right)^2}{2} \sum_{j\ upper\ wedge} \left(\varepsilon_m^m\right)^2 \left(\pi - \sum_{k=0}^{\infty} \frac{(-1)^k}{2k+1} \frac{L_m^{2k+1}}{h_{j-1,j,m}^{2k+1}} - \sum_{k=0}^{\infty} \frac{(-1)^k}{2k+1} \frac{L_m^{2k+1}}{h_{j,j+1,m}^{2k+1}}\right) \\
&= \frac{\left(\varepsilon_m^m\right)^2}{2} \sum_{j\ upper\ wedge} \left(\pi - \sum_{k=0}^{\infty} \frac{(-1)^k}{2k+1} N_b^{(2k+1)(1-D_{\mathcal{W}})\{x\}} \left(\varepsilon_m^m\right)^{2k+1} \mathcal{O}(1)\right) \\
&= \frac{\left(\varepsilon_m^m\right)^2}{2} \left(r_b^+ N_b^m - 1\right) \left(\pi - \sum_{k=0}^{\infty} \frac{(-1)^k}{2k+1} N_b^{(2k+1)(1-D_{\mathcal{W}})\{x\}} \left(\varepsilon_m^m\right)^{2k+1} \mathcal{O}(1)\right) \\
&= \frac{\left(\varepsilon_m^m\right)^2}{2} \left(\frac{\varepsilon_m^m}{4} r_b^+ N_b^{-\{x\}} - \frac{\left(\varepsilon_m^m\right)^2}{2}\right) \left(\pi - \sum_{k=0}^{\infty} \frac{(-1)^k}{2k+1} N_b^{(2k+1)(1-D_{\mathcal{W}})\{x\}} \left(\varepsilon_m^m\right)^{2k+1} \mathcal{O}(1)\right) \\
&= \frac{\pi}{2} \left(\frac{\left(\varepsilon_m^m\right)^3}{4} r_b^+ N_b^{-\{x\}} - \frac{\left(\varepsilon_m^m\right)^4}{2}\right) - \frac{\left(\varepsilon_m^m\right)^3}{4} r_b^+ \sum_{k=0}^{\infty} \frac{(-1)^k}{2k+1} N_b^{-((2k+1)D_{\mathcal{W}}-2k)\{x\}} \left(\varepsilon_m^m\right)^{2k+1} \mathcal{O}(1) \\
&\quad + \frac{\left(\varepsilon_m^m\right)^4}{4} \sum_{k=0}^{\infty} \frac{(-1)^k}{2k+1} N_b^{-((2k+1)D_{\mathcal{W}}-2k+1)\{x\}} \left(\varepsilon_m^m\right)^{2k+1} \mathcal{O}(1)\,,
\end{aligned} \tag{$\mathcal{R}$ 20}$$

where, for notational simplicity, and as done previously in Proposition 3.5, on page 56, we have used the estimates obtained in relation ($\mathcal{R}$9), given on page 27, for the elementary quotients $\dfrac{L_m}{h_{j-1,j,m}}$, in the form

$$\frac{h_{j-1,j,m}}{L_m} = L_m^{1-D_{\mathcal{W}}} \mathcal{O}(1) \quad , \quad \frac{h_{j,j+1,m}}{L_m} = L_m^{1-D_{\mathcal{W}}} \mathcal{O}(1)\,,$$

where, as in Proposition 3.5, on page 56 above, $\mathcal{O}(1)$ may depend on m, but is uniformly bounded away from 0 and ∞; more specifically,

$$0 < C_{inf} \leqslant \mathcal{O}(1) \leqslant C_{sup} < \infty \cdot$$

This ensures here that, for all $k \in \mathbb{N}$,

$$\frac{(-1)^k}{2k+1} N_b^{-((2k+1)D_{\mathcal{W}}-2k+1)\{x\}} \left(\varepsilon_m^m\right)^{2k+1} \mathcal{O}(1) \neq 0\,, \tag{$\mathcal{R}$ 21}$$

*iii. In the same way, given $m \in \mathbb{N}^\star$ sufficiently large, the contribution of the $r_b^- N_b^m - 1$ **lower wedges** to the tubular volume is given by*

$$\begin{aligned}\mathcal{V}_{m,\Gamma_{\mathcal{W}_m},\text{lower wedges}}\left(\varepsilon_m^m\right) = \quad & \frac{\pi}{2}\left(\frac{\left(\varepsilon_m^m\right)^3}{4} r_b^- N_b^{-\{x\}} - \frac{\left(\varepsilon_m^m\right)^4}{2}\right) \\ & -\frac{\left(\varepsilon_m^m\right)^3}{4} r_b^- \sum_{k=0}^{\infty} \frac{(-1)^k}{2k+1} N_b^{-((2k+1)D_{\mathcal{W}}-2k)\{x\}} \left(\varepsilon_m^m\right)^{2k+1} \mathcal{O}(1) \\ & +\frac{\left(\varepsilon_m^m\right)^4}{4} \sum_{k=0}^{\infty} \frac{(-1)^k}{2k+1} N_b^{-((2k+1)D_{\mathcal{W}}-2k+1)\{x\}} \left(\varepsilon_m^m\right)^{2k+1} \left(\varepsilon_m^m\right)^{2k+1} \mathcal{O}(1)\,. \end{aligned} \tag{$\mathcal{R}$ 22}$$

As previously, we obtain that, for all $k \in \mathbb{N}$,

$$\frac{(-1)^k}{2k+1} N_b^{-((2k+1)D_{\mathcal{W}}-2k+1)\{x\}} \left(\varepsilon_m^m\right)^{2k+1} \mathcal{O}(1) \neq 0\,. \tag{$\mathcal{R}$ 23}$$

Proposition 3.7 (**Negative Contribution of the Extra Outer Triangles to the Tubular Volume**)**.**

*i. Given $m \in \mathbb{N}^\star$ sufficiently large, the negative contribution of the $(N_b - r_b^+ - 1) N_b^m$ **extra outer lower triangles** to the tubular volume is given by*

$$\begin{aligned}\mathcal{V}_{m,\Gamma_{\mathcal{W}_m},\text{extra outer lower triangles}}\left(\varepsilon_m^m\right) &= -\frac{\varepsilon_m^m)}{2} \sum_{j\ triangle} \left\{b_{j-1,j,m} + b_{j,j+1,m}\right\} \\ &= -\frac{\varepsilon_m^m}{2} \sum_{j\ lower\ triangle} N_b^{(3-D_{\mathcal{W}})\{x\}} \left(\varepsilon_m^m\right)^2 \mathcal{O}(1) \\ &= -\frac{\varepsilon_m^m}{2} (N_b - r_b^+ - 1) N_b^m N_b^{(3-D_{\mathcal{W}})\{x\}} \left(\varepsilon_m^m\right)^2 \mathcal{O}(1) \\ &= -\frac{(\varepsilon_m^m)^2}{2} (N_b - r_b^+ - 1) N_b^{-\{x\}} N_b^{(3-D_{\mathcal{W}})\{x\}} \mathcal{O}(1)\,, \end{aligned} \tag{$\mathcal{R}$ 24}$$

where the coefficient r_b^+ is defined in formula ($\mathcal{R}$14) page 41, and where, as in Proposition 3.5, on page 56 above, $\mathcal{O}(1)$ may depend on m, but is uniformly bounded away from 0 and ∞; more specifically,

$$0 < C_{inf}^3 \leqslant \mathcal{O}(1) \leqslant C_{sup}^3 < \infty\,,$$

thanks to the estimates obtained in Corollary 3.4, on page 50, and where the coefficient r_b^+ is defined in formula ($\mathcal{R}$14), on page 41.

This ensures here that, for all $k \in \mathbb{N}$,

$$\frac{(-1)^k}{2k+1} N_b^{-(2k+1)(D_{\mathcal{W}}-1)\{x\}} \left(\varepsilon_m^m\right)^{2k+1} \mathcal{O}(1) \neq 0\,. \tag{$\mathcal{R}$ 25}$$

ii. In the same way, given $m \in \mathbb{N}^\star$ *sufficiently large, the negative contribution of the* $(N_b - r_b^- - 1)\, N_b^m$ ***extra outer upper triangles*** *to the tubular volume is given by*

$$\mathcal{V}_{m,\Gamma_{\mathcal{W}_m},\textit{extra outer upper triangles}}\left(\varepsilon_m^m\right) \;=\; -\frac{\left(\varepsilon_m^m\right)^2}{2}\,(N_b - r_b^- - 1)\,N_b^{-\{x\}}\,N_b^{(3-D_{\mathcal{W}})\{x\}}\,\mathcal{O}(1)\;, \tag{$\mathcal{R}$ 26}$$

again where, as in Proposition 3.5, on page 56 above, $\mathcal{O}(1)$ *may depend on* m*, but is uniformly bounded away from 0 and* ∞*; more specifically,*

$$0 < C_{inf}^3 \leqslant \mathcal{O}(1) \leqslant C_{sup}^3 < \infty\,,$$

and where the coefficient r_b^- *is defined in formula (*$\mathcal{R}$*15), on page 41.*

Proposition 3.8 (**Negative Contribution of the Overlapping Rectangles to the Tubular Volume**)**.**

Given $m \in \mathbb{N}^\star$ *sufficiently large, the negative contribution of the* ***upper and lower overlapping rectangles*** *to the tubular volume is given by*

$$\mathcal{V}_{m,\Gamma_{\mathcal{W}_m},\textit{upper and lower parallelograms}}\left(\varepsilon_m^m\right) = -\varepsilon_m^m \sum_{j\ \textit{upper and lower parallelogram}} b_{j-1,j,m} = -\left(\varepsilon_m^m\right)^2\,N_b^{(3-D_{\mathcal{W}})\{x\}}\,\mathcal{O}(1)\;, \tag{$\mathcal{R}$ 27}$$

where, as in Proposition 3.5, on page 56 above, $\mathcal{O}(1)$ *may depend on* m*, but is uniformly bounded away from 0 and* ∞*; more specifically,*

$$0 < C_{inf}^3 \leqslant \mathcal{O}(1) \leqslant C_{sup}^3 < \infty\,\cdot$$

Property 3.9 (**Staggered Sequence of** (m, ε_m^m)**–Neighborhoods**)**.**

Given $m \in \mathbb{N}$*, there exists an integer* $k_m \in \mathbb{N}$ *such that, for each integer* $k \geqslant k_m$*, the* $(m+k, \varepsilon_{m+k}^{m+k})$*–neighborhood of the* m^{th} *prefractal approximation* $\Gamma_{\mathcal{W}_m}$ *(where* ε_{m+k}^{m+k} *is the* $(m+k)^{th}$ *cohomolgy infinitesimal, as introduced in Definition 3.1, on page 37),*

$$\mathcal{D}\left(\Gamma_{\mathcal{W}_{m+k}}, \varepsilon_{m+k}^{m+k}\right) = \left\{M = (x,y) \in \mathbb{R}^2\,,\, d\left(M, \Gamma_{\mathcal{W}_{m+k}}\right) \leqslant \varepsilon_{m+k}^{m+k}\right\}\,, \tag{$\mathcal{R}$ 28}$$

is contained in the (m, ε_m^m)*–neighborhood of the* m^{th} *prefractal approximation* $\Gamma_{\mathcal{W}_m}$ *,*

$$\mathcal{D}\left(\Gamma_{\mathcal{W}_m}, \varepsilon_m^m\right) = \left\{M = (x,y) \in \mathbb{R}^2\,,\, d\left(M, \Gamma_{\mathcal{W}_m}\right) \leqslant \varepsilon_m^m\right\}\,; \tag{$\mathcal{R}$ 29}$$

namely,

$$\mathcal{D}\left(\Gamma_{\mathcal{W}_{m+k}}, \varepsilon_{m+k}^{m+k}\right) \subset \mathcal{D}\left(\Gamma_{\mathcal{W}_m}, \varepsilon_m^m\right)\,\cdot \tag{$\mathcal{R}$ 30}$$

Proof. This proof is based on the fact that the sequence of sets of vertices $(V_m)_{m\in\mathbb{N}}$ is increasing (see part *i.* of Property 2.4, on page 14), and that $V^\star = \bigcup_{n\in\mathbb{N}} V_n$ is dense in the Weierstrass Curve $\Gamma_{\mathcal{W}}$, along

with the fact that the prefractal graph sequence $\left(\Gamma_{\mathcal{W}_m}\right)_{m\in\mathbb{N}}$ converges to the Weierstrass Curve $\Gamma_{\mathcal{W}}$ (for example, in the sense of the Hausdorff metric on $\mathbb{R}^2$).

Given $m \in \mathbb{N}$, there exists an integer $k_{0,m} \in \mathbb{N}$ such that, for each integer $k \geqslant k_{0,m}$, we have that

$$d\left(\Gamma_{\mathcal{W}_m}, \Gamma_{\mathcal{W}_{m+k}}\right) = \inf_{\substack{0 \leqslant j \leqslant \#V_m - 1 \\ 0 \leqslant j' \leqslant \#V_{m+k} - 1}} \left\{ d\left(M_{j,m}, M_{j',m+k}\right),\ M_{j,m} \in V_m,\ M_{j',m+k} \in V_{m+k} \setminus V_m \right\} \leqslant \varepsilon_m^m .$$

We then deduce that for all $k \geqslant k_{0,m}$,

$$\Gamma_{\mathcal{W}_{m+k}} \subset \mathcal{D}\left(\Gamma_{\mathcal{W}_m}, \varepsilon_m^m\right) .$$

At the same time, since, for any $(m,k) \in \mathbb{N}^2$,

$$\varepsilon_{m+k}^{m+k} \leqslant \varepsilon_m^m ,$$

along with the fact that, for any $m \in \mathbb{N}$,

$$\lim_{k\to\infty} \varepsilon_{m+k}^{m+k} = 0 ,$$

we can find another integer $k_{1,m} \in \mathbb{N}$ such that, for each integer $k \geqslant k_{1,m}$, we have that

$$\mathcal{D}\left(\Gamma_{\mathcal{W}_{m+k}}, \varepsilon_{m+k}^{m+k}\right) \subset \mathcal{D}\left(\Gamma_{\mathcal{W}_m}, \varepsilon_m^m\right) .$$

The desired result is obtained by letting $k_m = \max\left\{k_{0,m}, k_{1,m}\right\}$.

□

Remark 3.3 (**Connection Between Fractality and the Cohomology Infinitesimal**).

As is mentioned in [DL22c], the cohomology infinitesimal (or, equivalently, the elementary length) – which obviously depends on the magnification scale (i.e., the chosen prefractal approximation) – can be seen as a transition scale between the fractal domain and the classical (or Euclidean) one. In fact, we could say that the system is fractal below this scale, and classical above (for the level of magnification considered). In the limit when the integer m associated with the prefractal approximation tends to infinity, the system is fractal below the cohomological infinitesimal (which is really an infinitesimal, in this case), i.e., at small scales, and is classical beyond, i.e., on a large scale. Note that this is in perfect agreement with what is evoked by the French physicist Laurent Nottale in [Not98] about scale–relativity.

The Complex Dimensions of a fractal set characterize their intrinsic vibrational properties. Thus far, the values of the Complex Dimensions were obtained by studying the oscillations of a small neighborhood of the boundary, i.e., of a tubular neighborhood, where points are located within an epsilon distance from any edge. In the case of our fractal Weierstrass Curve $\Gamma_{\mathcal{W}}$, which is, also, the limit of the sequence of (polygonal) prefractal approximations $\left(\Gamma_{\mathcal{W}_m}\right)_{m\in\mathbb{N}}$, it is natural – and consistent with the result of Property 3.9, on page 59 above – to envision the infinitesimal tubular neighborhood of $\Gamma_{\mathcal{W}}$ associated with the cohomology infinitesimal $\left(\varepsilon_m^m\right)_{m\in\mathbb{N}}$, as the limit of the (obviously convergent) sequence $\left(\mathcal{D}\left(\Gamma_{\mathcal{W}_m}, \varepsilon_m^m\right)\right)_{m\in\mathbb{N}}$ of ε_m^m–neighborhoods of $\Gamma_{\mathcal{W}_m}$, where, for each integer $m \in \mathbb{N}$, ε_m^m is the m^{th} cohomology infinitesimal introduced in Definition 3.1, on page 37 above.

4 Prefractal Tube Formulas, Complex Dimensions and Average Minkowski Content

4.1 Preliminaries

Property 4.1 (Fourier Series Expansion of the one–periodic Map $x \mapsto N_b^{-\{x\}}$ [LvF06]).

The fractional part map $\{\cdot\}$ is one–periodic. Hence, it is also the case of the map $x \mapsto N_b^{-\{x\}}$, which admits, with respect to the real variable x, the following Fourier Series expansion:

$$N_b^{-\{x\}} = \frac{N_b - 1}{N_b} \sum_{\ell \in \mathbb{Z}} \frac{e^{2\,i\,\pi\,m\,x}}{\ln N_b + 2\,i\,\ell\,\pi} = \frac{N_b - 1}{N_b} \sum_{\ell \in \mathbb{Z}} \frac{(N_b - 1)^{-i\,\ell\,\mathbf{p}}\,\left(\varepsilon_m^m\right)^{-i\,\ell\,\mathbf{p}}}{\ln N_b + 2\,i\,\ell\,\pi},$$

where, for each $\ell \in \mathbb{Z}$, the exponential Fourier coefficients c_ℓ have been obtained through

$$\begin{aligned} c_\ell = \int_0^1 N_b^{-t}\, e^{-2\,i\,\pi\,\ell\,t}\, dt &= \int_0^1 e^{-t\,\ln N_b}\, e^{-2\,i\,\pi\,\ell\,t}\, dt = -\frac{1}{\ln N_b + 2\,i\,\ell\,\pi}\left[e^{-t\,\ln N_b}\, e^{-2\,i\,\pi\,\ell\,t}\right]_{t=0}^1 \\ &= \frac{1}{\ln N_b + 2\,i\,\ell\,\pi}\left[1 - \frac{1}{N_b}\right] = \frac{N_b - 1}{N_b}\,\frac{1}{\ln N_b + 2\,i\,\ell\,\pi}\,. \end{aligned}$$

Thus, for any $x \in \mathbb{R}$,

$$N_b^{-\{x\}} = \frac{N_b - 1}{N_b} \sum_{\ell \in \mathbb{Z}} \frac{e^{2\,i\,\pi\,m\,x}}{\ln N_b + 2\,i\,\ell\,\pi}\,.$$

Note that since

$$x = -\ln_{N_b}\left((N_b - 1)\,\varepsilon_m^m\right),$$

one has, for every $m \in \mathbb{Z}$,

$$e^{2\,i\,\pi\,m\,x} = e^{-2\,i\,\pi\,m\,\ln_{N_b}\left((N_b-1)\,\varepsilon_m^m\right)} = e^{-2\,i\,\pi\,m\,\frac{\ln\left((N_b-1)\,\varepsilon_m^m\right)}{\ln N_b}}\,.$$

Definition 4.1 (Oscillatory Period).

Following [LvF00], [LvF06], [LRŽ17b], we introduce the *oscillatory period* of the Weierstrass IFD:

$$\mathbf{p} = \frac{2\,\pi}{\ln N_b}\,.$$

Definition 4.2 (ℓ^{th}–order Vibration Mode).

Given $\ell \in \mathbb{Z}$, we define *the ℓ^{th}–order vibration mode* as the one associated to $\ell\,\mathbf{p}$.

Property 4.2. *For any integer $\ell \in \mathbb{Z}$, as given in Property 4.1, on page 61,*

$$e^{2\,i\,\pi\,\ell\,x} = e^{-i\,\ell\,\mathbf{p}\,\ln\left((N_b-1)\,\varepsilon_m^m\right)} = \left((N_b-1)\,\varepsilon_m^m\right)^{-i\,\ell\,\mathbf{p}} = (N_b-1)^{-i\,\ell\,\mathbf{p}}\,\left(\varepsilon_m^m\right)^{-i\,\ell\,\mathbf{p}}\,,$$

where the oscillatory period $\mathbf{p}$ *has been introduced in Definition 4.1, on page 61 above.*

Thus, for any any $x \in \mathbb{R}$ *and any* $\varepsilon_m^m > 0$,

$$N_b^{-\{x\}} = \frac{N_b-1}{N_b}\,\sum_{\ell\,\in\,\mathbb{Z}}\frac{(N_b-1)^{-i\,\ell\,\mathbf{p}}\,\left(\varepsilon_m^m\right)^{-i\,\ell\,\mathbf{p}}}{\ln N_b + 2\,i\,\ell\,\pi}\quad,\quad N_b^{-D_{\mathcal{W}}\,\{x\}} = \frac{N_b^{D_{\mathcal{W}}}-1}{N_b^{D_{\mathcal{W}}}}\,\sum_{\ell\,\in\,\mathbb{Z}}\frac{\left(N_b^{D_{\mathcal{W}}}-1\right)^{-i\,\ell\,\mathbf{p}}\,\left(\varepsilon_m^m\right)^{-i\,\ell\,\mathbf{p}}}{D_{\mathcal{W}}\,\ln N_b + 2\,i\,\ell\,\pi}\,.$$

Definition 4.3 (**Effective Distance and Tube Zeta Functions Associated to an Arbitrary IFD of $\mathbb{R}^2$**)**.**

Let $\mathcal{F}^{\mathcal{I}}$ be an iterated fractal drum of $\mathbb{R}^2$; i.e., given a cohomology infinitesimal $\varepsilon_{\mathcal{F}} = \left(\varepsilon_{m,\mathcal{F}}^m\right)_{m\,\in\,\mathbb{N}}$, as introduced in Definition 3.2, on page 38, $\mathcal{F}^{\mathcal{I}}$ is a sequence of ordered pairs $\left(\mathcal{F}_m, \varepsilon_{m,\mathcal{F}}^m\right)_{m\,\in\,\mathbb{N}}$, where, for each $m \in \mathbb{N}$, $\mathcal{F}_m$ is the m^{th} prefractal approximation to a fractal curve $\mathcal{F}$.

We are assuming here that $\left(\varepsilon_{m,\mathcal{F}}^m\right)_{m\,\in\,\mathbb{N}}$ is a decreasing sequence of positive numbers tending to 0 as $m \to \infty$, such that, for all fixed $m \in \mathbb{N}$, $\lim\limits_{k_m\,\to\,\infty}\left(\varepsilon_{m,\mathcal{F}}^m - \varepsilon_{m+k_m,\mathcal{F}}^{m+k_m}\right) = 0$. This is the case, in particular, for the Weierstrass IFD, according to Definition 3.1, on page 37. Indeed, with the notation of the latter definition, we have that $\varepsilon_{m+1,\mathcal{F}}^{m+1} = \varepsilon_{m+1}^{m+1} = \dfrac{\varepsilon_m^m}{N_b}$, for all $m \in \mathbb{N}$. Hence, for any $k_m \in \mathbb{N}$, $\varepsilon_{m+k_m,\mathcal{F}}^{m+k_m} = \varepsilon_{m+k_m}^{m+k_m} = \dfrac{\varepsilon_m^m}{N_b^{k_m}}$.

Back to the general case of $\mathcal{F}^{\mathcal{I}}$, we hereafter consider the $\varepsilon_{m,\mathcal{F}}^m$–neighborhood (or $\varepsilon_{m,\mathcal{F}}^m$–tubular neighborhood) of $\mathcal{F}_m$,

$$\mathcal{D}\left(\mathcal{F}_m, \varepsilon_{m,\mathcal{F}}^m\right) = \left\{M \in \mathbb{R}^2\,,\, d\left(M, \mathcal{F}_m\right) \leqslant \varepsilon_{m,\mathcal{F}}^m\right\}\,, \tag{$\mathcal{R}$ 31}$$

of tubular volume (i.e., area) denoted $\mathcal{V}_{m,\mathcal{F}_m}\left(\varepsilon_{m,\mathcal{F}}^m\right)$.

In our present context, when it comes to obtaining the associated fractal tube zeta function, we cannot, as in the case of an arbitrary bounded subset of $\mathbb{R}^2$ (see [LRŽ17b], Definition 2.2.8, page 118), directly use an integral formula of the form

$$\tilde{\zeta}_{m,\mathcal{F}_m}(s) = \int_0^{\varepsilon_{m,\mathcal{F}}^m} t^{s-3}\,\mathcal{V}_{m,\mathcal{F}_m}(t)\,dt = \int_0^{\varepsilon_{m,\mathcal{F}}^m} t^{s-2}\,\mathcal{V}_{m,\mathcal{F}_m}(t)\,\frac{dt}{t}\,, \tag{$\mathcal{R}$ 32}$$

since the tube formulas that we will obtain in Subsection 4.2 below can only be expressed in an explicit way at a cohomology infinitesimal.

However, if, instead of considering the tube volume function at a given step m_0, we consider the more general tube volume functions *for all integers* $m \geqslant m_0$, we can then use Riemann sums, for the following nonuniform partition of the interval $\left[0, \varepsilon_{m,\mathcal{F}}^m\right]$: given an arbitrary nonnegative integer $k_m \geqslant m$,

$$\left[0, \varepsilon_{m,\mathcal{F}}^m\right] = \left[0, \varepsilon_{m\,k_m,\mathcal{F}}^{m\,k_m}\right] \bigcup \left\{\bigcup_{m+k_m+p\,=\,m\,k_m-2}^{m+k_m+p\,=\,m+k_m}\left[\varepsilon_{m+k_m+p+1,\mathcal{F}}^{m+k_m+p+1}, \varepsilon_{m+k+p,\mathcal{F}}^{m+k_m+p}\right]\right\} \bigcup \left[\varepsilon_{m+k_m,\mathcal{F}}^{m+k_m}, \varepsilon_{m,\mathcal{F}}^m\right]\,, \tag{$\mathcal{R}$ 33}$$

where the second union is taken over all $p \in \mathbb{N}$ satisfying the indicated relations and equalities.

Note that the mesh of the partition (i.e., the length of the largest subinterval) is

$$\varepsilon_{m,\mathcal{F}}^{m} - \varepsilon_{m+k,\mathcal{F}}^{m+k_m}, \quad \text{with} \quad \lim_{k_m \to \infty} \left(\varepsilon_{m,\mathcal{F}}^{m} - \varepsilon_{m+k_m,\mathcal{F}}^{m+k_m} \right) = 0 \cdot$$

We set

$$\sigma_{0,m\,k_m} = \varepsilon_{m\,k_m,\mathcal{F}}^{m\,k_m} \quad , \quad \sigma_{m,m+k_m} = \varepsilon_{m,\mathcal{F}}^{m} - \varepsilon_{m+k_m,\mathcal{F}}^{m+k_m}, \tag{$\mathcal{R}$ 34}$$

and, for all $p \in \{0, \cdots, m\,k_m - m - k_m - 2\}$,

$$\sigma_p = \varepsilon_{m+k_m+p,\mathcal{F}}^{m+k_m+p} - \varepsilon_{m+k_m+p+1,\mathcal{F}}^{m+k_m+p+1} \cdot \tag{$\mathcal{R}$ 35}$$

We can then introduce the Riemann sum

$$\begin{aligned} \mathcal{R}iemann\,(k_m, m, \mathcal{V}) \;\; = \;\; & \sigma_0 \left(\varepsilon_{m\,m,\mathcal{F}}^{m\,k_m} \right)^{s-3} \mathcal{V}_{m\,k_m,\mathcal{F}_{m\,k_m}} \left(\varepsilon_{m\,k,\mathcal{F}}^{m\,k_m} \right) + \sigma_{m+k_m} \left(\varepsilon_{m,\mathcal{F}}^{m} \right)^{s-3} \mathcal{V}_{m\,k_m,\mathcal{F}_{m\,k_m}} \left(\varepsilon_{m,\mathcal{F}}^{m} \right) \\ & + \sum_{0 \leqslant p \leqslant m\,k_m - m - k_m - 2} \sigma_p \left(\varepsilon_{m+k_m+p,\mathcal{F}}^{m+k_m+p} \right)^{s-3} \mathcal{V}_{m+k_m+p+1,\mathcal{F}_{m+k_m+p+1}} \left(\varepsilon_{m+k_m+p,\mathcal{F}}^{m+k_m+p} \right) \cdot \end{aligned} \tag{$\mathcal{R}$ 36}$$

We then have that

$$\lim_{k_m \to \infty} \mathcal{R}iemann\,(k_m, m, \mathcal{V}_m) = \int_0^{\varepsilon_{m,\mathcal{F}}^{m}} t^{s-2}\, \tilde{\mathcal{V}}_{m,\mathcal{F}_m}(t)\, \frac{dt}{t}, \tag{$\mathcal{R}$ 37}$$

where, for all sufficiently large $n \in \mathbb{N}^{\star}$, $\tilde{\mathcal{V}}_{n,\mathcal{F}_n}$ is the continuous function defined for all $t \in \left[0, \varepsilon_{n,\mathcal{F}}^{n}\right]$ by substituting t for $\varepsilon_{n,\mathcal{F}}^{n}$ in the expression for $\mathcal{V}_{n,\mathcal{F}_n}\left(\varepsilon_{n,\mathcal{F}}^{n}\right)$.

For the fractal power series obtained for $\tilde{\mathcal{V}}_{n,\mathcal{F}_n}$ in the case of the Weierstrass IFD of key interest to us in this paper, see Theorem 4.7, on page 72, in Subsection 4.2 below.

One can think of $\tilde{\mathcal{V}}_{n,\mathcal{F}_n} = \tilde{\mathcal{V}}_{n,\mathcal{F}_n}(t)$ as being *the effective volume* of the t–neighborhood of the n^{th} prefractal approximation to the fractal curve defined by the IFD $\mathcal{F}$, for every value of $t \in \left[0, \varepsilon_{n,\mathcal{F}}^{n}\right]$. Note that, in fact, $\tilde{\mathcal{V}}_{n,\mathcal{F}_n} = \tilde{\mathcal{V}}_{n,\mathcal{F}_n}(t)$ is given by the same (locally uniformly) convergent fractal power series for all nonzero $t \in \mathbb{C}$ with $|t| \leqslant \varepsilon_{n,\mathcal{F}}^{n}$ (by convention, $\tilde{\mathcal{V}}_{n,\mathcal{F}_n}(0) = \mathcal{V}_{n,\mathcal{F}_n}(0) = 0$); however, we will not make use of this observation in this paper.

We can then obtain the resulting m^{th} *effective local tube zeta function* $\tilde{\zeta}_{m,\mathcal{F}}^{e}$ – a generalization to IFDs of the usual definition referred to just above – defined for all s in $\mathbb{C}$ with sufficiently large real part (in fact, for $\mathcal{R}e(s) > D_{m,\mathcal{F}_m}$, where $D_{m,\mathcal{F}_m}$ is the abscissa of convergence of $\tilde{\zeta}_{m,\mathcal{F}_m}$), by

$$\tilde{\zeta}_{m,\mathcal{F}_m}^{e}(s) = \lim_{k \to \infty} \int_0^{\varepsilon_{m,\mathcal{F}}^{m}} t^{s-3}\, \tilde{\mathcal{V}}_{m,\mathcal{F}_m}(t)\, dt = \int_0^{\varepsilon_{m,\mathcal{F}}^{m}} t^{s-2}\, \tilde{\mathcal{V}}_{m,\mathcal{F}_m}(t)\, \frac{dt}{t} \cdot \tag{$\mathcal{R}$ 38}$$

Note that still for $\mathcal{R}e(s) > D_{m,\mathcal{F}}$, $\tilde{\zeta}_{m,\mathcal{F}_m}$ is also given by a limit of Riemann sums, as given in the identity ($\mathcal{R}$36), on page 63. This statement follows by combining relations ($\mathcal{R}$38) and ($\mathcal{R}$37)

As for the m^{th} *effective local distance zeta function* $\zeta_{m,\mathcal{F}}$, it can be deduced by the following *functional equation* (in the present case, when $\mathcal{F}_m \subset \mathbb{R}^2$), for the same value of $\varepsilon_{m,\mathcal{F}}^{m} > 0$,

$$\zeta_{m,\mathcal{F}_m}^{e}(s) = \left(\varepsilon_{m,\mathcal{F}}^{m}\right)^{s-2} \mathcal{V}_{m,\mathcal{F}_m}\left(\varepsilon_{m,\mathcal{F}}^{m}\right) + (2-s)\, \tilde{\zeta}_{m,\mathcal{F}_m}^{e}(s) \cdot \qquad (\blacklozenge) \tag{$\mathcal{R}$ 39}$$

Observe that since, by construction,

$$\mathcal{V}_{m,\mathcal{F}_m}\left(\varepsilon_{m,\mathcal{F}}^m\right) = \tilde{\mathcal{V}}_{m,\mathcal{F}_m}\left(\varepsilon_{m,\mathcal{F}}^m\right),$$

the associated functional equation of relation ($\mathcal{R}39$) just above is the exact analog of the functional equation connecting the usual tube and zeta functions of a bounded set (or, more generally, of a related fractal drum) in the standard higher–dimensional of Complex Dimensions developped in [LRŽ17b], as well as in [LRŽ17a], [LRŽ17c] and [LRŽ18].

Remark 4.1. We stress the fact that $\tilde{\zeta}_{m,\mathcal{F}_m}^e$ does not coincide with the usual tube zeta function $\tilde{\zeta}_{\mathcal{F}_m}$ associated with the m^{th} polygonal prefractal approximation $\mathcal{F}_m \subset \mathbb{R}^2$ to the fractal curve $\mathcal{F}$, given, as in [LRŽ17b], for all $s \in \mathbb{C}$ with $\mathcal{R}e(s)$ sufficiently large, by

$$\tilde{\zeta}_{\mathcal{F}_m}(s) = \int_0^{\varepsilon_{m,\mathcal{F}}^m} t^{s-3}\,\mathcal{V}_{m,\mathcal{F}_m}(t)\,dt = \int_0^{\varepsilon_{m,\mathcal{F}}^m} t^{s-2}\,\mathcal{V}_{m,\mathcal{F}_m}(t)\,\frac{dt}{t}\cdot$$

Similarly, $\zeta_{m,\mathcal{F}_m}^e$ does not coincide with the usual distance zeta function $\zeta_{\mathcal{F}_m}$ associated with the m^{th} polygonal prefractal approximation $\mathcal{F}_m \subset \mathbb{R}^2$ to the fractal curve $\mathcal{F}$, given, as in [LRŽ17b], for all $s \in \mathbb{C}$ with $\mathcal{R}e(s)$ sufficiently large, by

$$\zeta_{\mathcal{F}_m}(s) = \int_{M \in \mathcal{D}\left(\Gamma_{\mathcal{F}_m}, \varepsilon_{m,\mathcal{F}}^m\right)} \left(d\left(M, \mathcal{F}_m\right)\right)^{s-2}\ dt\,,$$

where $\mathcal{D}\left(\Gamma_{\mathcal{F}_m}, \varepsilon_{m,\mathcal{F}}^m\right)$ is the $\varepsilon_{m,\mathcal{F}}^m$–neighborhood (or $\varepsilon_{m,\mathcal{F}}^m$–tubular neighborhood) of $\mathcal{F}_m$, given by

$$\mathcal{D}\left(\Gamma_{\mathcal{F}_m}, \varepsilon_{m,\mathcal{F}}^m\right) = \left\{M \in \mathbb{R}^2,\, d\left(M, \mathcal{F}_m\right) \leqslant \varepsilon_{m,\mathcal{F}}^m\right\}\cdot$$

This entire comment applies, in particular, to the Weierstrass IFD, which is the central object of this paper.

Notation 11 (**Natural Volume Extension**)**.**

For the sake of simplicity, given $m \in \mathbb{N}$, we will from now on call *the* m^{th} *natural volume extension*, the volume extension function $\tilde{\mathcal{V}}_{m,\mathcal{F}_m}$ associated with $\mathcal{V}_{m,\mathcal{F}_m}$. Alternatively, as was mentioned earlier, $\tilde{\mathcal{V}}_{m,\mathcal{F}_m}$ will be called *the* m^{th} *effective tubular volume*. This notation and terminology apply, in particular, to the different volume functions involved in the discussion of the Weierstrass IFD in Subsection 4.2 below.

Remark 4.2 (**Consistency of our Approach in the Case of the Weierstrass IFD – Connection with Reality**)*.*

As shown in Remark 3.1, on page 37, the m^{th} prefractal approximations to the Weierstrass Curve become closer and closer as m increases. Hence, it makes sense to consider a continuous version of the tubular volume, where the discrete and the continuous, in a sense, eventually merge, for all $m \in \mathbb{N}^\star$ sufficiently large.

We can also note that, in real life, fractality is not always the result of a discrete process. On the contrary, fractal shapes develop continuously, as is the case, for instance, in biology.

Remark 4.3. It follows from the above relation ($\mathcal{R}39$), on page 63, along with the results (and their proofs) in [LRŽ17b], Corollary 2.2.20, on page 127, that, in a given domain of $\mathbb{C}$, the effective fractal zeta functions $\zeta^e_{m,\mathcal{F}_m}$ and $\widetilde{\zeta}^e_{m,\mathcal{F}_m}$ have the same poles (denoted by ω) with residues connected by the relation

$$\operatorname{res}\left(\widetilde{\zeta}^e_{m,\mathcal{F}_m},\omega\right)=\frac{1}{2-\omega}\operatorname{res}\left(\zeta^e_{m,\mathcal{F}_m},\omega\right),\qquad(\blacklozenge\blacklozenge)\tag{$\mathcal{R}40$}$$

in case $\omega\neq 2$ is a simple pole; and, similarly for the principal parts of $\zeta^e_{m,\mathcal{F}_m}$ and $\widetilde{\zeta}^e_{m,\mathcal{F}_m}$ at ω, in case $\omega\neq 2$ is a multiple pole. It follows, in particular, that, in the present new sense, the Complex Dimensions of $\mathcal{F}_m$ can be indifferently defined as the (visible) poles of the effective distance zeta function $\zeta^e_{m,\mathcal{F}_m}$ or of the effective tube zeta function $\widetilde{\zeta}^e_{m,\mathcal{F}_m}$.

We will show in Subsection 4.2 below that, in the case of the Weierstrass IFD, and for all integers m sufficiently large, $\widetilde{\zeta}^e_{m,\mathcal{F}_m}$ (and hence also, $\zeta^e_{m,\mathcal{F}_m}$, in light of relation ($\mathcal{R}40$), on page 65 above), has a meromorphic continuation to all of $\mathbb{C}$ and has Minkowski dimension strictly smaller than 2; so that its Complex Dimensions are simple and have real part strictly smaller than 2. Hence, for any Complex Dimension ω of the Weierstrass IFD, we have that ω is simple and $\omega\neq 2$. (See, especially, Theorem 4.8, on page 76, and Theorem 4.10, on page 81, along with Corollary 4.9, on page 80).

4.2 Prefractal Tube Formulas and Prefractal Effective Zeta Functions

In order to obtain the main results of this section – namely, Theorem 4.7, on page 72, Theorem 4.8, on page 76, and 4.11, on page 83, along with Corollary 4.9, on page 80, and Theorem 4.10, on page 81 below, we consider the contribution to the (pre)fractal tube formulas brought by the various types of geometric elements in the ε^m_m–neighborhood of $\Gamma_{\mathcal{W}_m}$, here, the rectangles and the wedges (in Property 4.3, on page 65, and Property 4.4, on page 68 respectively), thereby supplementing the study of the positive or negative contributions of the rectangles, triangles and extreme wedges carried out earlier in Section 3, and synthetized in Propositions 3.5–3.8, on pages 56–59 above. We stress the fact that, due to the above computations, the value of the m^{th} cohomology infinitesimal ε^m_m has to be *sufficiently small*. This means, in particular, that $m\in\mathbb{N}^\star$ has to be sufficiently large, throughout this subsection.

In the sequel, in the case when $\mathcal{F}$ is the Weierstrass IFD, we will write, for example, $\widetilde{\mathcal{V}}_{m,\Gamma_{\mathcal{W}_m}}$, $\mathcal{V}_{m,\Gamma_{\mathcal{W}_m}}$, $\widetilde{\zeta}^e_{m,\Gamma_{\mathcal{W}}}$, $\zeta^e_{m,\Gamma_{\mathcal{W}}}$, instead of $\widetilde{\mathcal{V}}_{m,\mathcal{F}_m}$, $\mathcal{V}_{m,\mathcal{F}_m}$, $\widetilde{\zeta}^e_{m,\mathcal{F}_m}$, $\zeta^e_{m,\mathcal{F}_m}$, respectively. And similarly for the corresponding expressions associated with the contributions of the rectangles, wedges, outer triangles and parallelograms, for instance, as in Section 3 above.

Property 4.3 (**Tube Formula and Effective Tube Zeta Function Associated to the Contribution of the Rectangles to the Tubular Volume**).

Given $m\in\mathbb{N}^\star$, with Notation 11, on page 64, the contribution $\widetilde{\mathcal{V}}_{m,\Gamma_{\mathcal{W}_m},Rectangles}\left(\varepsilon^m_m\right)$ of the $2\left(N_b-1\right)N_b^m$ ***rectangles*** *to the effective tubular volume $\widetilde{\mathcal{V}}_{m,\Gamma_{\mathcal{W}_m}}\left(\varepsilon^m_m\right)$ is*

$$\begin{aligned}\widetilde{\mathcal{V}}_{m,\Gamma_{\mathcal{W}_m},Rectangles}\left(\varepsilon^m_m\right)&=2\sum_{k=0}^{\infty}\binom{\frac{1}{2}}{k}N_b^{-(1-k(2-D_{\mathcal{W}}))\{x\}}\left(\varepsilon^m_m\right)^{2-D_{\mathcal{W}}+k(2-D_{\mathcal{W}})}\mathcal{O}(1)\\&=2\sum_{k=0}^{\infty}\binom{\frac{1}{2}}{k}\frac{N_b^{1-k(2-D_{\mathcal{W}})}-1}{N_b^{1-k(2-D_{\mathcal{W}})}}\sum_{\ell\in\mathbb{Z}}\frac{\left(N_b-1\right)^{-i\ell\mathbf{p}}\left(\varepsilon^m_m\right)^{2-D_{\mathcal{W}}+k(2-D_{\mathcal{W}})-i\ell\mathbf{p}}}{(1-k(2-D_{\mathcal{W}}))\ln N_b+2i\ell\pi}\mathcal{O}(1)\,.\end{aligned}\tag{$\mathcal{R}41$}$$

Recall from the discussion in Subsection 4.1 that, by construction,

$$\tilde{\mathcal{V}}_{m,\Gamma_{\mathcal{W}_m},Rectangles}\left(\varepsilon_m^m\right) = \mathcal{V}_{m,\Gamma_{\mathcal{W}_m},Rectangles}\left(\varepsilon_m^m\right) \cdot$$

For the sake of clarity, and in order to avoid confusion between various occurrences of $\mathcal{O}(1)$, we will write relation ($\mathcal{R}41$) in the form

$$\tilde{\mathcal{V}}_{m,\Gamma_{\mathcal{W}_m},Rectangles}\left(\varepsilon_m^m\right) = C_{Rectangles} \sum_{k=0}^{\infty} \binom{\frac{1}{2}}{k} \frac{N_b^{1-k(2-D_{\mathcal{W}})} - 1}{N_b^{1-k(2-D_{\mathcal{W}})}} \sum_{\ell \in \mathbb{Z}} \frac{(N_b-1)^{-i\ell\mathbf{p}} \left(\varepsilon_m^m\right)^{2-D_{\mathcal{W}}+k(2-D_{\mathcal{W}})-i\ell\mathbf{p}}}{(1-k(2-D_{\mathcal{W}}))\ln N_b + 2i\ell\pi}, \tag{$\mathcal{R}42$}$$

where $C_{Rectangles}$ denotes a strictly positive and finite constant, depending on $m \in \mathbb{N}^\star$, but uniformly bounded away from 0 and ∞ (i.e., here and in the sequel, independently of $m \in \mathbb{N}^\star$ large enough); see Proposition 3.5, on page 56.

The associated m^{th} (local) effective tube zeta function *(see Definition 4.3, on page 62 above) is first obtained, for any complex number s such that $\mathcal{R}e(s) > D_{\mathcal{W}}$, as follows:*

$$\begin{aligned}
\tilde{\zeta}^e_{m,Rectangles}(s) &= \int_0^{\varepsilon_m^m} t^{s-3}\, \tilde{\mathcal{V}}_{m,\Gamma_{\mathcal{W}_m},Rectangles}(t)\, dt \\
&= C_{Rectangles} \sum_{k=0}^{\infty} \binom{\frac{1}{2}}{k} \frac{N_b^{1-k(2-D_{\mathcal{W}})} - 1}{N_b^{1-k(2-D_{\mathcal{W}})}} \sum_{\ell \in \mathbb{Z}} \frac{(N_b-1)^{-i\ell\mathbf{p}}}{(1-k(2-D_{\mathcal{W}}))\ln N_b + 2i\ell\pi} \int_0^{\varepsilon_m^m} t^{s-3}\, t^{2-D_{\mathcal{W}}+k(2-D_{\mathcal{W}})-i\ell\mathbf{p}}\, dt \\
&= C_{Rectangles} \sum_{k=0}^{\infty} \binom{\frac{1}{2}}{k} \frac{N_b^{1-k(2-D_{\mathcal{W}})} - 1}{N_b^{1-k(2-D_{\mathcal{W}})}} \sum_{\ell \in \mathbb{Z}} \frac{(N_b-1)^{-i\ell\mathbf{p}}}{(1-k(2-D_{\mathcal{W}}))\ln N_b + 2i\ell\pi} \frac{\left(\varepsilon_m^m\right)^{s-D_{\mathcal{W}}+k(2-D_{\mathcal{W}})-i\ell\mathbf{p}}}{s-D_{\mathcal{W}}+k\,(2-D_{\mathcal{W}})-i\ell\mathbf{p}} \cdot
\end{aligned} \tag{$\mathcal{R}43$}$$

where, as in Notation 11, on page 64 (and the discussion preceeding it), $\tilde{\mathcal{V}}_{m,\Gamma_{\mathcal{W}_m},Rectangles}$ is the natural volume extension function associated with $\mathcal{V}_{m,\Gamma_{\mathcal{W}_m},Rectangles}$, which means that $\tilde{\mathcal{V}}_{m,\Gamma_{\mathcal{W}_m},Rectangles}$ is the function defined for all $t \in \left[0, \varepsilon_m^m\right]$ by substituting t for ε_m^m in the fractal power series obtained for $\mathcal{V}_{m,Rectangles}\left(\varepsilon_m^m\right)$ in relation ($\mathcal{R}42$), or, equivalently, in relation ($\mathcal{R}41$).

We call this zeta function $\tilde{\zeta}^e_{m,Rectangles}$ the m^{th} local effective tube zeta function *(associated with the rectangles), because it is the zeta function associated* ***not only*** *with the m^{th} prefractal approximation to the Weierstrass Curve $\Gamma_{\mathcal{W}}$, but, also,* ***with the infinitesimal*** *ε_m^m which conveys* ***the scaling relation associated to the limit fractal object****; i.e., $\Gamma_{\mathcal{W}}$. The same comment holds for the forthcoming local zeta functions introduced in Properties 4.4–4.6, on pages 68—71.*

By meromorphic continuation to all of $\mathbb{C}$, one then obtains the (local) effective tube zeta function $\tilde{\zeta}^e_{m,Rectangles}$ for all $s \in \mathbb{C}$, as given by the last two equalities in relation ($\mathcal{R}43$) just above.

Furthermore, the abscissa of absolute convergence of the Dirichlet–type integral (DTI) involved in the definition of $\tilde{\zeta}^e_{m,Rectangles}$, in the sense of [LRŽ17b] (Appendix A), is equal to $D_{\mathcal{W}}$.

The associated Complex Dimensions arise as

$$D_{\mathcal{W}} - k\,(2-D_{\mathcal{W}}) + i\ell\mathbf{p} \quad , \quad \text{with } k \in \mathbb{N}\,,\ \ell \in \mathbb{Z}\,\cdot$$

Note that, thanks to the results of Corollary 2.15, on page 27, the one–periodic function (with respect to the variable $\ln_{N_b}\left(\varepsilon_m^m\right)^{-1}$*, see Property 4.1, on page 61), associated to the above Complex Dimensions with real part* $D_{\mathcal{W}}$*, is bounded between two strictly positive and finite constants.*

Remark 4.4. In the proof of Theorem 4.8, on page 76, we will show that the series appearing on the right–hand side of the expression of $\tilde{\mathcal{V}}_{m,\Gamma_{\mathcal{W}_m},\text{Rectangles}}\left(\varepsilon_m^m\right)$ in formulas ($\mathcal{R}41$)–($\mathcal{R}42$) in Property 4.3, on page 65 (for all $m \geqslant 1$ large enough) is absolutely convergent – and hence also, convergent. We will also explain how to derive the expression for the tube zeta function $\tilde{\zeta}_{m,\text{Rectangles}}$ (again, for all $m \geqslant 1$ large enough), via an application of the (truncated) Mellin transform to the function $t \mapsto \tilde{\mathcal{V}}_{m,\text{Rectangles}}(t)$, defined for all $t \in \left[0, \varepsilon_m^m\right]$, followed by meromorphic continuation to all of $\mathbb{C}$. We refer to that same proof for the other statements concerning $\tilde{\zeta}^e_{m,\text{Rectangles}}$ and the associated (possible) poles (i.e., the Complex Dimensions of the Weierstrass IFD).

An entirely similar comment could be made (still for all $m \geqslant 1$ sufficiently large) about $\tilde{\mathcal{V}}_{m,\Gamma_{\mathcal{W}_m},\text{wedges}}\left(\varepsilon_m^m\right)$ and $\tilde{\zeta}^e_{m,\text{wedges}}$ in Property 4.4, on page 68, $\tilde{\mathcal{V}}_{m,\Gamma_{\mathcal{W}_m},\text{extra outer triangles}}\left(\varepsilon_m^m\right)$ and $\tilde{\zeta}^e_{m,\text{extra outer triangles}}$ in Property 4.5, on page 70, $\tilde{\mathcal{V}}_{m,\Gamma_{\mathcal{W}_m},\text{parallelograms}}\left(\varepsilon_m^m\right)$ and $\tilde{\zeta}^e_{m,\text{parallelograms}}$ in Property 4.6, on page 71, as well as about

$$\begin{aligned}\tilde{\mathcal{V}}_{m,\Gamma_{\mathcal{W}_m}}\left(\varepsilon_m^m\right) \;=\; & \tilde{\mathcal{V}}_{m,\Gamma_{\mathcal{W}_m},\text{Rectangles}}\left(\varepsilon_m^m\right) + \tilde{\mathcal{V}}_{m,\Gamma_{\mathcal{W}_m},\text{wedges}}\left(\varepsilon_m^m\right) \\ & + \tilde{\mathcal{V}}_{m,\Gamma_{\mathcal{W}_m},\text{extra outer triangles}}\left(\varepsilon_m^m\right) + \tilde{\mathcal{V}}_{m,\Gamma_{\mathcal{W}_m},\text{parallelograms}}\left(\varepsilon_m^m\right),\end{aligned} \tag{$\mathcal{R}$ 44}$$

and

$$\tilde{\zeta}^e_{m,\mathcal{W}_m}(s) = \tilde{\zeta}^e_{m,\text{Rectangles}}(s) + \tilde{\zeta}^e_{m,\text{wedges}}(s) + \tilde{\zeta}^e_{m,\text{extra outer triangles}}(s) + \tilde{\zeta}^e_{m,\text{parallelograms}}(s), \tag{$\mathcal{R}$ 45}$$

in Theorem 4.7, on page 72, and Theorem 4.8, on page 76.

Remark 4.5. Recall from [LRŽ17b] that the abscissa of convergence σ_m of $\tilde{\zeta}^e_{m,\text{Rectangles}}$ is the unique (possibly extended) real number σ_m such that the DTI defining $\tilde{\zeta}^e_{m,\text{Rectangles}}$ (in the first equality in relation ($\mathcal{R}43$) above, on page 66), converges for $\mathcal{R}e(s) > \sigma_m$ and diverges for $\mathcal{R}e(s) < \sigma_m$. Here, in the light of the identity ($\mathcal{R}43$), we have that $\sigma_m = D_{\mathcal{W}}$, for all $m \in \mathbb{N}^\star$ large enough. An analogous comment applies to all the other DTIs encountered in this subsection, and in Subsection 4.3, including, especially, $\tilde{\zeta}^e_{m,\text{wedges}}$, $\tilde{\zeta}^e_{m,\text{extra outer triangles}}$, $\tilde{\zeta}^e_{m,\text{parallelograms}}$.

Property 4.4 (Tube Formula and Effective Tube Zeta Function Associated to the Contribution of the Wedges to the Tubular Volume).

*Given $m \in \mathbb{N}^\star$ sufficiently large, with Notation 11, on page 64, the contribution of the **wedges** to the effective tubular volume $\tilde{\mathcal{V}}_{m,\Gamma_{\mathcal{W}_m}}\left(\varepsilon_m^m\right)$ is*

$$
\begin{aligned}
\tilde{\mathcal{V}}_{m,\Gamma_{\mathcal{W}_m},wedges}\left(\varepsilon_m^m\right) = \quad & \tilde{\mathcal{V}}_{m,\Gamma_{\mathcal{W}_m},upper\ wedges}\left(\varepsilon_m^m\right) + \tilde{\mathcal{V}}_{m,\Gamma_{\mathcal{W}_m},lower\ wedges}\left(\varepsilon_m^m\right) + \tilde{\mathcal{V}}_{m,\Gamma_{\mathcal{W}_m},extreme\ wedges}\left(\varepsilon_m^m\right) \\
= \quad & \frac{r_b\,\pi\,\left(\varepsilon_m^m\right)^3}{8}\,N_b^{-\{x\}} - \frac{\pi\,\left(\varepsilon_m^m\right)^4}{2} + \pi\,\left(\varepsilon_m^m\right)^2 \\
& -\frac{\left(\varepsilon_m^m\right)^3}{4}\,r_b\,\sum_{k=0}^{\infty}\frac{(-1)^k}{2\,k+1}\,N_b^{-((2\,k+1)\,D_{\mathcal{W}}-2\,k)\,\{x\}}\,\left(\varepsilon_m^m\right)^{2\,k+1}\,\mathcal{O}(1) \\
& +\frac{\left(\varepsilon_m^m\right)^4}{2}\,\sum_{k=0}^{\infty}\frac{(-1)^k}{2\,k+1}\,N_b^{-((2\,k+1)\,D_{\mathcal{W}}-2\,k+1)\,\{x\}}\,\left(\varepsilon_m^m\right)^{2\,k+1}\,\mathcal{O}(1) \\
= \quad & \frac{r_b\,\pi}{8}\,\frac{N_b-1}{N_b}\,\sum_{\ell\in\mathbb{Z}}\frac{(N_b-1)^{-i\,\ell\,\mathbf{p}}\,\left(\varepsilon_m^m\right)^{3-i\,\ell\,\mathbf{p}}}{\ln N_b + 2\,i\,\ell\,\pi} - \frac{\pi\,\left(\varepsilon_m^m\right)^4}{2} + \pi\,\left(\varepsilon_m^m\right)^2 \\
& -\frac{1}{4}\,r_b\,\sum_{k=0}^{\infty}\frac{(-1)^k}{2\,k+1}\,\frac{N_b^{((2\,k+1)\,D_{\mathcal{W}}-2\,k)}-1}{N_b^{((2\,k+1)\,D_{\mathcal{W}}-2\,k)}}\,\sum_{\ell\in\mathbb{Z}}\frac{(N_b^{((2\,k+1)\,D_{\mathcal{W}}-2\,k)}-1)^{-i\,\ell\,\mathbf{p}}\,\left(\varepsilon_m^m\right)^{2\,k+1-i\,\ell\,\mathbf{p}}}{((2\,k+1)\,D_{\mathcal{W}}-2\,k)\,\ln N_b + 2\,i\,\ell\,\pi}\,\mathcal{O}(1) \\
& +\frac{1}{2}\,\sum_{k=0}^{\infty}\frac{(-1)^k}{2\,k+1}\,\frac{N_b^{(2\,k+1)\,(D_{\mathcal{W}}-1)}-1}{N_b^{(2\,k+1)\,(D_{\mathcal{W}}-1)}}\,\sum_{\ell\in\mathbb{Z}}\frac{(N_b^{(2\,k+1)\,D_{\mathcal{W}}-2\,k+1}-1)^{-i\,\ell\,\mathbf{p}}\,\left(\varepsilon_m^m\right)^{5+2\,k-i\,\ell\,\mathbf{p}}}{((2\,k+1)\,D_{\mathcal{W}}-2\,k+1)\,\ln N_b + 2\,i\,\ell\,\pi}\,.
\end{aligned}
\tag{$\mathcal{R}$ 46}
$$

Recall from Subsection 4.1 that

$$
\tilde{\mathcal{V}}_{m,\Gamma_{\mathcal{W}_m},\star,wedges}\left(\varepsilon_m^m\right) = \mathcal{V}_{m,\Gamma_{\mathcal{W}_m},\star,wedges}\left(\varepsilon_m^m\right)\,,
$$

where $\star$ = upper, lower, or extreme. Hence, in light of the first equality in relation ($\mathcal{R}$46), an analogous identity holds if $\star, wedges$ is replaced by "wedges" .

As before, for the sake of clarity, we will rewrite relation ($\mathcal{R}$46) in the form

$$
\begin{aligned}
\tilde{\mathcal{V}}_{m,\Gamma_{\mathcal{W}_m},wedges}\left(\varepsilon_m^m\right) = \quad & C^1_{wedges}\,\sum_{\ell\in\mathbb{Z}}\frac{(N_b-1)^{-i\,\ell\,\mathbf{p}}\,\left(\varepsilon_m^m\right)^{3-i\,\ell\,\mathbf{p}}}{\ln N_b + 2\,i\,\ell\,\pi} - \frac{\pi\,\left(\varepsilon_m^m\right)^4}{2} + \pi\,\left(\varepsilon_m^m\right)^2 \\
& -C^2_{wedges}\,\sum_{k=0}^{\infty}\frac{(-1)^k}{2\,k+1}\,\frac{N_b^{((2\,k+1)\,D_{\mathcal{W}}-2\,k)}-1}{N_b^{((2\,k+1)\,D_{\mathcal{W}}-2\,k)}}\,\sum_{\ell\in\mathbb{Z}}\frac{(N_b^{((2\,k+1)\,D_{\mathcal{W}}-2\,k)}-1)^{-i\,\ell\,\mathbf{p}}\,\left(\varepsilon_m^m\right)^{2\,k+1-i\,\ell\,\mathbf{p}}}{((2\,k+1)\,D_{\mathcal{W}}-2\,k)\,\ln N_b + 2\,i\,\ell\,\pi} \\
& +C^3_{wedges}\,\sum_{k=0}^{\infty}\frac{(-1)^k}{2\,k+1}\,\frac{N_b^{(2\,k+1)\,(D_{\mathcal{W}}-1)}-1}{N_b^{(2\,k+1)\,(D_{\mathcal{W}}-1)}}\,\sum_{\ell\in\mathbb{Z}}\frac{(N_b^{(2\,k+1)\,D_{\mathcal{W}}-2\,k+1}-1)^{-i\,\ell\,\mathbf{p}}\,\left(\varepsilon_m^m\right)^{5+2\,k-i\,\ell\,\mathbf{p}}}{((2\,k+1)\,D_{\mathcal{W}}-2\,k+1)\,\ln N_b + 2\,i\,\ell\,\pi}\,,
\end{aligned}
\tag{$\mathcal{R}$ 47}
$$

where C^1_{wedges}, C^2_{wedges}, *and* C^3_{wedges} *denote strictly positive and finite constants depending on* m, *but uniformly bounded away from* 0 *and* ∞ *(see Proposition 3.6, on page 57).*

The associated (local) effective tube zeta function *(see Definition 4.3, on page 62 above) is first obtained, for any complex number* s *such that* $\mathcal{R}e(s) > D_{\mathcal{W}}$, *as follows:*

$$
\begin{aligned}
\tilde{\zeta}^e_{m,wedges}(s) = & \int_0^{\varepsilon_m^m} t^{s-3}\, \tilde{\mathcal{V}}_{m,,\Gamma_{\mathcal{W}_m},wedges}(t)\, dt \\
= & \quad C^1_{wedges} \sum_{\ell\in\mathbb{Z}} \frac{(N_b-1)^{-i\,\ell\,\mathbf{p}}}{\ln N_b + 2\,i\,\ell\,\pi} \int_0^{\varepsilon_m^m} t^{s-i\,\ell\,\mathbf{p}}\, dt + \pi \int_0^{\varepsilon_m^m} t^{s-1}\, dt - \frac{\pi}{2} \int_0^{\varepsilon_m^m} t^{s+1}\, dt \\
& - C^2_{wedges} \sum_{k=0}^{\infty} \frac{(-1)^k}{2\,k+1} \frac{N_b^{((2\,k+1)\,D_{\mathcal{W}}-2\,k)}-1}{N_b^{((2\,k+1)\,D_{\mathcal{W}}-2\,k)}} \sum_{\ell\in\mathbb{Z}} \frac{(N_b^{((2\,k+1)\,D_{\mathcal{W}}-2\,k)}-1)^{-i\,\ell\,\mathbf{p}}}{((2\,k+1)\,D_{\mathcal{W}}-2\,k)\,\ln N_b + 2\,i\,\ell\,\pi} \int_0^{\varepsilon_m^m} t^{s+2\,k+1-i\,\ell\,\mathbf{p}}\, dt \\
& + C^3_{wedges} \sum_{k=0}^{\infty} \frac{(-1)^k}{2\,k+1} \frac{(-1)^k}{2\,k+1} \frac{N_b^{(2\,k+1)\,(D_{\mathcal{W}}-2\,k+1)}-1}{N_b^{(2\,k+1)\,D_{\mathcal{W}}-2\,k+1)}} \frac{(N_b^{(2\,k+1)\,D_{\mathcal{W}}-2\,k+1}-1)^{-i\,\ell\,\mathbf{p}}}{((2\,k+1)\,D_{\mathcal{W}}-2\,k+1)\,\ln N_b + 2\,i\,\ell\,\pi} \int_0^{\varepsilon_m^m} t^{s-2+2\,k-i\,\ell\,\mathbf{p}}\, dt \\
= & \quad C^1_{wedges} \sum_{\ell\in\mathbb{Z}} \frac{(N_b-1)^{-i\,\ell\,\mathbf{p}}}{\ln N_b + 2\,i\,\ell\,\pi} \frac{(\varepsilon_m^m)^{s+1-i\,\ell\,\mathbf{p}}}{s+1-i\,\ell\,\mathbf{p}} + \frac{\pi\,(\varepsilon_m^m)^s}{s} - \frac{\pi\,(\varepsilon_m^m)^{s+2}}{2\,(s+2)} \\
& - C^2_{wedges} \sum_{k=0}^{\infty} \frac{(-1)^k}{2\,k+1} \frac{N_b^{((2\,k+1)\,D_{\mathcal{W}}-2\,k)}-1}{N_b^{((2\,k+1)\,D_{\mathcal{W}}-2\,k)}} \sum_{\ell\in\mathbb{Z}} \frac{(N_b^{((2\,k+1)\,D_{\mathcal{W}}-2\,k)}-1)^{-i\,\ell\,\mathbf{p}}}{((2\,k+1)\,D_{\mathcal{W}}-2\,k)\,\ln N_b + 2\,i\,\ell\,\pi} \frac{(\varepsilon_m^m)^{s+2\,k-1-i\,\ell\,\mathbf{p}}}{s+2\,k-1-i\,\ell\,\mathbf{p}} \\
& + C^3_{wedges} \sum_{k=0}^{\infty} \frac{(-1)^k}{2\,k+1} \frac{N_b^{(2\,k+1)\,(D_{\mathcal{W}}-2\,k+1)}-1}{N_b^{(2\,k+1)\,D_{\mathcal{W}}-2\,k+1)}} \sum_{\ell\in\mathbb{Z}} \frac{(N_b^{(2\,k+1)\,D_{\mathcal{W}}-2\,k+1}-1)^{-i\,\ell\,\mathbf{p}}}{((2\,k+1)\,D_{\mathcal{W}}-2\,k+1)\,\ln N_b + 2\,i\,\ell\,\pi} \frac{(\varepsilon_m^m)^{s+3+2\,k-i\,\ell\,\mathbf{p}}}{s+3+2\,k-i\,\ell\,\mathbf{p}}\,.
\end{aligned}
\tag{$\mathcal{R}$ 48}
$$

By meromorphic continuation to all of $\mathbb{C}$, *one then obtains* $\tilde{\zeta}^e_{m,wedges}$, *the (local) effective tube zeta function (associated with the wedges), for all* $s \in \mathbb{C}$, *as given by the last two equalities in relation ($\mathcal{R}$48) just above.*

The associated Complex Dimensions arise as

$$
-1 + i\,\ell\,\mathbf{p} \quad , \quad 1 - 2\,k + i\,\ell\,\mathbf{p} \quad , \quad -3 - 2\,k + i\,\ell\,\mathbf{p} \quad , \quad \textit{with } k \in \mathbb{N}\,,\ \ell \in \mathbb{Z}\,, \textit{ along with } 0 \textit{ and } -2\,\cdot
$$

Note that for $k \geqslant 2$ *(and any* $\ell \in \mathbb{Z}$*), the last two families of (possible) Complex Dimensions fully overlap. We will take this fact into account in Theorem 4.10, on page 81, and Theorem 4.11, on page 83 below.*

Property 4.5 (**Tube Formula and Effective Tube Zeta Function Associated to the Contribution of the Extra Outer Triangles to the Tubular Volume**).

Given $m \in \mathbb{N}^\star$ sufficiently large, with Notation 11, on page 64, we obtain, for the negative contribution of the ***extra outer triangles*** *to the effective tubular volume $\tilde{\mathcal{V}}_{m,\Gamma_{\mathcal{W}_m}}\left(\varepsilon_m^m\right)$,*

$$\begin{aligned}
\tilde{\mathcal{V}}_{m,\Gamma_{\mathcal{W}_m},\textit{extra outer triangles}}\left(\varepsilon_m^m\right) &= \tilde{\mathcal{V}}_{m,\Gamma_{\mathcal{W}_m},\textit{extra outer lower triangles}}\left(\varepsilon_m^m\right) + \tilde{\mathcal{V}}_{m,\Gamma_{\mathcal{W}_m},\textit{extra outer upper triangles}}\left(\varepsilon_m^m\right) \\
&= -\frac{\left(\varepsilon_m^m\right)^2}{2}\, N_b^{(3-D_{\mathcal{W}})\,\{x\}}\, \mathcal{O}(1) \\
&= -\frac{N_b^{D_{\mathcal{W}}-3}-1}{N_b^{D_{\mathcal{W}}-3}} \sum_{\ell\in\mathbb{Z}} \frac{\left(N_b^{D_{\mathcal{W}}-3}-1\right)^{-i\,\ell\,\mathbf{p}}\,\left(\varepsilon_m^m\right)^{2-i\,\ell\,\mathbf{p}}}{(D_{\mathcal{W}}-3)\,\ln N_b + 2\,i\,\ell\,\pi}\,\mathcal{O}(1)\,,
\end{aligned} \tag{$\mathcal{R}$ 49}$$

with

$$0 < C_{inf}^3 \leqslant \mathcal{O}(1) \leqslant C_{sup}^3 < \infty\,.$$

Recall from Subsection 4.1 that $\tilde{\mathcal{V}}_{m,\Gamma_{\mathcal{W}_m},\star}\left(\varepsilon_m^m\right) = \mathcal{V}_{m,\Gamma_{\mathcal{W}_m},\star}\left(\varepsilon_m^m\right)$, where $\star$ = extra outer lower triangles, or extra outer upper triangles. Hence, in light of the first equality in relation ($\mathcal{R}$49), we also have that $\tilde{\mathcal{V}}_{m,\Gamma_{\mathcal{W}_m},\textit{extra outer triangles}}\left(\varepsilon_m^m\right) = \mathcal{V}_{m,\Gamma_{\mathcal{W}_m},\textit{extra outer triangles}}\left(\varepsilon_m^m\right)$.

As previously, for the sake of clarity, we will write relation ($\mathcal{R}$49) in the following form:

$$\tilde{\mathcal{V}}_{m,,\Gamma_{\mathcal{W}_m},\textit{extra outer triangles}}\left(\varepsilon_m^m\right) = -C_{\textit{triangles}} \sum_{\ell\in\mathbb{Z}} \frac{\left(N_b^{D_{\mathcal{W}}-3}-1\right)^{-i\,\ell\,\mathbf{p}}\,\left(\varepsilon_m^m\right)^{2-i\,\ell\,\mathbf{p}}}{(D_{\mathcal{W}}-3)\,\ln N_b + 2\,i\,\ell\,\pi}\,, \tag{$\mathcal{R}$ 50}$$

where $C_{\textit{triangles}}$ denotes a strictly positive and finite constant, depending on m, but uniformly bounded away from 0 and ∞ (in $m \in \mathbb{N}^\star$ sufficiently large); see Proposition 3.7, on page 58. More specifically,

$$0 < C_{inf}^3 \leqslant C_{\textit{triangles}} \leqslant C_{sup}^3 < \infty\,.$$

The associated (local) effective tube zeta function *(see Definition 4.3, on page 62 above) is first obtained, for any complex number s such that $\mathcal{R}e(s) > D_{\mathcal{W}}$, as follows:*

$$\begin{aligned}
\tilde{\zeta}^e_{m,\textit{extra outer triangles}}(s) &= \int_0^{\varepsilon_m^m} t^{s-3}\,\tilde{\mathcal{V}}_{m,,\Gamma_{\mathcal{W}_m},\textit{extra outer triangles}}(t)\,dt \\
&= -C_{\textit{triangles}} \sum_{\ell\in\mathbb{Z}} \frac{\left(N_b^{D_{\mathcal{W}}-3}-1\right)^{-i\,\ell\,\mathbf{p}}}{(2-3\,D_{\mathcal{W}})\,\ln N_b + 2\,i\,\ell\,\pi} \int_0^{\varepsilon_m^m} t^{s-2-i\,\ell\,\mathbf{p}}\,dt \\
&= -C_{\textit{triangles}} \sum_{\ell\in\mathbb{Z}} \frac{\left(N_b^{D_{\mathcal{W}}-3}-1\right)^{-i\,\ell\,\mathbf{p}}}{(D_{\mathcal{W}}-3)\,\ln N_b + 2\,i\,\ell\,\pi}\,\frac{\left(\varepsilon_m^m\right)^{s-1-i\,\ell\,\mathbf{p}}}{s-1-i\,\ell\,\mathbf{p}}\,.
\end{aligned} \tag{$\mathcal{R}$ 51}$$

By meromorphic continuation to all of $\mathbb{C}$, one then obtains $\tilde{\zeta}^e_{m,\textit{extra triangles}}$, the (local) effective tube zeta function (associated with the extra outer triangles), for all $s \in \mathbb{C}$, as given by the last two

equalities in relation (R51) just above.

The associated Complex Dimensions arise as

$$1 + i\,\ell\,\mathbf{p}\,,\ \textit{with}\ \ell \in \mathbb{Z}\,\cdot$$

Property 4.6 (**Tube Formula and Effective Tube Zeta Function Associated to the Contribution of the Parallelograms to the Tubular Volume**).

Given $m \in \mathbb{N}^\star$ sufficiently large, with Notation 11, on page 64, the last contribution to the effective tubular volume $\tilde{\mathcal{V}}_{m,\Gamma_{\mathcal{W}_m}}\left(\varepsilon_m^m\right)$, coming from the parallelograms, is given by

$$\begin{aligned}\tilde{\mathcal{V}}_{m,\Gamma_{\mathcal{W}_m},\textit{parallelograms}}\left(\varepsilon_m^m\right) &= \tilde{\mathcal{V}}_{m,\Gamma_{\mathcal{W}_m},\textit{lower parallelograms}}\left(\varepsilon_m^m\right) + \tilde{\mathcal{V}}_{m,\Gamma_{\mathcal{W}_m},\textit{upper parallelograms}}\left(\varepsilon_m^m\right)\\ &= -C_{\textit{parallelograms}} \sum_{\ell\in\mathbb{Z}} \frac{\left(N_b^{D_{\mathcal{W}}-3}-1\right)^{-i\,\ell\,\mathbf{p}}\,\left(\varepsilon_m^m\right)^{2-i\,\ell\,\mathbf{p}}}{(D_{\mathcal{W}}-3)\,\ln N_b + 2\,i\,\ell\,\pi}\,,\end{aligned} \tag{$\mathcal{R}$ 52}$$

where $C_{\textit{parallelograms}}$ denotes a strictly positive and finite constant, depending on m, but uniformly bounded away from 0 and ∞ (see Proposition 3.8, on page 59). More specifically, again,

$$0 < C_{inf}^3 \leqslant C_{\textit{parallelograms}} \leqslant C_{sup}^3 < \infty\,\cdot$$

Also, recall from Subsection 4.1 that, by construction,

$$\tilde{\mathcal{V}}_{m,\Gamma_{\mathcal{W}_m},\textit{lower parallelograms}}\left(\varepsilon_m^m\right) = \mathcal{V}_{m,\Gamma_{\mathcal{W}_m},\textit{lower parallelograms}}\left(\varepsilon_m^m\right)\,,$$

and similarly, if "lower parallelograms" is replaced by "upper parallelograms". Hence, an entirely analogous relation holds if "parallelograms" is substituted for "lower parallelograms".

The associated (local) effective tube zeta function $\tilde{\zeta}^e_{m,\textit{parallelograms}}$ *(see Definition 4.3, on page 62 above) is then first obtained, for any complex number s such that $\mathcal{R}e(s) > D_{\mathcal{W}}$, as follows:*

$$\begin{aligned}\tilde{\zeta}^e_{m,\textit{parallelograms}}(s) &= \int_0^{\varepsilon_m^m} t^{s-3}\,\tilde{\mathcal{V}}_{m,\Gamma_{\mathcal{W}_m},\textit{parallelograms}}(t)\,dt\\ &= -C_{\textit{parallelograms}} \sum_{\ell\in\mathbb{Z}} \frac{\left(N_b^{2-3\,D_{\mathcal{W}}}-1\right)^{-i\,\ell\,\mathbf{p}}}{(2-3\,D_{\mathcal{W}})\,\ln N_b + 2\,i\,\ell\,\pi}\ \int_0^{\varepsilon_m^m} t^{s-2-i\,\ell\,\mathbf{p}}\,dt\\ &= -C_{\textit{parallelograms}} \sum_{\ell\in\mathbb{Z}} \frac{\left(N_b^{D_{\mathcal{W}}-3}-1\right)^{-i\,\ell\,\mathbf{p}}}{(D_{\mathcal{W}}-3)\,\ln N_b + 2\,i\,\ell\,\pi}\ \frac{\left(\varepsilon_m^m\right)^{s-1-i\,\ell\,\mathbf{p}}}{s-1-i\,\ell\,\mathbf{p}}\,\cdot\end{aligned} \tag{$\mathcal{R}$ 53}$$

By meromorphic continuation to all of $\mathbb{C}$, one then obtains $\tilde{\zeta}^e_{m,\textit{parallelograms}}$, the (local) effective tube zeta function (associated with the parallelograms), for all $s \in \mathbb{C}$, as given by the last two equalities in relation (R53) just above.

The associated Complex Dimensions arise as

$$1 + i\,\ell\,\mathbf{p}\,,\ \textit{with}\ \ell \in \mathbb{Z}\,\cdot$$

The above results stated in Properties 4.3–4.6, on pages 65–71, can now be combined in order to yield the following key theorems:

Theorem 4.7 (**Fractal Tube Formula for The Weierstrass IFD**).

Given $m \in \mathbb{N}$ sufficiently large, the m^{th} total contribution to the tubular volume $\mathcal{V}_{m,\Gamma_{\mathcal{W}_m}}\left(\varepsilon_m^m\right)$, *or two-dimensional Lebesgue measure of the ε_m^m–neighborhood of the m^{th} prefractal approximation $\Gamma_{\mathcal{W}_m}$,*

$$\mathcal{D}\left(\varepsilon_m^m\right) = \left\{M = (x,y) \in \mathbb{R}^2, d\left(M, \Gamma_{\mathcal{W}_m}\right) \leqslant \varepsilon_m^m\right\}, \tag{$\mathcal{R}$ 54}$$

where $\varepsilon = \left(\varepsilon_m^m\right)_{m \in N}$ is the cohomology infinitesimal, as introduced in Definition 3.1, on page 37, is given by

$$\begin{aligned}\tilde{\mathcal{V}}_{m,\Gamma_{\mathcal{W}_m}}\left(\varepsilon_m^m\right) \quad = \quad & \tilde{\mathcal{V}}_{m,\Gamma_{\mathcal{W}_m},Rectangles}\left(\varepsilon_m^m\right) + \tilde{\mathcal{V}}_{m,\Gamma_{\mathcal{W}_m},wedges}\left(\varepsilon_m^m\right) \\ & + \tilde{\mathcal{V}}_{m,\Gamma_{\mathcal{W}_m},\Gamma_{\mathcal{W}_m},extra\ outer\ triangles}\left(\varepsilon_m^m\right) + \tilde{\mathcal{V}}_{m,\Gamma_{\mathcal{W}_m},parallelograms}\left(\varepsilon_m^m\right),\end{aligned} \tag{$\mathcal{R}$ 55}$$

i.e.,

$$\begin{aligned}\tilde{\mathcal{V}}_{m,\Gamma_{\mathcal{W}_m}}\left(\varepsilon_m^m\right) \quad = \quad & C_{Rectangles} \sum_{k=0}^{\infty} \binom{\frac{1}{2}}{k} \frac{N_b^{1-k(2-D_{\mathcal{W}})} - 1}{N_b^{1-k(2-D_{\mathcal{W}})}} \sum_{\ell \in \mathbb{Z}} \frac{(N_b-1)^{-i\ell\mathbf{p}}}{(1-k(2-D_{\mathcal{W}}))\ln N_b + 2i\ell\pi} \left(\varepsilon_m^m\right)^{2-D_{\mathcal{W}}+k(2-D_{\mathcal{W}})-i\ell\mathbf{p}} \\ & + C_{wedges}^1 \sum_{\ell \in \mathbb{Z}} \frac{(N_b-1)^{-i\ell\mathbf{p}} \left(\varepsilon_m^m\right)^{3-i\ell\mathbf{p}}}{\ln N_b + 2i\ell\pi} + \pi\left(\varepsilon_m^m\right)^2 - \frac{\pi\left(\varepsilon_m^m\right)^4}{2} \\ & - C_{wedges}^2 \sum_{k=0}^{\infty} \frac{(-1)^k}{2k+1} \frac{N_b^{((2k+1)D_{\mathcal{W}}-2k)} - 1}{N_b^{((2k+1)D_{\mathcal{W}}-2k)}} \sum_{\ell \in \mathbb{Z}} \frac{(N_b^{((2k+1)D_{\mathcal{W}}-2k)} - 1)^{-i\ell\mathbf{p}} \left(\varepsilon_m^m\right)^{2k+1-i\ell\mathbf{p}}}{((2k+1)D_{\mathcal{W}} - 2k)\ln N_b + 2i\ell\pi} \\ & + C_{wedges}^3 \sum_{k=0}^{\infty} \frac{(-1)^k}{2k+1} \frac{N_b^{(2k+1)(D_{\mathcal{W}}-1)} - 1}{N_b^{(2k+1)(D_{\mathcal{W}}-1)}} \sum_{\ell \in \mathbb{Z}} \frac{(N_b^{(2k+1)D_{\mathcal{W}}-2k+1} - 1)^{-i\ell\mathbf{p}} \left(\varepsilon_m^m\right)^{5+2k-i\ell\mathbf{p}}}{((2k+1)D_{\mathcal{W}} - 2k + 1)\ln N_b + 2i\ell\pi} \\ & - \left(C_{triangles} + C_{parallelograms}\right) \sum_{\ell \in \mathbb{Z}} \frac{\left(N_b^{2-3D_{\mathcal{W}}} - 1\right)^{-i\ell\mathbf{p}}}{(2-3D_{\mathcal{W}})\ln N_b + 2i\ell\pi} \left(\varepsilon_m^m\right)^{2-i\ell\mathbf{p}},\end{aligned} \tag{$\mathcal{R}$ 56}$$

where $C_{rectangles}$, C_{wedges}^{ℓ}, $\ell = 1, 2, 3$, $C_{triangles}$, and $C_{parallelograms}$ denote the strictly positive and finite constants respectively introduced in Properties 4.3–4.6, on pages 65–71 above. Recall that these constants depend on m, but are uniformly bounded away from 0 and ∞ (in $m \in \mathbb{N}^{\star}$ large enough).

Also, recall from the discussion in Subsection 4.1 that, by construction,

$$\tilde{\mathcal{V}}_{m,\Gamma_{\mathcal{W}_m}}\left(\varepsilon_m^m\right) = \mathcal{V}_{m,\Gamma_{\mathcal{W}_m}}\left(\varepsilon_m^m\right).$$

Actually, this identity follows from the corresponding identity for each of the terms on the right–hand side of relation ($\mathcal{R}$55).

For the sake of clarity, and in order to highlight the role played by the one–periodic functions (with respect to the variable $\ln_{N_b}\left(\varepsilon_m^m\right)^{-1}$*, see Property 4.1, on page 61), one can exchange the sums over* k *and* m*, which enables one to obtain an expression of the following form:*

$$\begin{aligned}\tilde{\mathcal{V}}_{m,\Gamma_{\mathcal{W}_m}}\left(\varepsilon_m^m\right) \;=\; & \sum_{\ell\in\mathbb{Z},\,k\in\mathbb{N}} f_{k,\ell,Rectangles}\left(\varepsilon_m^m\right)^{2-D_{\mathcal{W}}+k\,(2-D_{\mathcal{W}})-i\,\ell\,\mathbf{p}} \\ & + \sum_{\ell\in\mathbb{Z},\,k\in\mathbb{N}} \left(f_{k,\ell,wedges,1}\,\left(\varepsilon_m^m\right)^{3-i\,\ell\,\mathbf{p}} + \,f_{k,\ell,wedges,2}\,\left(\varepsilon_m^m\right)^{1+2\,k-i\,\ell\,\mathbf{p}} + f_{k,\ell,wedges,3}\,\left(\varepsilon_m^m\right)^{5+2\,k-i\,\ell\,\mathbf{p}}\right) \\ & + \sum_{\ell\in\mathbb{Z},\,k\in\mathbb{N}} f_{k,\ell,triangles,\ parallelograms}\left(\varepsilon_m^m\right)^{2-i\,\ell\,\mathbf{p}} + \pi\left(\varepsilon_m^m\right)^2 - \frac{\pi\left(\varepsilon_m^m\right)^4}{2}\,,\end{aligned} \tag{$\mathcal{R}$ 57}$$

where the notation $f_{k,\ell,Rectangles}$*,* $f_{k,\ell,wedges,\ell'}$*,* $1\leqslant\ell'\leqslant 3$*, and* $f_{k,\ell,triangles,\ parallelograms}$*, respectively account for the nonzero coefficients associated to the sums corresponding to the contribution of the rectangles, wedges, triangles and parallelograms, respectively given by:*

$$f_{k,\ell,Rectangles} \;=\; C_{Rectangles}\binom{\frac{1}{2}}{k}\frac{N_b^{1-k\,(2-D_{\mathcal{W}})}-1}{N_b^{1-k\,(2-D_{\mathcal{W}})}}\,\frac{(N_b-1)^{-i\,\ell\,\mathbf{p}}}{(1-k\,(2-D_{\mathcal{W}}))\,\ln N_b+2\,i\,\ell\,\pi}\,; \tag{$\mathcal{R}$ 58}$$

$$f_{k,\ell,wedges,1} \;=\; C_{wedges}^1\,\frac{(N_b-1)^{-i\,\ell\,\mathbf{p}}}{\ln N_b+2\,i\,\ell\,\pi}\,; \tag{$\mathcal{R}$ 59}$$

$$f_{k,\ell,wedges,2} \;=\; -C_{wedges}^2\sum_{k=0}^{\infty}\frac{(-1)^k}{2\,k+1}\,\frac{N_b^{((2\,k+1)\,D_{\mathcal{W}}-2\,k)}-1}{N_b^{((2\,k+1)\,D_{\mathcal{W}}-2\,k)}}\;\frac{(N_b^{((2\,k+1)\,D_{\mathcal{W}}-2\,k)}-1)^{-i\,\ell\,\mathbf{p}}}{((2\,k+1)\,D_{\mathcal{W}}-2\,k)\,\ln N_b+2\,i\,\ell\,\pi}\,; \tag{$\mathcal{R}$ 60}$$

$$f_{k,\ell,wedges,3} \;=\; C_{wedges}^3\,\tfrac{(-1)^k}{2\,k+1}\,\frac{N_b^{(2\,k+1)\,(D_{\mathcal{W}}-1)}-1}{N_b^{(2\,k+1)\,(D_{\mathcal{W}}-1)}}\,\frac{(N_b^{(2\,k+1)\,D_{\mathcal{W}}-2\,k+1}-1)^{-i\,\ell\,\mathbf{p}}}{((2\,k+1)\,D_{\mathcal{W}}-2\,k+1)\,\ln N_b+2\,i\,\ell\,\pi}\,; \tag{$\mathcal{R}$ 61}$$

$$f_{k,\ell,triangles,\ parallelograms} \;=\; -\left(C_{triangles}+C_{parallelograms}\right)\,\frac{\left(N_b^{2-3\,D_{\mathcal{W}}}-1\right)^{-i\,\ell\,\mathbf{p}}}{(2-3\,D_{\mathcal{W}})\,\ln N_b+2\,i\,\ell\,\pi}\;. \tag{$\mathcal{R}$ 62}$$

Note that those coefficients do not depend on ε_m^m*, and satisfy the following uniform estimates (independent of* $m\in\mathbb{N}^\star$ *sufficiently large):*

$$\left|f_{k,\ell,Rectangles}\right| \;\leqslant\; C_{Rectangles}\binom{\frac{1}{2}}{k}\frac{1}{2\,\ell\,\pi}\,; \tag{$\mathcal{R}$ 63}$$

$$\left|f_{k,\ell,wedges,1}\right| \;\leqslant\; \frac{C_{wedges}^1}{2\,\ell\,\pi}\,; \tag{$\mathcal{R}$ 64}$$

$$\left|f_{k,\ell,wedges,2}\right| \;\leqslant\; \frac{C_{wedges}^2}{2\,k+1}\,\frac{1}{2\,\ell\,\pi}\,; \tag{$\mathcal{R}$ 65}$$

$$\left|f_{k,\ell,wedges,3}\right| \;\leqslant\; \frac{C_{wedges}^3}{2\,k+1}\,\frac{1}{2\,\ell\,\pi}\,; \tag{$\mathcal{R}$ 66}$$

$$\left|f_{k,\ell,triangles,\ parallelograms}\right| \;\leqslant\; \left(C_{triangles}+C_{parallelograms}\right)\cdot \tag{$\mathcal{R}$ 67}$$

Finally, each of the double sums in formulae ($\mathcal{R}$*55), on page 72, and (*$\mathcal{R}$*57), on page 73, is absolutely convergent (and hence, convergent).*

Proof. Indeed, by construction, the identity ($\mathcal{R}55$), on page 72, holds. Therefore, all of the main statements in the theorem concerning the m^{th} effective tubular volume $\tilde{\mathcal{V}}_{m,\Gamma_{\mathcal{W}_m}}\left(\varepsilon_m^m\right)$ follow by combining Properties 4.3–4.6, on pages 65–71 above.

Finally, we justify the uniform estimates ($\mathcal{R}63$)– ($\mathcal{R}67$) in the following manner:

We have that

$$\begin{aligned}
\left|f_{k,\ell,\text{Rectangles}}\right| &\leqslant C_{\text{Rectangles}}\binom{\frac{1}{2}}{k}\frac{\left|N_b^{1-k\,(2-D_{\mathcal{W}})}-1\right|}{N_b^{1-k\,(2-D_{\mathcal{W}})}}\,\frac{1}{\sqrt{\left(1-k\,(2-D_{\mathcal{W}})\right)^2\,\left(\ln N_b\right)^2+4\,\ell^2\,\pi^2}}\\
&\leqslant C_{\text{Rectangles}}\binom{\frac{1}{2}}{k}\frac{1}{\sqrt{\left(1-k\,(2-D_{\mathcal{W}})\right)^2\,\left(\ln N_b\right)^2+4\,\ell^2\,\pi^2}}\\
&\leqslant C_{\text{Rectangles}}\binom{\frac{1}{2}}{k}\frac{1}{2\,\ell\,\pi}\,;
\end{aligned}$$

$$\left|f_{k,\ell,\text{wedges},1}\right| \leqslant C^1_{\text{wedges}}\,\frac{1}{\sqrt{\left(\ln N_b\right)^2+4\,\ell^2\,\pi^2}} \leqslant \frac{C^1_{\text{wedges}}}{2\,\ell\,\pi}\,;$$

$$\begin{aligned}
\left|f_{k,\ell,\text{wedges},2}\right| &\leqslant \frac{C^2_{\text{wedges}}}{2\,k+1}\left|\frac{N_b^{((2\,k+1)\,D_{\mathcal{W}}-2\,k)}-1}{N_b^{((2\,k+1)\,D_{\mathcal{W}}-2\,k)}}\right|\,\frac{1}{\sqrt{\left((2\,k+1)\,D_{\mathcal{W}}-2\,k\right)^2\,\left(\ln N_b\right)^2+4\,\ell^2\,\pi^2}}\\
&\leqslant \frac{C^2_{\text{wedges}}}{2\,k+1}\,\frac{1}{\sqrt{\left((2\,k+1)\,D_{\mathcal{W}}-2\,k\right)^2\,\left(\ln N_b\right)^2+4\,\ell^2\,\pi^2}}\\
&\leqslant \frac{C^2_{\text{wedges}}}{2\,k+1}\,\frac{1}{2\,\ell\,\pi}\,;
\end{aligned}$$

$$\begin{aligned}
\left|f_{k,\ell,\text{wedges},3}\right| &\leqslant \frac{C^3_{\text{wedges}}}{2\,k+1}\left|\frac{N_b^{(2\,k+1)\,(D_{\mathcal{W}}-1)}-1}{N_b^{(2\,k+1)\,(D_{\mathcal{W}}-1)}}\right|\,\frac{1}{\sqrt{\left((2\,k+1)\,D_{\mathcal{W}}-2\,k+1\right)^2\,\left(\ln N_b\right)^2+4\,\ell^2\,\pi^2}}\\
&\leqslant \frac{C^3_{\text{wedges}}}{2\,k+1}\,\frac{1}{\sqrt{\left((2\,k+1)\,D_{\mathcal{W}}-2\,k+1\right)^2\,\left(\ln N_b\right)^2+4\,\ell^2\,\pi^2}}\\
&\leqslant \frac{C^3_{\text{wedges}}}{2\,k+1}\,\frac{1}{2\,\ell\,\pi}\,;
\end{aligned}$$

$$\begin{aligned}
\left|f_{k,\ell,\text{triangles, parallelograms}}\right| &\leqslant \left(C_{\text{triangles}}+C_{\text{parallelograms}}\right)\,\frac{1}{\sqrt{\left(2-3\,D_{\mathcal{W}}\right)^2\,\left(\ln N_b\right)^2+4\,\ell^2\,\pi^2}}\\
&\leqslant \left(C_{\text{triangles}}+C_{\text{parallelograms}}\right)\,\frac{1}{2\,\ell\,\pi}\,.
\end{aligned}$$

This concludes the proof of the theorem.

□

Remark 4.6 (**Periodic Functions Associated to the Poles of the Zeta Functions**).

The one–periodic functions (with respect to the variable $\ln_{N_b}\left(\varepsilon_m^m\right)^{-1}$, see Property 4.1, on page 61), respectively associated to the following values,

i. $D_{\mathcal{W}} - k\,(2 - D_{\mathcal{W}})$, with $k \in \mathbb{N}$,

ii. 1,

are nonconstant, since their m^{th} Fourier coefficients, with $m \in \mathbb{Z}$, $m \neq 0$, which are respectively proportional to the strictly positive and finite constants $C_{\text{Rectangles}}$, C_{wedges}^{ℓ}, for $1 \leqslant \ell \leqslant 3$, and $C_{\text{triangles}} + C_{\text{parallelograms}}$, are thus nonzero. We refer to Theorem 4.11, on page 83 below, for the specific manner in which these periodic functions arise. (See also Subsection 4.3.2, on page 83.)

4.3 Complex Dimensions

We deduce at once the Complex Dimensions of the Weierstrass IFD from the fractal tube formula and the expression for the (local) effective tube zeta function obtained in Theorem 4.7, on page 72 above, and Theorem 4.8, on page 76 below, respectively.

4.3.1 Main Results

Following (as well as adapting to IFDs) [LRŽ17b], we hereafter define the local and global effective tube zeta functions of the sequence of Weierstrass IFDs associated to the cohomology infinitesimal, as introduced in Definition 3.1, on page 37.

Definition 4.4 (**Local Tube Zeta Function for the Weierstrass Iterated Fractal Drums**).

In the sequel, for each $m \in \mathbb{N}$, $\widetilde{\zeta}_{m,\mathcal{W}}^{e}$ denotes the m^{th} effective tubular zeta function associated with $\mathcal{V}_{m,\Gamma_{\mathcal{W}_m}}\left(\varepsilon_m^m\right)$ – and hence also, associated with the corresponding natural volume extension function $\widetilde{\mathcal{V}}_{m,\Gamma_{\mathcal{W}_m}}\left(\varepsilon_m^m\right)$; see Definition 4.3, on page 62, along with Notation 11, on page 64. More specifically, it is initially defined by the following truncated Mellin transform, for all $s \in \mathbb{C}$ with $\mathcal{R}e(s)$ sufficiently large (in fact, for all $s \in \mathbb{C}$ with $\mathcal{R}e(s) > D_{\mathcal{W}}$),

$$\widetilde{\zeta}_{m,\Gamma_{\mathcal{W}_m}}^{e}(s) = \int_0^{\varepsilon_m^m} t^{s-3}\,\widetilde{\mathcal{V}}_{m,\Gamma_{\mathcal{W}_m}}(t)\,dt\,\cdot \tag{$\mathcal{R}$ 68}$$

We also call $\widetilde{\zeta}_{m,\Gamma_{\mathcal{W}_m}}^{e}$ the m^{th} *local effective tube zeta function* (or the m^{th} *prefractal effective tube zeta function*) of the Weierstrass IFD, for the same reason as the one provided in Property 4.3, on page 65.

Theorem 4.8 (**Local and Global Tube Zeta Function for the Weierstrass Iterated Fractal Drums [DL23b]**).

With the notation and terminology of Definition 4.4 just above, $\widetilde{\zeta}^{e}_{\Gamma_{\mathcal{W}}}$, *the* global effective tube zeta function *of the Weierstrass IFD, defined by analogy with the work in [LRŽ17b], admits a (necessarily unique) meromorphic continuation to all of* $\mathbb{C}$, *and is given, for any* $s \in \mathbb{C}$, *by the following expression (see [DL23b] for the proof of the existence of the limit, which is locally uniform on* $\mathbb{C}$*):*

$$\widetilde{\zeta}^{e}_{\Gamma_{\mathcal{W}}}(s) = \lim_{m\to\infty} \widetilde{\zeta}^{e}_{m,\Gamma_{\mathcal{W}_m}}(s)\,, \tag{$\mathcal{R}$ 69}$$

where, for all $m \in \mathbb{N}$ *sufficiently large, the* m^{th} local effective tube zeta function $\widetilde{\zeta}^{e}_{m,\mathcal{W}}$ *is given, for any* $s \in \mathbb{C}$, *by*

$$\begin{aligned}
\widetilde{\zeta}^{e}_{m,\Gamma_{\mathcal{W}_m}}(s) \;=\; & \sum_{\ell\in\mathbb{Z},\,k\in\mathbb{N}} f_{k,\ell,Rectangles}\,\frac{(\varepsilon_m^m)^{s-D_{\mathcal{W}}+k\,(2-D_{\mathcal{W}})-i\,\ell\,\mathbf{p}}}{s-D_{\mathcal{W}}+k\,(2-D_{\mathcal{W}})-i\,\ell\,\mathbf{p}} \\
& + \sum_{\ell\in\mathbb{Z},\,k\in\mathbb{N}} \left\{ f_{\ell,k,wedges,1}\,\frac{(\varepsilon_m^m)^{s+1-i\,\ell\,\mathbf{p}}}{s+1-i\,\ell\,\mathbf{p}} + f_{\ell,k,wedges,2}\,\frac{(\varepsilon_m^m)^{s+2\,k-1-i\,\ell\,\mathbf{p}}}{s+2\,k-1-i\,\ell\,\mathbf{p}} + f_{\ell,k,wedges,3}\,\frac{(\varepsilon_m^m)^{s+3+2\,k-i\,\ell\,\mathbf{p}}}{s+3+2\,k-i\,\ell\,\mathbf{p}} \right\} \\
& + \sum_{\ell\in\mathbb{Z},\,k\in\mathbb{N}} f_{k,\ell,triangles,\ parallelograms}\,\frac{(\varepsilon_m^m)^{s-1-i\,\ell\,\mathbf{p}}}{s-1-i\,\ell\,\mathbf{p}} + \frac{\pi\,(\varepsilon_m^m)^{s}}{s} - \frac{\pi\,(\varepsilon_m^m)^{s+2}}{4\,(s+2)}\,,
\end{aligned} \tag{$\mathcal{R}$ 70}$$

where, as already introduced in Theorem 4.7, on page 72, the coefficients $f_{k,\ell,Rectangles}$, $f_{\ell,k,wedges,j}$, *for* $1 \leqslant j \leqslant 3$, *and* $f_{\ell,k,triangles,\ parallelograms}$, *respectively, depend on* m,*but are uniformly bounded (in* $m \in \mathbb{N}^{\star}$ *large enough) and account for the nonzero coefficients associated to the sums corresponding to the contribution of the rectangles, wedges, triangles and parallelograms.*

Note that, in light of Definition 4.3, on page 62, $\widetilde{\zeta}^{e}_{m,\Gamma_{\mathcal{W}_m}}$ *is a (tamed) Dirichlet-type integral (in the sense of [LRŽ17b], Appendix A) and hence, admits an abscissa of (absolute) convergence.*

Furthermore, still for all $m \in \mathbb{N}^{\star}$ *sufficiently large, the abscissa of convergence of* $\widetilde{\zeta}^{e}_{m,\Gamma_{\mathcal{W}_m}}$ *is equal to*

$$D_{\mathcal{W}} = 2 + \frac{\ln\lambda}{\ln b} = 2 - \ln_b\,\frac{1}{\lambda}\,\cdot$$

As is proved in [DL23b], $\widetilde{\zeta}^{e}_{m,\Gamma_{\mathcal{W}_m}}$, *the* m^{th} *local tube zeta function of the Weierstrass IFD, is the contribution of the* m^{th} *prefractal approximation* $\Gamma_{\mathcal{W}_m}$ *to* $\widetilde{\zeta}^{e}_{\Gamma_{\mathcal{W}}}$, *the global effective tube zeta function of the Weierstrass IFD.*

Proof. Since, by definition (see Definition 4.4, on page 75),

$$\widetilde{\zeta}^{e}_{m,\Gamma_{\mathcal{W}_m}}(s) = \int_0^{\varepsilon_m^m} t^{s-3}\,\widetilde{\mathcal{V}}_{m,\Gamma_{\mathcal{W}_m}}(t)\,dt\,, \tag{$\mathcal{R}$ 71}$$

for all $s \in \mathbb{C}$ with $\mathcal{R}e(s)$ sufficiently large (in fact, for $\mathcal{R}e(s) > D_{\mathcal{W}}$), and according to Theorem 4.8, on page 76 in Section 4.2,

$$\begin{aligned}
\widetilde{\mathcal{V}}_{m,\Gamma_{\mathcal{W}_m}}\left(\varepsilon_m^m\right) \;=\; & \widetilde{\mathcal{V}}_{m,\Gamma_{\mathcal{W}_m},\mathrm{Rectangles}}\left(\varepsilon_m^m\right) + \widetilde{\mathcal{V}}_{m,\Gamma_{\mathcal{W}_m},\mathrm{wedges}}\left(\varepsilon_m^m\right) \\
& + \widetilde{\mathcal{V}}_{m,\Gamma_{\mathcal{W}_m},\text{extra outer triangles}}\left(\varepsilon_m^m\right) + \widetilde{\mathcal{V}}_{m,\Gamma_{\mathcal{W}_m},\text{parallelograms}}\left(\varepsilon_m^m\right)\,,
\end{aligned} \tag{$\mathcal{R}$ 72}$$

we have that (still for $\mathcal{R}e(s) > D_{\mathcal{W}}$),

$$\begin{aligned}\tilde{\zeta}^{e}_{m,\Gamma_{\mathcal{W}_m}}(s) \;\; = \;\; & \tilde{\zeta}^{e}_{m,\text{Rectangles}}(s) + \tilde{\zeta}^{e}_{m,\text{wedges}}(s) \\ & + \tilde{\zeta}^{e}_{m,\text{extra outer triangles}}(s) + \tilde{\zeta}^{e}_{m,\text{parallelograms}}(s)\,,\end{aligned} \tag{$\mathcal{R}$ 73}$$

and still in light of Theorem 4.7, on page 72, combined with the definition of $\tilde{\mathcal{V}}_{m,\Gamma_{\mathcal{W}_m}}(t)$, for any $t \in \left[0, \varepsilon_m^m\right]$, and of $\tilde{\zeta}^{e}_{m,\Gamma_{\mathcal{W}_m}} = \tilde{\zeta}^{e}_{m,\Gamma_{\mathcal{F}_m}}$ (see Definition 4.3, on page 62, where $\mathcal{F}_m = \Gamma_{\mathcal{W}_m}$ denotes the m^{th} component of the Weierstrass IFD – or, equivalently, the m^{th} prefractal approximation to the Weierstrass Curve), it follows that, for all $m \in \mathbb{N}^{\star}$ sufficiently large, $\tilde{\zeta}^{e}_{m,\Gamma_{\mathcal{W}_m}}$ has a meromorphic continuation to all of $\mathbb{C}$ given by formula ($\mathcal{R}$70) in Theorem 4.8, on page 76.

Finally, the fact that, for all m sufficiently large, the abscissa of convergence of $\tilde{\zeta}^{e}_{m,\Gamma_{\mathcal{W}_m}}$ coincides with $D_{\mathcal{W}}$ follows by combining formula ($\mathcal{R}$70), on page 76 (for all $s \in \mathbb{C}$) and the method of proof of Theorem 2.1 on page 57 in [LRŽ17b].

Alternatively, the fact that, for all $m \in \mathbb{N}$ sufficiently large, the abscissa of convergence D_m of $\tilde{\zeta}^{e}_{m,\Gamma_{\mathcal{W}_m}}$ is equal to

$$D_{\mathcal{W}} = 2 + \frac{\ln \lambda}{\ln b} = 2 - \ln_b \frac{1}{\lambda}\,, \tag{$\mathcal{R}$ 74}$$

follows from relation ($\mathcal{R}$70), given on page 76. Indeed, by definition, $\tilde{\zeta}^{e}_{m,\Gamma_{\mathcal{W}_m}}$ is a tamed Dirichlet-type integral (DTI), in the sense of [LRŽ17b], Appendix A, Definitions A.1.2 and A.1.3, on page 579. Hence, since $\tilde{\zeta}^{e}_{m,\Gamma_{\mathcal{W}_m}}$ is meromorphic in all of $\mathbb{C}$ and, in particular, in a neighborhood of $D_{\mathcal{W}}$, the abscissa of convergence of $\tilde{\zeta}^{e}_{m,\Gamma_{\mathcal{W}_m}}$ exists and coincides with the largest real part of the poles of $\tilde{\zeta}^{e}_{m,\Gamma_{\mathcal{W}_m}}$; that is, here, in light of relation ($\mathcal{R}$70) and of Theorem 4.10, on page 81 below (a corollary of the above Theorem 4.8, given on page 76, and which implies that $D_{\mathcal{W}}$ is an actual pole of $\tilde{\zeta}^{e}_{m,\Gamma_{\mathcal{W}_m}}$), D_m coincides with $D_{\mathcal{W}}$, as given by relation ($\mathcal{R}$74) above.

The fact that the first series, $\Sigma_{Rectangles} = \Sigma_{Rectangles}(t)$ (appearing in relation ($\mathcal{R}$76)), is locally uniformly convergent (and hence, pointwise convergent), follows from the following uniform estimate (valid for all $s \in \mathbb{C}$, with $\mathcal{R}e(s) \geqslant \alpha$, where $\alpha \in \mathbb{R}$ is arbitrary),

$$\begin{aligned}\forall\,(k,\ell) \in \mathbb{N}\times\mathbb{Z}\,:\;\; \left|\left(\varepsilon_m^m\right)^{s-D_{\mathcal{W}}+k\,(2-D_{\mathcal{W}})-i\,\ell\,\mathbf{p}}\right| \;\; & \leqslant \;\; \left(\varepsilon_m^m\right)^{\alpha-D_{\mathcal{W}}+k\,(2-D_{\mathcal{W}})-i\,\ell\,\mathbf{p}} \\ & \lesssim \;\; \left(\left(\frac{1}{2}\right)^{2-D_{\mathcal{W}}}\right)^{k}\,,\end{aligned} \tag{$\mathcal{R}$ 75}$$

provided $0 < \varepsilon_m^m \leqslant \dfrac{1}{2}$, which is true for all m sufficiently large.

More specifically, we combine the uniform estimate of relation ($\mathcal{R}$75), on page 77, together with the fact that, for $(k,\ell) \in \mathbb{N}\times\mathbb{Z}$ and independently of $m \in \mathbb{N}^{\star}$ large enough), the coefficients $f_{k,\ell,\text{Rectangles}}$ are uniformly bounded.

Also, we reason in exactly the same manner with each of the two double sums in relation ($\mathcal{R}$70), on page 76, defining the remaining effective tube zeta functions contributing to $\tilde{\zeta}^{e}_{m,\Gamma_{\mathcal{W}_m}}$.

It then suffices to apply the same reasoning as the one described in Remark 4.7, on page 80 just below to conclude that, for all m large enough, $\tilde{\zeta}^{e}_{m,\Gamma_{\mathcal{W}_m}}$ is meromorphic on all of $\mathbb{C}$, as desired.

Next, we justify the fact that, for all $s \in \mathbb{C}$, $\widetilde{\zeta}^{e}_{m,\Gamma_{\mathcal{W}_m}}(s)$ is given by relation ($\mathcal{R}70$) in Theorem 4.8, on page 76 above.

In order to see this, we apply Definition 4.3, on page 62, of the m^{th} effective tubular volume $\widetilde{\mathcal{V}}_{m,\Gamma_{\mathcal{W}_m}} = \widetilde{\mathcal{V}}_{m,\Gamma_{\mathcal{W}_m}}(t)$, for all $t \in \left[0, \varepsilon_m^m\right]$. Accordingly, as was alluded to above, for these values of t, and for all $m \in \mathbb{N}^{\star}$ sufficiently large, $\widetilde{\mathcal{V}}_{m,\Gamma_{\mathcal{W}_m}}(t)$ is given by (the sum of) the fractal power series appearing on the right–hand side of relation ($\mathcal{R}56$), on page 72 (or, equivalently, in relation ($\mathcal{R}57$), on page 73), in the fractal tube formula for the Weierstrass IFD obtained in Theorem 4.7, on page 72, but where ε_m^m is replaced by $t \in \left[0, \varepsilon_m^m\right]$.

Then, the same estimate as in relation ($\mathcal{R}75$), on page 77 just above, but now still with ε_m^m replaced by t, and m_0 large enough such that $0 < \varepsilon_q^q \leqslant \dfrac{1}{2}$, for all $q \geqslant m_0$ (and hence, also, $0 < t \leqslant \dfrac{1}{2}$) shows that the general term of the first series, namely,

$$\sum_{k \in \mathbb{N},\, \ell \in \mathbb{Z}} \binom{\frac{1}{2}}{k} \frac{N_b^{1-k(2-D_{\mathcal{W}})} - 1}{N_b^{1-k(2-D_{\mathcal{W}})}} \frac{(N_b - 1)^{-i\ell\mathbf{p}}}{(1 - k(2 - D_{\mathcal{W}}))\ln N_b + 2i\ell\pi}\, t^{2-D_{\mathcal{W}}+k(2-D_{\mathcal{W}})-i\ell\mathbf{p}},$$

appearing in the first term of the right–hand side of relation ($\mathcal{R}55$) in Theorem 4.7, on page 72 (yielding $\mathcal{V}_{m,\Gamma_{\mathcal{W}_m}}\left(\varepsilon_m^m\right)$) implies easily that

$$\begin{aligned}
\Sigma_{Rectangles}(t) &= \int_0^{\varepsilon_m^m} t^{s-3} \sum_{k \in \mathbb{N},\, \ell \in \mathbb{Z}} \binom{\frac{1}{2}}{k} \frac{N_b^{1-k(2-D_{\mathcal{W}})} - 1}{N_b^{1-k(2-D_{\mathcal{W}})}} \frac{(N_b - 1)^{-i\ell\mathbf{p}}}{(1 - k(2 - D_{\mathcal{W}}))\ln N_b + 2i\ell\pi}\, t^{2-D_{\mathcal{W}}+k(2-D_{\mathcal{W}})-i\ell\mathbf{p}}\, dt \\
&= \sum_{k \in \mathbb{N},\, \ell \in \mathbb{Z}} \binom{\frac{1}{2}}{k} \frac{N_b^{1-k(2-D_{\mathcal{W}})} - 1}{N_b^{1-k(2-D_{\mathcal{W}})}} \frac{(N_b - 1)^{-i\ell\mathbf{p}}}{(1 - k(2 - D_{\mathcal{W}}))\ln N_b + 2i\ell\pi} \int_0^{\varepsilon_m^m} t^{s-3}\, t^{2-D_{\mathcal{W}}+k(2-D_{\mathcal{W}})-i\ell\mathbf{p}},
\end{aligned} \tag{$\mathcal{R}76$}$$

viewed as a function of $t \in \left[0, \varepsilon_m^m\right]$, still for a fixed $m \geqslant m_0$ – converges normally (and thus also, uniformly) in t on $\left[0, \varepsilon_m^m\right]$. The same reasoning can be applied to each of the remaining series; i.e.,

$$\Sigma^1_{wedges}(t) = \sum_{\ell \in \mathbb{Z}} \frac{(N_b - 1)^{-i\ell\mathbf{p}}\, t^{3-i\ell\mathbf{p}}}{\ln N_b + 2i\ell\pi}, \tag{$\mathcal{R}77$}$$

$$\Sigma^2_{wedges}(t) = \sum_{k \in \mathbb{N},\, \ell \in \mathbb{Z}} \frac{(-1)^k}{2k+1} \frac{N_b^{((2k+1)D_{\mathcal{W}}-2k)} - 1}{N_b^{((2k+1)D_{\mathcal{W}}-2k)}} \sum_{\ell \in \mathbb{Z}} \frac{(N_b^{((2k+1)D_{\mathcal{W}}-2k)} - 1)^{-i\ell\mathbf{p}}\, t^{2k+1-i\ell\mathbf{p}}}{((2k+1)D_{\mathcal{W}} - 2k)\ln N_b + 2i\ell\pi}, \tag{$\mathcal{R}78$}$$

$$\Sigma^3_{wedges}(t) = \sum_{k \in \mathbb{N},\, \ell \in \mathbb{Z}} \frac{(-1)^k}{2k+1} \frac{N_b^{(2k+1)(D_{\mathcal{W}}-1)} - 1}{N_b^{(2k+1)(D_{\mathcal{W}}-1)}} \frac{(N_b^{(2k+1)(D_{\mathcal{W}}-1)} - 1)^{-i\ell\mathbf{p}}\, t^{5+2k-i\ell\mathbf{p}}}{(2k+1)(D_{\mathcal{W}} - 1)\ln N_b + 2i\ell\pi}, \tag{$\mathcal{R}79$}$$

$$\Sigma_{triangles\,and\,parallelograms}(t) = \sum_{\ell \in \mathbb{Z}} \frac{\left(N_b^{2-3D_{\mathcal{W}}} - 1\right)^{-i\ell\mathbf{p}}}{(2 - 3D_{\mathcal{W}})\ln N_b + 2i\ell\pi}\, t^{2-i\ell\mathbf{p}}, \tag{$\mathcal{R}80$}$$

appearing on the right–hand side of the second equality of relation ($\mathcal{R}55$) in Theorem 4.7, on page 72. Hence, by Weierstrass' theorem (for uniformly convergent series of functions), we can interchange series and integrals in the expression for $\widetilde{\zeta}^{e}_{m,\Gamma_{\mathcal{W}_m}}(s)$, given for a fixed arbitrary $s \in \mathbb{C}$, such that $\mathcal{R}e(s) > D_{\mathcal{W}}$, by the truncated Mellin transform,

$$\widetilde{\zeta}^{e}_{m,\Gamma_{\mathcal{W}_m}}(s) = \int_0^{\varepsilon_m^m} t^{s-3}\, \widetilde{\mathcal{V}}_{m,\Gamma_{\mathcal{W}_m}}(t)\, dt\,. \tag{$\mathcal{R}81$}$$

In fact, with the notation of Properties 4.3–4.6, on pages 65–71, we have that (still for all $m \geqslant m_0$, $\widetilde{\zeta}^{e}_{m,\Gamma_{\mathcal{W}_m}}(s)$ is given by relation ($\mathcal{R}57$), on page 73, first for all $s \in \mathbb{C}$ with $\mathcal{R}e(s) \geqslant D_{\mathcal{W}}$ – and then, by

the principle of analytic (i.e., meromorphic) continuation, for all $s \in \mathbb{C}$, since, as was explained above, each of the series in relations ($\mathcal{R}$76)–($\mathcal{R}$80), on pages 78–78 above, converges and is a meromorphic function of s on all of $\mathbb{C}$.

Here is a direct way to establish the meromorphicity of $\widetilde{\zeta}^{e}_{m,\Gamma_{\mathcal{W}_m}}$ (for all $m \geqslant m_0$) and to identify its (possible) poles, without using the chordal metric on the Riemann sphere (see Remark 4.7, on page 80 below, for a closely related use of this latter metric.)

Let ω be a potential pole (i.e., a possible Complex Dimension, as given by Theorem 4.10, on page 81 below), say,

$$\omega = \omega_{k,\ell} = D_{\mathcal{W}} - k\,(2 - D_{\mathcal{W}}) + i\,\ell\,\mathbf{p}\,,$$

with $k \in \mathbb{N}$ and $\ell \in \mathbb{Z}$.

Then, by excizing an arbitrary small compact disk $\mathcal{D}_\omega$ centered at ω from a slightly larger open disk $\mathcal{D}^+_\omega$ (also centered at ω), it follows, much as in the above discussion, that the corresponding double series of holomorphoc functions in the resulting domain $\mathcal{D}^+_\omega \setminus \overline{\mathcal{D}_\omega}$ is normally – and hence, also uniformly – convergent in $\mathcal{D}^+_\omega \setminus \overline{\mathcal{D}_\omega}$.

Hence, since $\mathcal{D}_\omega$ can be chosen arbitrarily small, we deduce from Weierstrass' theorem for series of holomorphic functions that the sum of the double series appearing in the right-hand side of formula ($\mathcal{R}$70) in Theorem 4.8, on page 76, is holomorphic in $\mathcal{D}^+_\omega \setminus \overline{\mathcal{D}_\omega}$, which is an arbitrary small pointed neighborhood of ω – and thus, that

$$\begin{aligned}
\Sigma(s) = & \sum_{\ell\in\mathbb{Z},\,k\in\mathbb{N}} f_{k,\ell,\text{Rectangles}}\,\frac{\left(\varepsilon_m^m\right)^{s-D_{\mathcal{W}}+k\,(2-D_{\mathcal{W}})-i\,\ell\,\mathbf{p}}}{s-D_{\mathcal{W}}+k\,(2-D_{\mathcal{W}})-i\,\ell\,\mathbf{p}} \\
& + \sum_{\ell\in\mathbb{Z},\,k\in\mathbb{N}} \left\{ f_{\ell,k,\text{wedges},1}\,\frac{\left(\varepsilon_m^m\right)^{s+1-i\,\ell\,\mathbf{p}}}{s+1-i\,\ell\,\mathbf{p}} + f_{\ell,k,\text{wedges},2}\,\frac{\left(\varepsilon_m^m\right)^{s+2\,k-1-i\,\ell\,\mathbf{p}}}{s+2\,k-1-i\,\ell\,\mathbf{p}} + f_{\ell,k,\text{wedges},3}\,\frac{\left(\varepsilon_m^m\right)^{s+3+2\,k-i\,\ell\,\mathbf{p}}}{s+3+2\,k-i\,\ell\,\mathbf{p}} \right\} \\
& + \sum_{\ell\in\mathbb{Z},\,k\in\mathbb{N}} f_{k,\ell,\text{triangles, parallelograms}}\,\frac{\left(\varepsilon_m^m\right)^{s-1-i\,\ell\,\mathbf{p}}}{s-1-i\,\ell\,\mathbf{p}}
\end{aligned} \qquad (\mathcal{R}\,82)$$

is holomorphic away from any potential singularity $\omega_{k,\ell} = D_{\mathcal{W}} - k\,(2 - D_{\mathcal{W}}) + i\,\ell\,\mathbf{p}$.

Now, by using the uniform convergence in $\mathcal{D}^+_\omega \setminus \overline{\mathcal{D}_\omega}$, we can interchange limits and deduce that the following limits exist in $\mathbb{C}$, and are given as follows:

$$\text{res}\left(\Sigma, \omega_{k,\ell}\right) = \lim_{s\to\omega_{k,\ell}} \left(s - \omega_{k,\ell}\right)\,\Sigma(s)\,, \qquad (\mathcal{R}\,83)$$

from which we deduce that Σ has at most a simple pole at $\omega = \omega_{k,\ell}$. Since $f_{k,\ell,\text{Rectangles}} \neq 0$, then $\omega = \omega_{k,\ell}$ is a simple pole of Σ, with associated residue $f_{k,\ell} \neq 0$, as implied by formula ($\mathcal{R}$83).

We conclude from the above discussion that Σ is meromorphic in all of $\mathbb{C}$, with potential poles (necessarily simple poles) the possible Complex Dimensions listed in Theorem 4.10, on page 81 below. Since we know that still for all sufficiently large values of the positive integer m,

$$\widetilde{\zeta}^{e}_{m,\Gamma_{\mathcal{W}_m}}(s) \;=\; \Sigma(s)\,, \qquad (\mathcal{R}\,84)$$

for all s in the domain (open right-half plane) $\mathcal{R}e(s) > D_{\mathcal{W}}$, we deduce from the principle of analytic (i.e., meromorphic) continuation that $\widetilde{\zeta}^{e}_{m,\Gamma_{\mathcal{W}_m}}$ has a meromorphic continuation to all of $\mathbb{C}$, coïnciding

with Σ in $\mathbb{C}$ – and hence, having the same potential (as well as actual) poles as Σ, and the same associated residues.

This completes the proof of Theorem 4.8 (page 76), which will also be used in part in order to prove Theorem 4.10, on page 81 (about the possible Complex Dimensions of $\tilde{\zeta}_{m,\Gamma_{\mathcal{W}_m}}$) and Remark 4.7, on page 80 below.

□

Remark 4.7. The fact that the global effective tube zeta function $\tilde{\zeta}^e_{\Gamma_{\mathcal{W}}}$ admits a meromorphic continuation to all of $\mathbb{C}$ is obtained by applying Weierstrass' theorem for (locally) uniformly convergent sequences of holomorphic functions. First, we note that, for all sufficiently large $m \in \mathbb{N}$, the set $\mathcal{Z}$ of possible poles of the local tube zeta function $\tilde{\zeta}^e_{m,\Gamma_{\mathcal{W}_m}}(s)$ does not depend on m, and is given by Theorem 4.10, pag 81 below. Note that $\mathcal{Z}$ is discrete, and thus closed in $\mathbb{C}$. It then makes sense to consider any of thoses poles, that we will denote by ω. The local tube zeta function $\tilde{\zeta}^e_{m,\Gamma_{\mathcal{W}_m}}$ is then holomorphic on the connected open subset of $\mathbb{C}$ given by $\mathbb{C} \setminus \mathcal{Z}$. We can clearly see that the sequence of functions $\left(\tilde{\zeta}^e_{m,\Gamma_{\mathcal{W}_m}}\right)_{m \geq m_0}$ converges normally (and hence, uniformly) in a connected open (and relatively compact) neighborhood of any given $\omega \in \mathcal{Z}$ – i.e., for $s = x + i\,y \in \mathbb{C}$ close to ω. Weierstrass' theorem, applied once again, then ensures the holomorphicity of the limit $\tilde{\zeta}^e_{\Gamma_{\mathcal{W}}}$ on the domain $\mathbb{C} \setminus \mathcal{Z}$. It follows that the global tube zeta function $\tilde{\zeta}^e_{\Gamma_{\mathcal{W}}}$ is meromorphic in all of $\mathbb{C}$, with possible set of poles given by $\mathcal{Z}$.

Corollary 4.9 (**(of Theorem 4.8, on page 76) Local and Global Distance Zeta Function for the Weierstrass Iterated Fractal Drums**).

By analogy with the functional equation given in [LRŽ17b] *(Theorem 2.2.1, page 112), along with Theorem 4.8, on page 76 just above, given the cohomology infinitesimal ε (see Definition 3.1, on page 37), the* global effective distance zeta function $\zeta^e_{\Gamma_{\mathcal{W}}}$ *is given, for any complex number s, by the following expression:*

$$\zeta^e_{\Gamma_{\mathcal{W}}}(s) = \lim_{m \to \infty} \zeta^e_{m,\Gamma_{\mathcal{W}_m}}(s)\,, \tag{$\mathcal{R}$ 85}$$

where, for all $m \in \mathbb{N}$ sufficiently large, $\zeta^e_{m,\Gamma_{\mathcal{W}_m}}$, the m^{th} local effective distance zeta function *of the Weierstrass IFD, is given, for any complex number s, by*

$$\begin{aligned} \zeta^e_{m,\Gamma_{\mathcal{W}_m}}(s) &= \left(\varepsilon_m^m\right)^{s-2} \tilde{\mathcal{V}}_{m,\Gamma_{\mathcal{W}_m}}\left(\varepsilon_m^m\right) + (2-s) \int_0^{\varepsilon_m^m} t^{s-3}\, \tilde{\mathcal{V}}_{m,\Gamma_{\mathcal{W}_m}}(t)\, dt \\ &= \left(\varepsilon_m^m\right)^{s-2} \tilde{\mathcal{V}}_{m,\Gamma_{\mathcal{W}_m}}\left(\varepsilon_m^m\right) + (2-s)\, \tilde{\zeta}^e_{m,\Gamma_{\mathcal{W}_m}}(s)\,, \end{aligned} \tag{$\mathcal{R}$ 86}$$

where $\tilde{\mathcal{V}}_{m,\Gamma_{\mathcal{W}_m}}$ denotes the m^{th} local effective tubular volume obtained in relations ($\mathcal{R}$56)–($\mathcal{R}$57) of Theorem 4.7, on page 72, and where $\tilde{\zeta}^e_{m,\Gamma_{\mathcal{W}_m}}(s)$ is given in relation ($\mathcal{R}$70) of Theorem 4.8, on page 76 (note that, by construction, $\tilde{\mathcal{V}}_{m,\Gamma_{\mathcal{W}_m}}\left(\varepsilon_m^m\right) = \mathcal{V}_{m,\Gamma_{\mathcal{W}_m}}\left(\varepsilon_m^m\right)$). The first equality in relation ($\mathcal{R}$86) is only valid for

$$\mathcal{R}e\,(s) > D_m = D_{\mathcal{W}}\,,$$

while the last one is valid for all s in $\mathbb{C}$. Furthermore, still for all $m \in \mathbb{N}$ sufficiently large, the distance zeta function $\zeta^e_{m,\Gamma_{\mathcal{W}_m}}$ admits a meromorphic continuation to all of $\mathbb{C}$, given by the last equality of relation ($\mathcal{R}$86) just above, with $\tilde{\zeta}^e_{m,\Gamma_{\mathcal{W}_m}}$ given as in Theorem 4.8, on page 76.

Remark 4.8. It follows from the above functional equation ($\mathcal{R}86$), on page 80, as well from the general theory developed in [LRŽ17b], that $\zeta^e_{m,\Gamma_{\mathcal{W}_m}}$ and $\widetilde{\zeta}^e_{m,\Gamma_{\mathcal{W}_m}}$ have exactly the same poles, with precisely related residues, for simple poles, which is the case here. Hence, they define the same Complex Dimensions. In light of Remark 4.7, on page 80 above, an analogous comment can be made about the global effective tube and distance zeta functions $\widetilde{\zeta}^e_{\Gamma_{\mathcal{W}}}$ and $\zeta^e_{\Gamma_{\mathcal{W}}}$.

We recall from [LRŽ17b] that the Complex Dimensions are defined as the poles of the meromorphic continuation of the tube (or, equivalently, the distance) zeta function. In our present setting, the set of Complex Dimensions of the Weierstrass IFD is the set of Complex Dimensions of the sequence of Weierstrass IFDs introduced in Remark 3.3, on page 60. Hence, those Complex Dimensions are the poles of the effective tube zeta functions – or, equivalently, the effective distance zeta functions – associated to those IFDs, respectively obtained in Theorem 4.8, on page 76 and Corollary 4.9, page 80 above.

Remarkably, in light of Theorem 4.8, on page 76, it turns out that the set of (possible) Complex Dimensions, defined as the set of (possible) poles of the m^{th} local effective tube zeta function $\widetilde{\zeta}^e_{m,\Gamma_{\mathcal{W}_m}}$ (or, equivalently, of $\zeta^e_{m,\Gamma_{\mathcal{W}_m}}$), does not change, for all sufficiently large $m \in \mathbb{N}^\star$; i.e., this set of (possible) Complex Dimensions – viewed as a multiset taking into account the multiplicities of the possible poles – stabilizes for all sufficiently large $m \in \mathbb{N}^\star$.

By definition, this set is then called the set of (possible) Complex Dimensions of the Weierstrass IFD $\Gamma^{\mathcal{I}}_{\mathcal{W}}$.

We expect this "stabilization phenomenon" to be common to a large class of IFDs associated with complicated fractals.

Observe that also in light of Theorem 4.8, on page 76, we could equivalenty define the set of (possible) Complex Dimensions of the Weierstrass IFD as the set of (possible) poles of the global effective tube zeta function $\widetilde{\zeta}^e_{\Gamma_{\mathcal{W}}}$ (or, equivalently, of the global effective distance zeta function $\zeta^e_{\Gamma_{\mathcal{W}}}$) of the Weierstrass IFD.

Theorem 4.10 (**Complex Dimensions of the Weierstrass IFD**).

The possible Complex Dimensions of the Weierstrass IFD $\Gamma^{\mathcal{I}}_{\mathcal{W}}$ are all simple, and given as follows:

$$D_{\mathcal{W}} - k\,(2 - D_{\mathcal{W}}) + i\,\ell\,\mathbf{p} \quad , \quad \text{with } k \in \mathbb{N}\,,\ \ell \in \mathbb{Z}\,,$$

$$1 - 2\,k + i\,\ell\,\mathbf{p} \quad , \quad \text{with } k \in \mathbb{N}\,,\ \ell \in \mathbb{Z}, \text{ along with } -2 \text{ and } 0\,,$$

where $\mathbf{p} = \dfrac{2\,\pi}{\ln N_b}$ *is the oscillatory period of the Weierstrass IFD.*

Furthermore, the one–periodic functions (with respect to the variable $\ln_{N_b}\left(\varepsilon_m^m\right)^{-1}$*, see Property 4.1, on page 61), respectively associated to the values* $D_{\mathcal{W}} - k\,(2 - D_{\mathcal{W}})$*,* $k \in \mathbb{N}$*, are nonconstant. (See also Subsection 4.3.2, on page 83 below for the exceptional cases.)*

In addition, all of the Fourier coefficients of the latter periodic functions are nonzero, which implies that there are infinitely many Complex Dimensions that are nonreal, including all of those with maximal real part $D_{\mathcal{W}}$*, which are the principal Complex Dimensions, in the terminology of [LRŽ17b], and therefore give rise to geometric oscillations (or vibrations) with the largest amplitude, in the fractal tube formula obtained in Theorem 4.7, on page 72 above and reformulated in Theorem 4.11, on*

page 83 below.

Finally, for each $k \in \mathbb{N}$ and $\ell \in \mathbb{Z}$, $D_{\mathcal{W}} - k\,(2 - D_{\mathcal{W}}) + i\,\ell\,\mathbf{p}$, $1 + i\,\ell\,\mathbf{p}$, -2 and 0 are all simple Complex Dimensions of the Weierstrass IFD; i.e., they are simple poles of the m^{th} tube (or, equivalently, of the distance) zeta functions, for all $m \in \mathbb{N}^{\star}$ sufficiently large.

Consequently, the Weierstrass IFD $\Gamma_{\mathcal{W}}^{\mathcal{I}}$ is fractal*, in the sense of the theory of Complex Dimensions developed in [LvF00], [LvF06], [LvF13], [LRŽ17b] and [Lap19].*

We refer to Subsection 4.3.2, on page 83, for a discussion of the exceptional cases, and to Subsection 4.3.3, on page 85 for a possible interpretation of our results.

Proof. The proof of this theorem is included in the latter part of the proof of Theorem 4.8, on page 76. □

Remark 4.9. The justification of this remark is also included in the latter part of proof of Theorem 4.8, given on page 76. Note, however, that we are giving here more precise statements and informations than in the aforementioned proof.

i. Let $m \in \mathbb{N}$ be arbitrary, but sufficiently large, so that both Theorem 4.8 (page 76) and Corollary 4.9 (page 80) are valid. Let ω be a potential pole (necessary simple) of $\widetilde{\zeta}^{e}_{m,\Gamma_{\mathcal{W}_m}}$ – or, equivalently, of $\zeta^{e}_{m,\Gamma_{\mathcal{W}_m}}$ (since $D_{\mathcal{W}} < 2$); ω is a possible Complex Dimension of the Weierstrass IFD, as given in Theorem 4.10, on page 81.

Say, for notational simplicity, that

$$\omega = \omega_{k,\ell} = D_{\mathcal{W}} - k\,(2 - D_{\mathcal{W}}) + i\,\ell\,\mathbf{p}\,, \tag{$\mathcal{R}$ 87}$$

for some $k \in \mathbb{N}$ and $\ell \in \mathbb{Z}$. Then, with the notation and the latter part of Theorem 4.8, given on page 76, we have that

$$\operatorname{res}\left(\widetilde{\zeta}^{e}_{m,\Gamma_{\mathcal{W}_m}}, \omega_{k,\ell}\right) = \lim_{s \to \omega_{k,\ell}} \left(s - \omega_{k,\ell}\right)\, \widetilde{\zeta}^{e}_{m,\Gamma_{\mathcal{W}_m}}(s) = f_{k,\ell,\text{Rectangles}} \tag{$\mathcal{R}$ 88}$$

and

$$\operatorname{res}\left(\zeta^{e}_{m,\Gamma_{\mathcal{W}_m}}, \omega_{k,\ell}\right) = \lim_{s \to \omega_{k,\ell}} \left(s - \omega_{k,\ell}\right)\, \zeta^{e}_{m,\Gamma_{\mathcal{W}_m}}(s) = \left(2 - \omega_{k,\ell}\right)\, f_{k,\ell,\text{Rectangles}} = \left(2 - \omega_{k,\ell}\right) \operatorname{res}\left(\widetilde{\zeta}^{e}_{m,\Gamma_{\mathcal{W}_m}}, \omega_{k,\ell}\right), \tag{$\mathcal{R}$ 89}$$

where the last equality follows from the functional equation connecting $\zeta^{e}_{m,\Gamma_{\mathcal{W}_m}}$ and $\widetilde{\zeta}^{e}_{m,\Gamma_{\mathcal{W}_m}}$ (much as in [LRŽ17b]), and as stated in relation ($\mathcal{R}$86) in Corollary 4.9, on page 80. Therefore, we see (much as in the end of the proof of Theorem 4.7, page 72), that $\omega = \omega_{k,\ell}$ is a pole (necessarily a simple pole of $\zeta^{e}_{m,\Gamma_{\mathcal{W}_m}}$, or, equivalently, of $\widetilde{\zeta}^{e}_{m,\Gamma_{\mathcal{W}_m}}$) – i.e., ω is a simple Complex Dimension of the Weierstrass IFD – if and only if $f_{k,\ell,\text{Rectangles}} \neq 0$, which, according to Theorem 4.7, on page 72, is always the case.

Furthermore, in this case, the residue of $\widetilde{\zeta}^{e}_{m,\Gamma_{\mathcal{W}_m}}$ (respectively, $\zeta^{e}_{m,\Gamma_{\mathcal{W}_m}}$) at ω is given by relation ($\mathcal{R}$88) (resp., by relation ($\mathcal{R}$89) just above.

ii. Moreover, also in agreement with the higher–dimensional theory developed in [LRŽ17b] (see also [LRŽ17a] and [LRŽ18], for example), the Complex Dimensions of the Weierstrass IFD can be defined indifferently via the m^{th} local effective tube zeta functions $\tilde{\zeta}^{e}_{m,\Gamma_{\mathcal{W}_m}}$ or via the m^{th} local effective distance zeta functions $\zeta^{e}_{m,\Gamma_{\mathcal{W}_m}}$, for all $m \in \mathbb{N}^{\star}$ sufficiently large.

iii. Parts *i.* and *ii.* of this remark are valid both for the potential (or possible) Complex Dimensions and for the exact Complex Dimensions of the Weierstrass IFD.

Theorem 4.11 (**Condensed Fractal Tube Formula for The Weierstrass IFD (Corollary of Theorem 4.7, on page 72).**

Given $m \in \mathbb{N}$ sufficiently large, the tubular effective volume $\tilde{\mathcal{V}}_{m,\Gamma_{\mathcal{W}_m}}\left(\varepsilon_m^m\right)$ *of the ε_m^m–neighborhood $\mathcal{D}\left(\varepsilon_m^m\right)$ of the Weierstrass IFD, can be expressed in the following manner:*

$$\begin{aligned}\tilde{\mathcal{V}}_{m,\Gamma_{\mathcal{W}_m}}\left(\varepsilon_m^m\right) \;=\; & \sum_{k=0}^{\infty}\left(\varepsilon_m^m\right)^{2-(D_{\mathcal{W}}-k\,(2-D_{\mathcal{W}}))}\,G_{k,D_{\mathcal{W}}}\left(\ln_{N_b}\left(\frac{1}{\varepsilon_m^m}\right)\right)\\ & +\sum_{k=0}^{\infty}\left(\varepsilon_m^m\right)^{2-(1-2\,k)}\,G_{k,1}\left(\ln_{N_b}\left(\frac{1}{\varepsilon_m^m}\right)\right)+\pi\,\left(\varepsilon_m^m\right)^2-\frac{\pi\,\left(\varepsilon_m^m\right)^4}{2}\,,\end{aligned} \tag{$\mathcal{R}$ 90}$$

where, for any fixed (but arbitrary) $k \in \mathbb{N}$, $G_{k,D_{\mathcal{W}}}$ and $G_{k,1}$ denote, respectively, continuous one–periodic functions (with respect to the variable $\ln_{N_b}\left(\varepsilon_m^m\right)^{-1}$, see Property 4.1, on page 61) associated to all of the Complex Dimensions of real parts $D_{\mathcal{W}}-k\,(2-D_{\mathcal{W}})$ and $1-2\,k$. Furthermore, all of the Fourier coefficients of the periodic functions $G_{k,D_{\mathcal{W}}}$ (for any $k \in \mathbb{N}$) and $G_{0,1}$ are nonzero. In particular, these periodic functions are not constant. Moreover, the functions $G_{0,D_{\mathcal{W}}}$ and $G_{0,1}$ are bounded away from zero and infinity.

This amounts to an expression of the form

$$\tilde{\mathcal{V}}_{m,\Gamma_{\mathcal{W}_m}}\left(\varepsilon_m^m\right)=\sum_{\substack{\alpha \text{ real part of a Complex Dimension}\\ \alpha \notin \{-2,0\}}}\left(\varepsilon_m^m\right)^{2-\alpha}\,G_{\alpha}\left(\ln_{N_b}\left(\frac{1}{\varepsilon_m}\right)\right)+\pi\,\left(\varepsilon_m^m\right)^2-\frac{\pi\,\left(\varepsilon_m^m\right)^4}{2}\,, \tag{$\mathcal{R}$ 91}$$

where, for any real part α of a Complex Dimension, with $\alpha \notin \{-2,0\}$, G_{α} denotes a continuous and one–periodic function.

4.3.2 Exceptional Cases

One might naturally question the following exceptional cases:

i. $D_{\mathcal{W}}-k_0\,(2-D_{\mathcal{W}})=0$, for some $k_0 \in \mathbb{N}$, which occurs when

$$D_{\mathcal{W}}=\frac{2\,k_0}{1+k_0}\,,\ \text{i.e.,}\ 2+\frac{\ln\lambda}{\ln N_b}=\frac{2\,k_0}{1+k_0}\,,\ \text{or}\ \lambda=N_b^{-\frac{2}{1+k_0}}\,.$$

According to the terminology of [LRŽ17b], Chapter 4, or [LvF06], Chapter 12, this first case corresponds to the situation when the Weierstrass Curve is *fractal in dimension 0.* We then happen to have a discrete line of Complex Dimensions with real part 0,

$$\mathcal{L}_0 = \{0 + i\,\ell\,\mathbf{p}\,,\ \ell\ \in\ \mathbb{Z}\} = \{i\,\ell\,\mathbf{p}\,,\ \ell\ \in\ \mathbb{Z}\}\ ,$$

which is obtained by merger with the discrete line of *actual* Complex Dimensions,

$$\mathcal{L}_{D_{\mathcal{W}},k_0} = \left\{ \underbrace{D_{\mathcal{W}} - k_0\ (2 - D_{\mathcal{W}})}_{0 \text{ here}} + i\,\ell\,\mathbf{p}\,,\ \ell\ \in\ \mathbb{Z} \right\}\ .$$

Note that the *actual* Complex Dimensions are *not double* (i.e., of multiplicity two). This directly comes from the expression obtained in relation ($\mathcal{R}70$) of Theorem 4.8, on page 76 for the effective fractal tube zeta function $\widetilde{\zeta}^e_{m,\Gamma_{\mathcal{W}_m}}$, which becomes here, for all m sufficiently large, and for any complex number s,

$$\begin{aligned}
\widetilde{\zeta}^e_{m,\Gamma_{\mathcal{W}_m}}(s) \quad &= \quad \sum_{\ell\in\mathbb{Z}} f_{k,\ell_0,\text{Rectangles}}\ \frac{(\varepsilon_m^m)^{s-i\,\ell\,\mathbf{p}}}{s - i\,\ell\,\mathbf{p}} \\
&= \quad \sum_{\ell\in\mathbb{Z},\ k\in\mathbb{N},\ k\neq k_0} f_{k,\ell,\text{Rectangles}}\ \frac{(\varepsilon_m^m)^{s-D_{\mathcal{W}}+k\,(2-D_{\mathcal{W}})-i\,\ell\,\mathbf{p}}}{s - D_{\mathcal{W}} + k\ (2 - D_{\mathcal{W}}) - i\,\ell\,\mathbf{p}} \\
&\quad + \sum_{\ell\in\mathbb{Z},\,k\in\mathbb{N}} \left(f_{k,\ell,\text{wedges},1}\ \frac{(\varepsilon_m^m)^{s+1-i\,\ell\,\mathbf{p}}}{s+1-i\,\ell\,\mathbf{p}} + f_{k,\ell,\text{wedges},2}\ \frac{(\varepsilon_m^m)^{s+2\,k-1-i\,\ell\,\mathbf{p}}}{s+2\,k-1-i\,\ell\,\mathbf{p}} + f_{\ell,k,\text{wedges},3}\ \frac{(\varepsilon_m^m)^{s+3+2\,k-i\,\ell\,\mathbf{p}}}{s+3+2\,k-i\,\ell\,\mathbf{p}} \right) \\
&\quad + \sum_{\ell\in\mathbb{Z},\,k\in\mathbb{N}} f_{\ell,k,\text{triangles, parallelograms}}\ \frac{(\varepsilon_m^m)^{s-1-i\,\ell\,\mathbf{p}}}{s-1-i\,\ell\,\mathbf{p}} + \frac{\pi\ (\varepsilon_m^m)^s}{s} - \frac{\pi\ (\varepsilon_m^m)^{s+2}}{4\,(s+2)}\ ,
\end{aligned} \tag{$\mathcal{R}\,92$}$$

where, as was already seen in Theorem 4.7, on page 72 the notation $f_{k,\ell,\text{Rectangles}}$, $f_{k,\ell,\text{wedges},\ell}$, with $1 \leqslant \ell \leqslant 3$, and $f_{k,\ell,\text{triangles, parallelograms}}$, respectively account for the coefficients associated to the sums corresponding to the contribution of the rectangles, wedges, triangles and parallelograms.

This could also be deduced from the fact if the pole $s = 0$ were double, we would have terms involving $\ln \varepsilon_m^m$ in the expression of $\widetilde{\zeta}^e_{m,\Gamma_{\mathcal{W}_m}}$, because, for any integer $\ell \in \mathbb{Z}$ and any complex number s,

$$\left(\varepsilon_m^m\right)^{s-i\,\ell\,\mathbf{p}} = e^{(s-i\,\ell\,\mathbf{p})\,\ln\varepsilon_m^m}\ ;$$

see [LvF06], Subsection 6.1.1, pages 180–182.

The novelty of this case is that we have Complex Dimensions above 0.

ii. $D_{\mathcal{W}} - k_1\ (2 - D_{\mathcal{W}}) = 1$, for some $k_1 \in \mathbb{N}$, which occurs when

$$D_{\mathcal{W}} = \frac{1 + 2\,k_1}{1 + k_1}\ ;\ \text{i.e., } 2 + \frac{\ln\lambda}{\ln N_b} = \frac{1 + 2\,k_1}{1 + k_1}\ \text{ or, equivalently, } \lambda = N_b^{-\frac{1}{1+k_1}}\ .$$

Since, here, $\lambda\,N_b \neq 1$, it follows that $k_1 \neq 0$.

According to the terminology mentioned in *i.*, this second case corresponds to the situation when the Weierstrass Curve is *fractal in dimension 1.* We then happen to have a discrete line of Complex Dimensions with real part 1,

$$\mathcal{L}_1 = \{1 + i\,\ell\,\mathbf{p}\,,\ \ell\ \in\ \mathbb{Z}\}\ ,$$

which is obtained by merger with the discrete line of *actual* Complex Dimensions,

$$\mathcal{L}_{D_{\mathcal{W}},k_1} = \left\{ \underbrace{D_{\mathcal{W}} - k_1\ (2 - D_{\mathcal{W}})}_{1 \text{ here}} + i\,\ell\,\mathbf{p}\,,\ \ell\ \in\ \mathbb{Z} \right\}\cdot$$

Note again that the *actual* Complex Dimensions are *not double*. As above, this directly comes from the expression obtained in relation ($\mathcal{R}70$) of Theorem 4.8, on page 76 for the fractal tube zeta function $\widetilde{\zeta}^{e}_{m,\Gamma_{\mathcal{W}_m}}$, which becomes here, for any complex number s,

$$\begin{aligned}
\widetilde{\zeta}^{e}_{m,\Gamma_{\mathcal{W}_m}}(s) \quad &= \quad \sum_{\ell\in\mathbb{Z}} \left(f_{k,\ell_1,\text{Rectangles}} + f_{\ell,0,\text{wedges},2}\right) \frac{\left(\varepsilon_m^m\right)^{s-1-i\,\ell\,\mathbf{p}}}{s-1-i\,\ell\,\mathbf{p}} \\
&= \quad \sum_{\ell\in\mathbb{Z},\,k\in\mathbb{N},\,k\neq k_1} f_{k,\ell,\text{Rectangles}}\ \frac{\left(\varepsilon_m^m\right)^{s-D_{\mathcal{W}}+k\,(2-D_{\mathcal{W}})-i\,\ell\,\mathbf{p}}}{s-D_{\mathcal{W}}+k\ (2-D_{\mathcal{W}})-i\,\ell\,\mathbf{p}} \\
&\qquad + \sum_{\ell\in\mathbb{Z},\,k\in\mathbb{N}^\star} f_{k,\ell,\text{wedges},2}\ \frac{\left(\varepsilon_m^m\right)^{s+2\,k-1-i\,\ell\,\mathbf{p}}}{s+2\,k-1-i\,\ell\,\mathbf{p}} \\
&\qquad + \sum_{\ell\in\mathbb{Z},\,k\in\mathbb{N}} \left(f_{k,\ell,\text{wedges},1}\ \frac{\left(\varepsilon_m^m\right)^{s+1-i\,\ell\,\mathbf{p}}}{s+1-i\,\ell\,\mathbf{p}} + f_{\ell,k,\text{wedges},3}\ \frac{\left(\varepsilon_m^m\right)^{s+3+2\,k-i\,\ell\,\mathbf{p}}}{s+3+2\,k-i\,\ell\,\mathbf{p}} \right) \\
&\qquad + \sum_{\ell\in\mathbb{Z},\,k\in\mathbb{N}} f_{k,\ell,\text{triangles, parallelograms}}\ \frac{\left(\varepsilon_m^m\right)^{s-1-i\,\ell\,\mathbf{p}}}{s-1-i\,\ell\,\mathbf{p}} + \frac{\pi\,\left(\varepsilon_m^m\right)^{s}}{s} - \frac{\pi\,\left(\varepsilon_m^m\right)^{s+2}}{4\,(s+2)}\cdot
\end{aligned} \tag{$\mathcal{R}\,93$}$$

What is new in this case is that we are sure that every possible Complex Dimension on $\mathcal{L}_1$, i.e., every complex number $1 + i\,\ell\,\mathbf{p}$, with $\ell\ \in\ \mathbb{Z}$, is an *actual* Complex Dimension of the Weierstrass Curve, because the same is true for each point of $\mathcal{L}_{D_{\mathcal{W}},k_1}$.

4.3.3 Possible Interpretation

Figure 18, on page 86, gives *the distribution of Complex Dimensions*. In order to understand their deeper meaning, one may consider an horizontal $\ell\,\mathbf{p}$ line, of equation $y = \ell\,\mathbf{p}$, where $\ell\ \in\ \mathbb{Z}$ is arbitrary (but fixed). Such a line corresponds to the ℓ^{th}–order vibration mode, but which can also be interpreted as coming from:

i. The vertical line $x = 0$, or, in other words, oscillations coming from *points*: indeed, the prefractal graph $\Gamma_{\mathcal{W}_m}$ is, at first, constituted of points.

ii. The vertical line $x = 1$, which this time correspond to oscillations coming from *lines* (or, rather, line segments): prefractal as it is, $\Gamma_{\mathcal{W}_m}$ is constituted of lines, in an Euclidean space of dimension two.

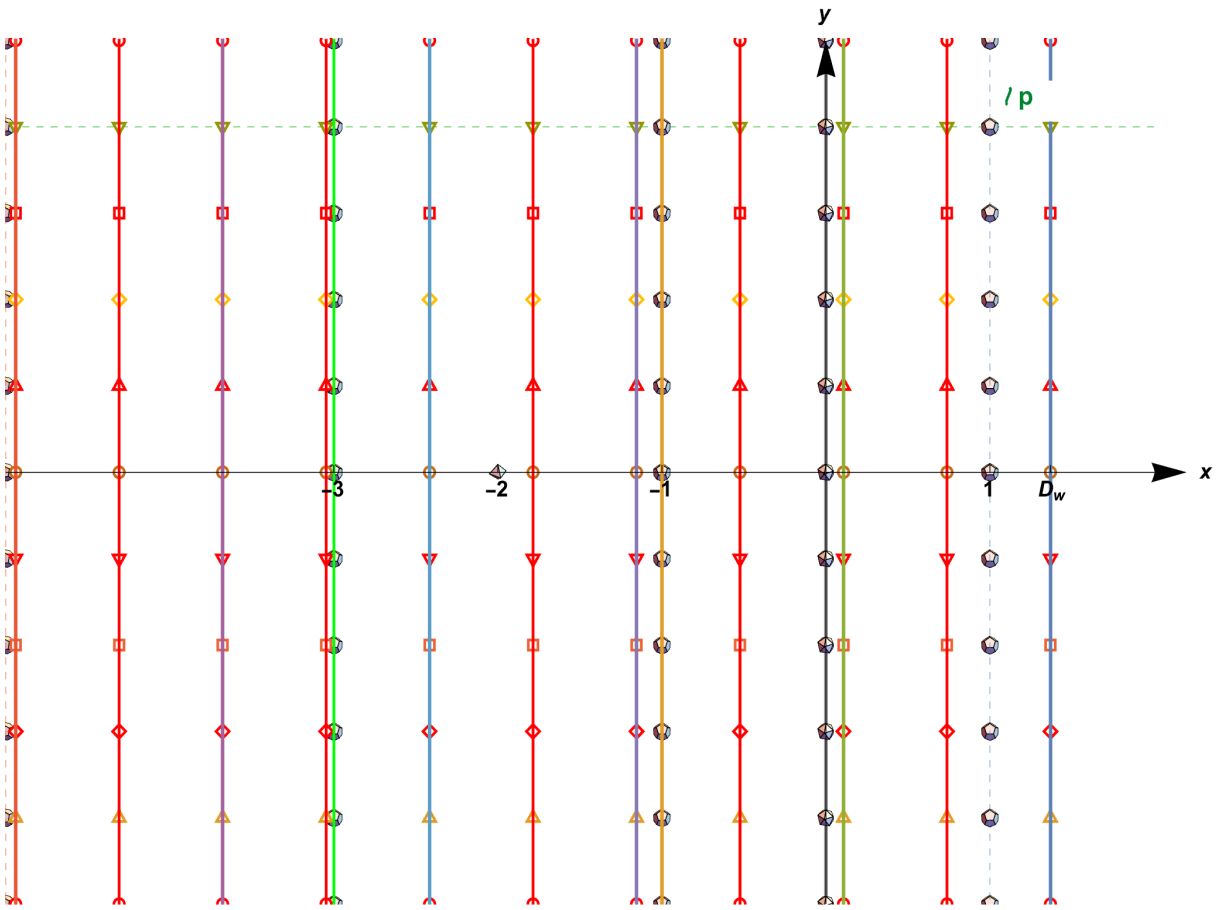

Figure 18: **The Complex Dimensions of the Weierstrass IFD. The nonzero Complex Dimensions are periodically distributed (with the same period $\mathbf{p} = \dfrac{2\pi}{\ln N_b}$, the oscillatory period of the Weierstrass IFD) along countably many vertical lines, with abscissae $D_{\mathcal{W}} - k\,(2 - D_{\mathcal{W}})$ and $1 - 2k$, where $k \in \mathbb{N}$ is arbitrary. In addition, 0 and −2 are Complex Dimensions of the Weierstrass IFD.**
For the sake of representation, there is a different color for each vertical line, and a specific symbol is used to plot the imaginary parts of the Complex Dimensions associated with a given vertical line. (See also Subsection 4.3.2, on page 83 for the exceptional cases.)

iii. The vertical line $x = D_{\mathcal{W}}$, which, this time, corresponds to oscillations coming from the whole prefractal $\Gamma_{\mathcal{W}_m}$ itself.

iv. The vertical lines $x = D_{\mathcal{W}} - k\,(2 - D_{\mathcal{W}})$, with k in $\mathbb{N}^* = \mathbb{N} \setminus \{0\}$.

For $k \leqslant m$, it corresponds to oscillations coming from the prefractal graphs $\Gamma_{\mathcal{W}_{m-k}}$, a phenomenon which can be understood via the following consideration:

Switching from the $(m-k)^{th}$ prefractal graph, to the m^{th} one, $0 < k \leqslant m$, is done by applying k iterates of the T_j maps,

$$T_{j_1 \cdots j_k} = T_{j_1} \circ \cdots \circ T_{j_k}\,. \tag{$\mathcal{R}$ 94}$$

In terms of the vertical distance between consecutive vertices, this amounts to a multiplication

of the amplitudes by the factor $\lambda^k = N_b^{-k\,(2-D_{\mathcal{W}})}$, associated to a sum of cosine expressions.

It thus provides an interesting interpretation of the real parts

$$D_{\mathcal{W}} - k\,(2 - D_{\mathcal{W}}) \quad , \quad \text{for } 0 < k \leqslant m\,, \tag{$\mathcal{R}$ 95}$$

insofar as the m^{th} prefractal graph bears – or, in a sense, *feels* – the oscillations of its predecessors.

There remains the lines $x = D_{\mathcal{W}} - k\,(2 - D_{\mathcal{W}})$, with $k > m$.

In order to interpret them, one could think in the same way, but, without associated graphs, how? Except if they could exist, in some way. This will be the purpose of a later extension of the prefractal sequence $\left(\Gamma_{\mathcal{W}_m}\right)_{m\in\mathbb{N}}$, a priori indexed by nonnegative integers, to negative ones, via the new concept of *antefractals*. However, this point will not be discussed in the present paper.

4.3.4 Analogy with the General Theory of Complex Dimensions

Our results in Theorem 4.7, on page 72 and Theorem 4.11, on page 83 above, on the fractal tube formula for the Weierstrass IFD are similar to the general (exact, pointwise) fractal tube formulas (via either tube or distance zeta functions) obtained in the higher–dimensional theory of Complex Dimensions in [LRŽ17b] (Chapter 5), or in [LRŽ18], and extending the fractal tube formulas for fractal strings obtained in [LvF00] and [LvF06] (Chapter 8). Compare, e.g., in the case of simple poles and under the hypothesis of strong languidity (a strong form of polynomial growth condition) of either $\widetilde{\zeta}^e_{m,\Gamma_{\mathcal{W}_m}}$ or $\zeta^e_{m,\Gamma_{\mathcal{W}_m}}$ [LRŽ17b], Theorem 5.1.16, page 427, or Theorem 5.3.17, page 449, respectively.

There is a notable difference, however, due to the great complexity of the Weierstrass Curve $\Gamma_{\mathcal{W}}$ and of the associated IFD $\Gamma^{\mathcal{I}}_{\mathcal{W}}$. Namely, the fractal tube formula is only given for the volume $\mathcal{V}_{m,\Gamma_{\mathcal{W}_m}}\left(\varepsilon^m_m\right)$ of the m^{th} prefractal approximation $\Gamma_{\mathcal{W}_m}$, and evaluated at the m^{th} cohomology infinitesimal ε^m_m, for all sufficiently large $m \in \mathbb{N}$.

Indeed, according to the aforementioned results from [LRŽ17b] and [LRŽ18], we would have, in particular, that the tubular volume is given as follows:

$$\mathcal{V}_{m,\Gamma_{\mathcal{W}_m}}\left(\varepsilon^m_m\right) = \sum_{\omega} \operatorname{res}\left(\widetilde{\zeta}^e_{m,\Gamma_{\mathcal{W}_m}},\omega\right)\left(\varepsilon^m_m\right)^{2-\omega} = \sum_{\omega} \frac{\operatorname{res}\left(\zeta^e_{m,\Gamma_{\mathcal{W}_m}},\omega\right)}{2-\omega}\left(\varepsilon^m_m\right)^{2-\omega}\,, \tag{$\mathcal{R}$ 96}$$

where, in each of these two sums, ω ranges through all of the Complex Dimensions of $\Gamma^{\mathcal{I}}_{\mathcal{W}}$ (i.e., the poles of either $\widetilde{\zeta}^e_{m,\Gamma_{\mathcal{W}_m}}$ or, equivalently, $\zeta^e_{m,\Gamma_{\mathcal{W}_m}}$).

Recall from equation ($\mathcal{R}$40)–(◆◆) in Remark 4.3, on page 65 above that

$$\operatorname{res}\left(\zeta^e_{m,\Gamma_{\mathcal{W}_m}},\omega\right) = (2-\omega)\operatorname{res}\left(\widetilde{\zeta}^e_{m,\Gamma_{\mathcal{W}_m}},\omega\right)\cdot \tag{$\mathcal{R}$ 97}$$

In order to obtain the fractal tube formula in Theorem 4.7, on page 72 (and hence also, in Theorem 4.11, on page 83), however, we did not need to appeal to the aforementioned results of the general theory, by first calculating $\widetilde{\zeta}^e_{m,\Gamma_{\mathcal{W}_m}}$ or $\zeta^e_{m,\Gamma_{\mathcal{W}_m}}$ (using their basic scaling and symmetry properties described in [LRŽ17b], along with the geometric properties of $\Gamma_{\mathcal{W}}$ described in Section 2 above) and then, verifying that the appropriate notion of strong languidity is satisfied. This could have been

done, but was unnecessary in our present situation.

Instead, as was explained earlier, we first directly calculated the tubular volume $\mathcal{V}_{m,\Gamma_{\mathcal{W}_m}}\left(\varepsilon_m^m\right)$ in Theorem 4.7, on page 72, and then deduced from the resulting fractal tube formula, via Mellin transformation, an explicit expression for the m^{th} local effective tube zeta function $\widetilde{\zeta}^e_{m,\Gamma_{\mathcal{W}_m}}$ – and further, for the m^{th} local effective distance zeta function $\zeta^e_{m,\Gamma_{\mathcal{W}_m}}$, via the functional equation recalled in relation (♦) of Remark 4.3, on page 65. Finally, as would have been the case if we had adopted the first method outlined above, we deduced (in Theorem 4.10, on page 81) the values of the (possible) Complex Dimensions of the Weierstrass IFD $\Gamma^{\mathcal{I}}_{\mathcal{W}}$, as the poles of $\widetilde{\zeta}^e_{m,\Gamma_{\mathcal{W}_m}}$ (or, equivalently, of $\zeta^e_{m,\Gamma_{\mathcal{W}_m}}$, since $D_{\mathcal{W}} < 2$).

4.4 Minkowski Dimension, Minkowski Nondegeneracy, and Average Minkowski Content

We next obtain new and refined results concerning the geometry – and, in particular, the Minkowski nondegeneracy, non Minkowski measurability, as well as the average Minkowski content of the Weierstrass IFD. For this purpose, and for the benefit of the reader who may not be familiar with these notions, we first state several definitions, which are now suitably adapted to our current setting and to the notions of effective tubular volumes.

In the spirit of the remainder of this paper, the definition of (upper, lower) Minkowski contents and dimensions, for example, will be given in terms of the cohomology infinitesimal $\left(\varepsilon_m^m\right)_{m=0}^{\infty}$, viewed as a sequence of positive scales tending to zero, as $m \to \infty$. So will the notions of Minkowski nondegeneracy and Minkowski measurability, as well as of effective average Minkowski content.

Definition 4.5 (**Lower and Upper r–Dimensional Minkowski Contents – Lower and Upper Minkowski Dimensions, and Minkowski Dimension of an IFD**)**.**

Let $\mathcal{F}^{\mathcal{I}}$ be an arbitrary iterated fractal drum of $\mathbb{R}^2$; see Definition 3.2, on page 38. More precisely, we hereafter consider the sequence of ordered pairs $\left(\mathcal{F}_m, \varepsilon^m_{\mathcal{F},m}\right)_{m\in\mathbb{N}}$, where, for each $m \in \mathbb{N}$, $\mathcal{F}_m$ is the m^{th} prefractal approximation to a fractal set $\mathcal{F}$, and where $\varepsilon^m_{\mathcal{F},m}$ is the associated m^{th} cohomology infinitesimal.

Then, given $r \geqslant 0$, $m \in \mathbb{N}$, and the $\varepsilon^m_{\mathcal{F},m}$–neighborhood (or tubular neighborhood) of $\mathcal{F}_m$,

$$\mathcal{D}_{\mathcal{F}_m}\left(\varepsilon^m_{\mathcal{F},m}\right) = \left\{M \in \mathbb{R}^2\,,\, d\left(M,\mathcal{F}_m\right) \leqslant \varepsilon^m_{\mathcal{F},m}\right\}\,, \tag{$\mathcal{R}$ 98}$$

of tubular volume $\mathcal{V}_{m,\mathcal{F}_m}\left(\varepsilon^m_{\mathcal{F},m}\right)$, we define, much as in [LRŽ17b], the *lower r–dimensional Minkowski content* (resp., the *upper r–dimensional Minkowski content*) of the IFD as

$$\mathcal{M}_{\star}{}^{r}\left(\mathcal{F}^{\mathcal{I}}\right) = \liminf_{m\to\infty} \frac{\mathcal{V}_{m,\mathcal{F}_m}\left(\varepsilon^m_{\mathcal{F},m}\right)}{\left(\varepsilon^m_{\mathcal{F},m}\right)^{2-r}} \quad \left(\text{resp.,}\ \mathcal{M}^{\star,r}\left(\mathcal{F}^{\mathcal{I}}\right) = \limsup_{m\to\infty} \frac{\mathcal{V}_{m,\mathcal{F}_m}\left(\varepsilon^m_{\mathcal{F},m}\right)}{\left(\varepsilon^m_{m}\right)^{2-r}}\right). \tag{$\mathcal{R}$ 99}$$

Recall that $\lim_{m\to\infty} \varepsilon^m_{\mathcal{F},m} = 0$; see Definition 3.2, on page 38, along with Definition 3.1, on page 37, for the special case of the Weierstrass IFD, for which we also have (in the present notation),

$$\mathcal{V}_{m,\mathcal{F}_m}\left(\varepsilon^m_{\mathcal{F},m}\right) = \widetilde{\mathcal{V}}_{m,\mathcal{F}_m}\left(\varepsilon^m_{\mathcal{F},m}\right)\,,$$

for all $m \in \mathbb{N}$.

Note that, by definition, we have that

$$0 \leqslant \mathcal{M}_{\star}{}^{r}\left(\mathcal{F}^{\mathcal{I}}\right) \leqslant \mathcal{M}^{\star,r}\left(\mathcal{F}^{\mathcal{I}}\right) \leqslant \infty \cdot \tag{$\mathcal{R}$ 100}$$

We then define the *lower Minkowski dimension* (resp., the *upper Minkowski dimension*) of the IFD by

$$\underline{D}\left(\mathcal{F}^{\mathcal{I}}\right) = \inf\left\{r \geqslant 0\,,\, \mathcal{M}_{\star}{}^{r}\left(\mathcal{F}^{\mathcal{I}}\right) < \infty\right\} \tag{$\mathcal{R}$ 101}$$

$$\left(\text{resp., } \overline{D}\left(\mathcal{F}^{\mathcal{I}}\right) = \inf\left\{r \geqslant 0\,,\, \mathcal{M}^{\star r}\left(\mathcal{F}^{\mathcal{I}}\right) < \infty\right\}\right) \cdot \tag{$\mathcal{R}$ 102}$$

As usual, by definition, the Minkowski dimension $D_{\mathcal{F}^{\mathcal{I}}} = D\left(\mathcal{F}^{\mathcal{I}}\right)$ of the IFD *exists* if

$$\underline{D}\left(\mathcal{F}^{\mathcal{I}}\right) = \overline{D}\left(\mathcal{F}^{\mathcal{I}}\right), \tag{$\mathcal{R}$ 103}$$

in which case, of course, we have that

$$D_{\mathcal{F}^{\mathcal{I}}} = D\left(\mathcal{F}^{\mathcal{I}}\right) = \underline{D}\left(\mathcal{F}^{\mathcal{I}}\right) = \overline{D}\left(\mathcal{F}^{\mathcal{I}}\right) \cdot \tag{$\mathcal{R}$ 104}$$

Definition 4.6 (**Minkowski Nondegeneracy and Minkowski Measurability of an IFD**).

Let $\mathcal{F}^{\mathcal{I}}$ be an arbitrary IFD. Assume that its Minkowski dimension $D_{\mathcal{F}^{\mathcal{I}}}$ exists, in the sense of Definition 4.5, on page 88 just above.

Then, with the same notation as in Definition 4.5, the IFD $\mathcal{F}^{\mathcal{I}}$ is said to be *Minkowski nondegenerate* if the lower and upper Minkowski contents,

$$\mathcal{M}_{\star}{}^{D_{\mathcal{F}^{\mathcal{I}}}}\left(\mathcal{F}^{\mathcal{I}}\right) = \liminf_{m\to\infty} \frac{\mathcal{V}_{m,\mathcal{F}_m}\left(\varepsilon^m_{\mathcal{F},m}\right)}{\left(\varepsilon^m_{\mathcal{F},m}\right)^{2-D_{\mathcal{F}^{\mathcal{I}}}}} \quad \text{and} \quad \mathcal{M}^{\star,D_{\mathcal{F}^{\mathcal{I}}}}\left(\mathcal{F}^{\mathcal{I}}\right) = \limsup_{m\to\infty} \frac{\mathcal{V}_{m,\mathcal{F}_m}(\varepsilon^m_{\mathcal{F},m})}{\left(\varepsilon^m_{\mathcal{F},m}\right)^{2-D_{\mathcal{F}^{\mathcal{I}}}}},$$

are respectively positive and finite. Recall that the inequalities in ($\mathcal{R}$100) always hold.

Finally, the IFD $\mathcal{F}^{\mathcal{I}}$ is said to be *Minkowski measurable* if it is Minkowski nondegenerate and

$$\mathcal{M}_{\star}{}^{D_{\mathcal{F}^{\mathcal{I}}}}\left(\mathcal{F}^{\mathcal{I}}\right) = \mathcal{M}^{\star,D_{\mathcal{F}^{\mathcal{I}}}}\left(\mathcal{F}^{\mathcal{I}}\right); \tag{$\mathcal{R}$ 105}$$

i.e., if the following limit exists in $]0,+\infty[$ (and necessarily equals this common value, denoted by $\mathcal{M}^{D_{\mathcal{F}^{\mathcal{I}}}}\left(\mathcal{F}^{\mathcal{I}}\right)$):

$$\mathcal{M}^{D_{\mathcal{F}^{\mathcal{I}}}}\left(\mathcal{F}^{\mathcal{I}}\right) = \lim_{m\to\infty} \frac{\mathcal{V}_{m,\mathcal{F}_m}\left(\varepsilon^m_{\mathcal{F},m}\right)}{\left(\varepsilon^m_{\mathcal{F},m}\right)^{2-D_{\mathcal{F}^{\mathcal{I}}}}} \cdot \tag{$\mathcal{R}$ 106}$$

Then, $\mathcal{M}^{D_{\mathcal{F}^{\mathcal{I}}}}\left(\mathcal{F}^{\mathcal{I}}\right)$ is called the *Minkowski content* of the IFD.

Remark 4.10. As was mentioned in Definition 4.6, on page 89 above, the IFD is said to be *Minkowski nondegenerate* if

$$0 < \mathcal{M}_{\star}{}^{D_{\mathcal{F}^{\mathcal{I}}}}\left(\mathcal{F}^{\mathcal{I}}\right) < \mathcal{M}^{\star,D_{\mathcal{F}^{\mathcal{I}}}}\left(\mathcal{F}^{\mathcal{I}}\right) < \infty \cdot \tag{$\mathcal{R}$ 107}$$

Equivalently, the IFD is Minkowski nondegenerate if there exists $d \geqslant 0$ such that,

$$0 < \mathcal{M}_{\star}^{\ d}\left(\mathcal{F}^{\mathcal{I}}\right) < \mathcal{M}^{\star\, d}\left(\mathcal{F}^{\mathcal{I}}\right), \tag{$\mathcal{R}$ 108}$$

which implies that the Minkowski dimension $D_{\mathcal{F}^{\mathcal{I}}}$ of the IFD exists and is equal to d.

Definition 4.7 (**Average Lower and Upper Minkowski Contents of an IFD**).

We hereafter use the same notation as in Definition 4.5, on page 88, and in Definition 4.6, on page 89 just above, where $\mathcal{F}^{\mathcal{I}}$ denotes an arbitrary iterated fractal drum of $\mathbb{R}^2$.

Then, by analogy with what can be found in [LRŽ17b], Definition 2.4.1, on page 178, we define, for all $m \in \mathbb{N}$ sufficiently large, the m^{th} *effective average lower–dimensional Minkowski content* (resp., the m^{th} *effective average upper–dimensional Minkowski content*) of $\mathcal{F}_m$ as

$$\widetilde{\mathcal{M}}_{\star}^{\ D_m,e}(\mathcal{F}_m) = \liminf_{r\to+\infty} \frac{1}{\ln r} \int_{\frac{1}{r}}^{\varepsilon_{\mathcal{F},m}^{m}} t^{D_m-3}\, \tilde{\mathcal{V}}_{m,\mathcal{F}_m}(t)\, dt \tag{$\mathcal{R}$ 109}$$

$$\left(\text{resp., } \widetilde{\mathcal{M}}^{\ \star,D_m,e}(\mathcal{F}_m) = \limsup_{r\to+\infty} \frac{1}{\ln r} \int_{\frac{1}{r}}^{\varepsilon_{\mathcal{F},m}^{m}} t^{D_m-3}\, \tilde{\mathcal{V}}_{m,\mathcal{F}_m}(t)\, dt\right), \tag{$\mathcal{R}$ 110}$$

where $\tilde{\mathcal{V}}_{m,\mathcal{F}_m}$ is the natural volume extension of $\mathcal{F}^{\mathcal{I}}$ (or m^{th} effective tubular volume of $\mathcal{F}_m$; see Notation 11, on page 64, along with Definition 4.3, on page 62), and where D_m denotes the abscissa of convergence of the m^{th} local effective tube zeta function $\tilde{\zeta}_{m,\mathcal{F}_m}^{e}$.

In the case when both of these values coincide, their common value, denoted by $\widetilde{\mathcal{M}}^{\ D_m,e}(\mathcal{F}_m)$, is called the m^{th} *local effective average Minkowski content* of $\mathcal{F}_m$, which is then said to *exist*. Accordingly,

$$\widetilde{\mathcal{M}}^{\ D_m,e}(\mathcal{F}_m) = \lim_{r\to+\infty} \frac{1}{\ln r} \int_{\frac{1}{r}}^{\varepsilon_{\mathcal{F},m}^{m}} t^{D_m-3}\, \tilde{\mathcal{V}}_{m,\mathcal{F}_m}(t)(t)\, dt\,. \tag{$\mathcal{R}$ 111}$$

We can now state several new geometric consequences of our above results, especially, Theorem 4.7, on page 72 and Theorem 4.11, on page 83.

Theorem 4.12 (**Lower, Upper and Average $D_{\mathcal{W}}$–Dimensional Minkowski Contents of the Weierstrass IFD**).

For any $m \in \mathbb{N}$, let us denote by D_m the abscissa of convergence of the m^{th} local effective tube zeta function $\tilde{\zeta}_{m,\mathcal{W}}^{e}$. Then, the Minkowski dimension of the Weierstrass IFD $\Gamma_{\mathcal{W}}^{\mathcal{I}}$ exists and equals $D_m = D_{\mathcal{W}}$, for any sufficiently large $m \in \mathbb{N}^{\star}$, where $D_{\mathcal{W}} = 2 - \ln_{N_b} \frac{1}{\lambda} \in]1,2[$ is the Minkowski dimension of the Weierstrass Curve; see Theorem 4.8, on page 76 above. Moreover, the lower and upper $D_{\mathcal{W}}$–dimensional Minkowski contents of the Weierstrass IFD $\Gamma_{\mathcal{W}}^{\mathcal{I}}$, respectively

$$\mathcal{M}_{\star}^{\ D_m}\left(\Gamma_{\mathcal{W}}^{\mathcal{I}}\right) = \mathcal{M}_{\star}^{\ D_{\mathcal{W}}}\left(\Gamma_{\mathcal{W}}^{\mathcal{I}}\right) \text{ and } \mathcal{M}^{\star,D_m}\left(\Gamma_{\mathcal{W}}^{\mathcal{I}}\right) = \mathcal{M}^{\star,D_{\mathcal{W}}}\left(\Gamma_{\mathcal{W}}^{\mathcal{I}}\right),$$

take strictly positive and finite values; more specifically, they are such that

$$0 < \frac{C_{Rectangles}}{N_b} < \mathcal{M}_{\star}^{\ D_m}\left(\Gamma_{\mathcal{W}}^{\mathcal{I}}\right) < \mathcal{M}^{\star,D_m}\left(\Gamma_{\mathcal{W}}^{\mathcal{I}}\right) \leqslant C_{Rectangles} < \infty, \tag{$\mathcal{R}$ 112}$$

where $C_{Rectangles}$ denotes the strictly positive and finite constant introduced in Property 4.3, on page 65.

Recall that $C_{Rectangles}$ may depend on $m \in \mathbb{N}^\star$, but is uniformly bounded away from 0 and infinity (with bounds independent of $m \in \mathbb{N}^\star$ large enough). Hence, the same is true of

$$\mathcal{M}_\star{}^{D_m}\left(\Gamma_{\mathcal{W}}^{\mathcal{I}}\right) = \mathcal{M}_\star{}^{D_{\mathcal{W}}}\left(\Gamma_{\mathcal{W}}^{\mathcal{I}}\right) \text{ and } \mathcal{M}^\star{}^{,D_m}\left(\Gamma_{\mathcal{W}}^{\mathcal{I}}\right) = \mathcal{M}^\star{}^{,D_{\mathcal{W}}}\left(\Gamma_{\mathcal{W}}^{\mathcal{I}}\right),$$

where $D_m = D_{\mathcal{W}}$, for all sufficiently large $m \in \mathbb{N}^\star$.

In addition, the values of $\mathcal{M}_\star{}^{D_{\mathcal{W}}}\left(\Gamma_{\mathcal{W}}^{\mathcal{I}}\right)$ and $\mathcal{M}^\star{}^{,D_{\mathcal{W}}}\left(\Gamma_{\mathcal{W}}^{\mathcal{I}}\right)$ are respectively equal to the minimum and maximum value of the one–periodic function $G_{D_{\mathcal{W}}} = G_{0,D_{\mathcal{W}}}$ introduced in Theorem 4.11, on page 83, associated to D_m in the expression of the fractal tube formula given in the same theorem (recall that the periodicity is with respect to the variable $\ln_{N_b}\left(\varepsilon_m^m\right)^{-1}$, see Property 4.1, on page 61).

Finally, for all sufficiently large $m \in \mathbb{N}^\star$, the m^{th} local effective average Minkowski content exists and is given by the mean value of the one–periodic function $G_{D_m} = G_{D_{\mathcal{W}}}$, as well as by the residues of $\tilde{\zeta}^e_{m,\Gamma_{\mathcal{W}_m}}$ at $s = D_m = D_{\mathcal{W}}$:

$$\widetilde{\mathcal{M}}^{\,D_m,e}\left(\Gamma_{\mathcal{W}_m}\right) = \int_0^1 G_{D_{\mathcal{W}}}(x)\,dx = res\left(\tilde{\zeta}^e_{m,\Gamma_{\mathcal{W}_m}}, D_m\right) = \frac{res\left(\zeta^e_{m,\Gamma_{\mathcal{W}_m}}, D_m\right)}{2 - D_m}\cdot \tag{$\mathcal{R}$ 113}$$

Hence, $\widetilde{\mathcal{M}}^{D_m,e}\left(\Gamma_{\mathcal{W}_m}\right)$ is nontrivial; in fact,

$$0 < \mathcal{M}_\star{}^{D_m}\left(\Gamma_{\mathcal{W}}^{\mathcal{I}}\right) < \widetilde{\mathcal{M}}^{\,D_m,e}\left(\Gamma_{\mathcal{W}_m}\right) < \mathcal{M}^\star{}^{,D_m}\left(\Gamma_{\mathcal{W}}^{\mathcal{I}}\right) < \infty\cdot$$

More specifically, still for all m large enough and thus, with $D_m = D_{\mathcal{W}}$, the m^{th} local effective average Minkowski content $\widetilde{\mathcal{M}}^{\,D_m,e}\left(\Gamma_{\mathcal{W}_m}\right)$ may depend on $m \in \mathbb{N}^\star$, but is uniformly bounded away from 0 and ∞ (with bounds independent of $m \in \mathbb{N}^\star$ large enough).

Proof. In light of Theorem 4.7, on page 72 (and of Definition 4.5, on page 88), one has

$$\begin{aligned}
\mathcal{M}^\star{}^{,D_m}\left(\Gamma_{\mathcal{W}}^{\mathcal{I}}\right) = & \limsup_{m\to\infty}\Bigg\{\sum_{\ell\in\mathbb{Z},\,k\in\mathbb{N}} f_{k,\ell,\text{Rectangles}}\left(\varepsilon_m^m\right)^{k(2-D_{\mathcal{W}})-i\,\ell\,\mathbf{p}} \\
& + \left(\varepsilon_m^m\right)^{D_{\mathcal{W}}}\sum_{\ell\in\mathbb{Z},\,k\in\mathbb{N}}\Big\{f_{k,\ell,\text{wedges},1}\left(\varepsilon_m^m\right)^{1-i\,\ell\,\mathbf{p}} + f_{k,\ell,\text{wedges},2}\left(\varepsilon_m^m\right)^{-1+2\,k-i\,\ell\,\mathbf{p}} + f_{k,\ell,\text{wedges},3}\left(\varepsilon_m^m\right)^{3+2\,k-i\,\ell\,\mathbf{p}}\Big\} \\
& + \left(\varepsilon_m^m\right)^{D_{\mathcal{W}}}\sum_{\ell\in\mathbb{Z},\,k\in\mathbb{N}} f_{k,\ell,\text{triangles, parallelograms}}\left(\varepsilon_m^m\right)^{-i\,\ell\,\mathbf{p}} + \left(\varepsilon_m^m\right)^{D_{\mathcal{W}}}\pi - \left(\varepsilon_m^m\right)^{D_{\mathcal{W}}}\frac{\pi\left(\varepsilon_m^m\right)^2}{2}\Bigg\} \\
= & \limsup_{m\to\infty}\sum_{\ell\in\mathbb{Z}} f_{m,0,\text{Rectangles}}\left(\varepsilon_m^m\right)^{-i\,\ell\,\mathbf{p}} \\
= & \limsup_{m\to\infty} C_{\text{Rectangles}}\,\frac{N_b-1}{N_b}\sum_{\ell\in\mathbb{Z}}\frac{(N_b-1)^{-i\,\ell\,\mathbf{p}}}{\ln N_b + 2\,i\,\ell\,\pi}\left(\varepsilon_m^m\right)^{-i\,\ell\,\mathbf{p}} = \limsup_{x\to+\infty} C_{\text{Rectangles}}\,N_b^{-\{x\}}\cdot
\end{aligned} \tag{$\mathcal{R}$ 114}$$

In the same way,

$$\mathcal{M}_\star{}^{D_{\mathcal{W}}}\left(\Gamma_{\mathcal{W}}^{\mathcal{I}}\right) = \liminf_{x\to+\infty} C_{\text{Rectangles}}\,N_b^{-\{x\}}\cdot \tag{$\mathcal{R}$ 115}$$

Thanks to Property 4.2, on page 62, and since $0 \leqslant \{x\} < 1$, where $\{x\}$ denotes the fractional part of $x \in \mathbb{R}$, we have that

$$N_b^{-\{x\}} = \frac{N_b - 1}{N_b} \sum_{\ell \in \mathbb{Z}} \frac{(N_b-1)^{-i\,\ell\,\mathbf{p}} \left(\varepsilon_m^m\right)^{-i\,\ell\,\mathbf{p}}}{\ln N_b + 2\,i\,\ell\,\pi}\,, \quad \text{with } x = -\ln_{N_b}\left((N_b-1)\,\varepsilon_m^m\right), \tag{$\mathcal{R}$ 116}$$

This yields $\dfrac{1}{N_b} < N_b^{-\{x\}} \leqslant 1$, and thus, in light of Theorem 4.8, on page 76, and with $D_m = D_{\mathcal{W}}$ given as in the theorem, we have that, for all $m \in \mathbb{N}^\star$ large enough,

$$\frac{C_{\text{Rectangles}}}{N_b} < {\mathcal{M}_\star}^{D_m}\left(\Gamma_{\mathcal{W}}^{\mathcal{I}}\right) < \mathcal{M}^{\star,D_m}\left(\Gamma_{\mathcal{W}}^{\mathcal{I}}\right) \leqslant C_{\text{Rectangles}}\,. \tag{$\mathcal{R}$ 117}$$

The constant $C_{\text{Rectangles}}$ being strictly positive and finite (see Property 4.3, on page 65), this accounts for a strictly positive (resp., finite) value of the lower (resp., upper) Minkowski content ${\mathcal{M}_\star}^{D_m}\left(\Gamma_{\mathcal{W}}^{\mathcal{I}}\right)$ (resp., $\mathcal{M}^{\star,D_m}\left(\Gamma_{\mathcal{W}}^{\mathcal{I}}\right)$).

Also, still for all $m \in \mathbb{N}$ sufficiently large, the one–periodic function (with respect to the variable $\ln_{N_b}\left(\varepsilon_m^m\right)^{-1}$, see Property 4.1, on page 61),

$$G_{D_{\mathcal{W}}} = G_{0,D_{\mathcal{W}}} : \quad x \mapsto \frac{N_b - 1}{N_b}\, C_{\text{Rectangles}} \sum_{\ell \in \mathbb{Z}} \frac{(N_b-1)^{-i\,\ell\,\mathbf{p}} \left(\varepsilon_m^m\right)^{-i\,\ell\,\mathbf{p}}}{\ln N_b + 2\,i\,\ell\,\pi} = N_b^{-\{x\}}\,, \tag{$\mathcal{R}$ 118}$$

associated to the value $D_{\mathcal{W}} = D_m$ is nonconstant, because it has nonzero m^{th} Fourier coefficients, with $m \neq 0$, as can be seen from the fractal tube formula, and as stated in Theorem 4.11, on page 83. (Note that the function $G_{D_{\mathcal{W}}} = G_{D_m}$ may depend on m sufficiently large.)

The last part of the theorem, regarding the m^{th} local effective average Minkowski content $\widetilde{\mathcal{M}}^{D_m,e}\left(\Gamma_{\mathcal{W}_m}\right)$ of the Weierstrass IFD (as introduced in Definition 4.7, on page 90), follows at once from the method of proof of [LRŽ17b], Theorem 2.3.25, on page 157. Note that the fact that $\widetilde{\mathcal{M}}^{D_m,e}\left(\Gamma_{\mathcal{W}_m}\right)$ is uniformly bounded away from 0 and infinity (in $m \in \mathbb{N}^\star$ large enough) follows from relation ($\mathcal{R}$88) on page 82. Indeed, recall from Property 4.3 on page 65 that the coefficients $f_{k,\ell,\text{Rectangles}}$ are uniformly bounded away from 0 and infinity (with bounds independent of $m \in \mathbb{N}^\star$ large enough).

□

Corollary 4.13 (**(of Theorem 4.12) Minkowski Dimension – Minkowski Nondegeneracy**)**.**

The Weierstrass IFD is Minkowski nondegenerate. Furthermore, the number $D_{\mathcal{W}} = 2 - \ln_{N_b}\dfrac{1}{\lambda}$ *is a simple Complex Dimension of the IFD, and it coincides with the Minkowski Dimension of* $\Gamma_{\mathcal{W}}$*, which must also exist. Moreover, the Weierstrass IFD is not Minkowski measurable.*

Proof. In light of Theorem 4.12, on page 90, the nondegeneracy directly follows from the definition. The statement concerning $D_m = D_{\mathcal{W}}$ (for all $m \in \mathbb{N}$ sufficiently large) then follows from Definition 4.6, on page 89, in particular.

Furthermore, the Weierstrass IFD is not Minkowski measurable; i.e., here,

$$\mathcal{M}_{\star}^{D_m}\left(\Gamma_{\mathcal{W}}^{\mathcal{I}}\right) < \mathcal{M}^{\star,D_m}\left(\Gamma_{\mathcal{W}}^{\mathcal{I}}\right).$$

This last statement also follows from Theorem 4.12, on page 90, because the one–periodic function $G_{D_{\mathcal{W}}} = G_{D_m}$ is nonconstant, and so, by the method of proof of the results in [LRŽ17b], Theorem 2.3.25, on page 157,

$$\widetilde{\mathcal{M}_{\star}}^{D_m,e}\left(\Gamma_{\mathcal{W}_m}\right) = \min_{[0,1]} G_{D_{\mathcal{W}}} < \max_{[0,1]} G_{D_{\mathcal{W}}} = \widetilde{\mathcal{M}}^{\star,D_m,e}\left(\Gamma_{\mathcal{W}_m}\right). \tag{$\mathcal{R}$ 119}$$

Moreover, since, for all $m \in \mathbb{N}$ sufficiently large, the m^{th} local effective distance zeta function $\zeta^{e}_{m,\Gamma_{\mathcal{W}_m}}$ associated to the Weierstrass IFD can clearly be meromorphically extended to a connected neighborhood of $s = D_{\mathcal{W}}$ in the Complex Plane, $D_{\mathcal{W}}$ is a simple pole of $\zeta^{e}_{m,\Gamma_{\mathcal{W}_m}}$. As was pointed out at the end of Theorem 4.12, given on page 90, in agreement with the general theory in [LRŽ17b] (see Theorem 2.3.25, page 157).

□

Remark 4.11. Let us call the *global lower* (resp., *upper*) *effective average Minkowski content of the Weierstrass IFD* $\Gamma_{\mathcal{W}}^{\mathcal{I}}$, and denote by $\widetilde{\mathcal{M}_{\star}}^{D_{\mathcal{W}},e}\left(\Gamma_{\mathcal{W}}^{\mathcal{I}}\right)$ (resp., $\widetilde{\mathcal{M}\star}^{D_{\mathcal{W}},e}\left(\Gamma_{\mathcal{W}}^{\mathcal{I}}\right)$) the following lower (resp., upper) limit of the corresponding m^{th} local effective average Minkowski contents, with $D_m = D_{\mathcal{W}}$, for all $m \in \mathbb{N}^{\star}$ sufficiently large:

$$\widetilde{\mathcal{M}_{\star}}^{D_{\mathcal{W}},e}\left(\Gamma_{\mathcal{W}}^{\mathcal{I}}\right) = \liminf_{m\to\infty} \widetilde{\mathcal{M}_{\star}}^{D_m,e}\left(\Gamma_{\mathcal{W}_m}\right) \tag{$\mathcal{R}$ 120}$$

$$\left(\text{resp., } \widetilde{\mathcal{M}^{\star}}^{D_{\mathcal{W}},e}\left(\Gamma_{\mathcal{W}}^{\mathcal{I}}\right) = \limsup_{m\to\infty} \widetilde{\mathcal{M}\star}^{D_m,e}\left(\Gamma_{\mathcal{W}_m}\right)\right)$$

Then, it follows from Theorem 4.12, on page 90, that the above quantities are well defined and bouded away from 0 and ∞. Furthermore, they coincide; so that the *global effective average Minkowski content of the Weierstrass IFD* $\Gamma_{\mathcal{W}}^{\mathcal{I}}$, denoted by $\widetilde{\mathcal{M}}^{D_{\mathcal{W}},e}\left(\Gamma_{\mathcal{W}}^{\mathcal{I}}\right)$), exists.

In light of relation ($\mathcal{R}$112), and since $D_m = D_{\mathcal{W}}$, for all $m \in \mathbb{N}^{\star}$ sufficiently large, we obtain that

$$0 < \frac{C_{\text{Rectangles}}}{N_b} < \mathcal{M}_{\star}^{D_{\mathcal{W}}}\left(\Gamma_{\mathcal{W}}^{\mathcal{I}}\right) \leqslant \widetilde{\mathcal{M}}^{\star,D_{\mathcal{W}},e}\left(\Gamma_{\mathcal{W}_m}\right) \leqslant \mathcal{M}^{\star D_{\mathcal{W}}}\left(\Gamma_{\mathcal{W}}^{\mathcal{I}}\right) \leqslant C_{\text{Rectangles}} < \infty. \tag{$\mathcal{R}$ 121}$$

In addition, since $D_m = D_{\mathcal{W}}$, and, by relation ($\mathcal{R}$113),

$$\widetilde{\mathcal{M}}^{D_{\mathcal{W}},e}\left(\Gamma_{\mathcal{W}_m}\right) = \operatorname{res}\left(\tilde{\zeta}^{e}_{m,\Gamma_{\mathcal{W}_m}}, D_{\mathcal{W}}\right) = \frac{\operatorname{res}\left(\zeta^{e}_{m,\Gamma_{\mathcal{W}_m}}, D_{\mathcal{W}}\right)}{2 - D_{\mathcal{W}}}, \tag{$\mathcal{R}$ 122}$$

for all $m \in \mathbb{N}^{\star}$ sufficiently large, as well as (see Theorem 4.8, on page 76, and its proof),

$$\operatorname{res}\left(\tilde{\zeta}^{e}_{\Gamma_{\mathcal{W}}}, D_{\mathcal{W}}\right) = \lim_{m\to\infty} \operatorname{res}\left(\tilde{\zeta}^{e}_{m,\Gamma_{\mathcal{W}_m}}, D_{\mathcal{W}}\right), \tag{$\mathcal{R}$ 123}$$

which follows from the local uniform convergence (as $m \to \infty$) on $\mathbb{C}$ of $\tilde{\zeta}^{e}_{m,\Gamma_{\mathcal{W}_m}}$ (resp., $\zeta^{e}_{m,\Gamma_{\mathcal{W}_m}}$) to $\tilde{\zeta}^{e}_{\Gamma_{\mathcal{W}}}$ (resp., to $\zeta^{e}_{\Gamma_{\mathcal{W}}}$).

By combining relation ($\mathcal{R}$122) and relation ($\mathcal{R}$123), we see that $\widetilde{\mathcal{M}}^{D_{\mathcal{W}},e}\left(\Gamma_{\mathcal{W}}^{\mathcal{I}}\right)$ exists and satisfies

$$\widetilde{\mathcal{M}}^{D_{\mathcal{W}},e}\left(\Gamma_{\mathcal{W}}^{\mathcal{I}}\right) = \lim_{m\to\infty} \mathcal{M}^{\star,D_{\mathcal{W}},e}\left(\Gamma_{\mathcal{W}_m}\right) = \operatorname{res}\left(\tilde{\zeta}^{e}_{\Gamma_{\mathcal{W}}}, D_{\mathcal{W}}\right) = \frac{\operatorname{res}\left(\zeta^{e}_{\Gamma_{\mathcal{W}}}, D_{\mathcal{W}}\right)}{2 - D_{\mathcal{W}}}. \tag{$\mathcal{R}$ 124}$$

Finally, in light of relation ($\mathcal{R}121$), we deduce from relation ($\mathcal{R}124$) that

$$0 < \frac{1}{N_b} \liminf_{m\to\infty} C_{\text{Rectangles}} \leqslant {\mathcal{M}_\star}^{D_{\mathcal{W}}}\left(\Gamma_{\mathcal{W}}^{\mathcal{I}}\right) \leqslant \widetilde{\mathcal{M}}^{D_{\mathcal{W}},e}\left(\Gamma_{\mathcal{W}}^{\mathcal{I}}\right) \leqslant {\mathcal{M}^\star}^{D_{\mathcal{W}}}\left(\Gamma_{\mathcal{W}}^{\mathcal{I}}\right) \leqslant \limsup_{m\to\infty} C_{\text{Rectangles}} < \infty \cdot \tag{$\mathcal{R}$ 125}$$

In conclusion, the global effective average Minkowski content $\widetilde{\mathcal{M}}^{D_{\mathcal{W}},e}\left(\Gamma_{\mathcal{W}}^{\mathcal{I}}\right)$ of the Weierstrass IFD $\Gamma_{\mathcal{W}}^{\mathcal{I}}$, exists, is positive and finite, satisfies the estimates in relation ($\mathcal{R}125$), and is expressed via relation ($\mathcal{R}124$) in terms of the residues at $s = D_{\mathcal{W}}$ of the global effective tube and distance zeta functions of $\Gamma_{\mathcal{W}}^{\mathcal{I}}$.

Accordingly, in particular, the relation between the m^{th} local effective average Minkowski content and the residues at $s = D_{\mathcal{W}}$ of the m^{th} local effective tube and distance zeta functions, for all $m \in \mathbb{N}^\star$ sufficiently large (see relation ($\mathcal{R}113$), on page 91) remains precisely the same between their global counterparts.

4.5 The Noninteger Case

An interesting question is the generalization of our previous results to *the noninteger case*; i.e., to the case when the Weierstrass function $\mathcal{W}$ is defined, for any real number x, by

$$\mathcal{W}(x) = \sum_{n=0}^{\infty} \lambda^n \cos\left(2\,\pi\, b^n\, x\right) , \tag{$\mathcal{R}$ 126}$$

where the real number b does not belong to the set of natural integers.

We plan to provide the details in a later work, but for now limit ourselves to a few comments.

From the geometric point of view, one cannot handle things in the same way. For instance, one cannot resort to a finite IFS, and the function, apart from its parity, has no periodicity property.

Yet, the associated graph being the attractor of the infinite set of maps, $\mathcal{T}_{\mathcal{W}} = \{T_i\}_{i\in\mathbb{Z}}$, such that, for any integer i and (x, y) in $\mathbb{R}^2$,

$$T_i(x, y) = \left(\frac{x+i}{b}, \lambda\, y + \cos\left(2\,\pi\,\left(\frac{x+i}{b}\right)\right)\right) , \tag{$\mathcal{R}$ 127}$$

it is natural to consider the associated *infinite IFS* (IIFS), $\mathcal{T}_{\mathcal{W}}$. As a consequence, the resulting prefractal graphs are infinite ones.

The local Hölder and reverse–Hölder continuity properties of the Weierstrass function then enable us to resort to estimates that are equivalent to the ones obtained in Corollary 2.11, on page 24, and Corollary 2.12, on page 24, and, consequently, to the resulting ones about the elementary heights obtained in Corollary 2.15, on page 27.

As for the effective tubular neighborhood, due to the polygonal approximations induced by the prefractals, it is still obtained by means of rectangles and wedges.

In the integer case, extra terms coming from overlapping rectangles vanished, thanks to the symmetry with respect to the vertical line $x = \frac{1}{2}$, as described in Proposition 3.4, on page 50. In the non-integer case, one simply replaces this symmetry with the one with respect to the vertical axis $x = 0$.

In this light, it is expected that a similar method, suitably adapted, would lead to a fractal tube formula of the same type as the one obtained in Theorem 4.7, on page 72, where the powers of the small parameter ε_m^m would be, respectively, and as previously,

$$\left(\varepsilon_m^m\right)^{2-D_{\mathcal{W}}+k\,(2-D_{\mathcal{W}})-i\,\ell\,\mathbf{p}} \quad , \quad \left(\varepsilon_m^m\right)^{3-i\,\ell\,\mathbf{p}} \quad , \quad \left(\varepsilon_m^m\right)^{1+2\,k-i\,\ell\,\mathbf{p}} \quad , \quad \left(\varepsilon_m^m\right)^{5+2\,k-i\,\ell\,\mathbf{p}} \quad , \quad \left(\varepsilon_m^m\right)^{2-i\,\ell\,\mathbf{p}} \quad , \quad \left(\varepsilon_m^m\right)^2 \quad , \quad (\mathcal{R}\,128)$$

which would yield the same results concerning the possible Complex Dimensions, along with the upper and lower, as well as the average, Minkowski contents of the Weierstrass Curve.

As in the integer case, the terms involving $\left(\varepsilon_m^m\right)^{2-D_{\mathcal{W}}+k\,(2-D_{\mathcal{W}})-i\,\ell\,\mathbf{p}}$ come from the contribution of the rectangles. The one–periodic functions (with respect to the variable $\ln_b\left(\varepsilon_m^m\right)^{-1}$ this time), respectively associated to the values $D_{\mathcal{W}}-k\,(2-D_{\mathcal{W}})$, $k\in\mathbb{N}$, are thus nonconstant, with all of their Fourier coefficients being nonzero. Hence, as in Theorem 4.10, on page 81, for each $k\in\mathbb{N}$ and $\ell\in\mathbb{Z}$, $D_{\mathcal{W}}-k\,(2-D_{\mathcal{W}})+i\,\ell\,\mathbf{p}$, are all simple Complex Dimensions of the Weierstrass Curve; i.e., they are simple poles of the tube (or, equivalently, of the distance) zeta function.

We also mention that we could deal with the case $\lambda\,b<1$, exactly in the same manner, and with the same conclusions. Actually, it is noteworthy that, in the present paper, all of our results remain valid when $\lambda\,N_b<1$, where $b=N_b$ is an integer greater than or equal to two. Observe that in the latter case, the Weierstrass Curve $\Gamma_{\mathcal{W}}$ is of class C^1, but is still fractal, because it has nonreal Complex Dimensions (in fact, infinitely many of them).

5 Concluding Comments

In the light of our results, the box dimension $D_{\mathcal{W}}$ stands as a simple pole of the tube and distance zeta functions associated to the Weierstrass IFD. It is also the abscissa of holomorphic continuation of those functions, which therefore cannot be extended holomorphically to the left of $D_{\mathcal{W}}$. According to [LRŽ17b], part c. of Theorem 2.1.11, page 57, and the last statement of Theorem 2.2.11, page 121, this additional result follows from the fact that, for all $m\in\mathbb{N}$ sufficiently large, $D_m=D_{\mathcal{W}}$ exists, ${\mathcal{M}_\star}^{D_{\mathcal{W}}}\left(\Gamma_{\mathcal{W}}^{\mathcal{I}}\right)>0$ and $D_{\mathcal{W}}<2$. It can also be deduced from Theorem 4.7, on page 72, or else from Theorem 4.10, on page 81.

A natural question which arises is wether the Complex Dimensions of the considered fractal – in our case, the Weierstrass Curve – are the same as those of the prefractal approximations. In [DL23b], by means of the exact sequence of the local effective fractal zeta functions associated with the sequence of polygonal neighborhoods which converge to the Curve, we prove that the limit (or global) fractal zeta function – the one associated with the limit fractal object – has the same poles as the fractal zeta function at each step of the prefractal approximation, and, hence, that the Complex Dimensions of the fractal are the same as the Complex Dimensions of each prefractal approximation. As is shown in [DL23b], the determination of the explicit Complex Dimensions of the IFD is a compulsory step in order to obtain the Complex Dimensions of the limit fractal Curve.

Now, as was alluded to in the Introduction, the determination of the possible Complex Dimensions of a fractal object, being deeply connected with its intrinsic vibrational properties, is thus directly associated to its cohomological properties: what are the topological invariants of the Weierstrass Curve? This is the question we try to answer in the second part of our study, [DL22c], where we determine the fractal cohomology of the Weierstrass Curve.

Behind the fractal series expansion of the Weierstrass function, another expansion, indexed by the Complex Dimensions obtained in our fractal tube formulas (see Theorem 4.7, on page 72 and

Theprem 4.11, on page 83 above), naturally arises. Intuitively, one understands that the terms of the expansion come from the cohomology groups associated to the prefractal sequence of finite graphs that converges towards the Curve. This is all the more interesting, as those groups possess the same symmetries as the Curve, which means that a specific differentiation could be achieved on this, however, everywhere singular object; see [DL22a] and [DL22c].

As was mentioned in Subsection 4.5, on page 94, we also intend, in a future work, to extend our results to the general case, i.e., when the Weierstrass function $\mathcal{W}$ is defined, for any real number x, by

$$\mathcal{W}(x) = \sum_{n=0}^{\infty} \lambda^n \cos\left(2\,\pi\, b^n\, x\right)$$

where the real number b does not belong to the set of natural integers. This goes along with a generalization of the results of the present paper to a large class of Weierstrass-like functions (see the paper [Dav19]), including the Takagi function, the Knopp functions and the Koch parametrized Curve; see [DL23a].

The reader may wonder where there is an intrinsic way of obtaining the global fractal zeta functions introduced and studied in Theorem 4.8 and Corollary 4.9 (on pages 76 and 80, respectively), that would be more in keeping with the general theory of Complex Dimensions (as developed in [LRŽ17a]–[LRŽ17c] and [LRŽ18]) and its natural extensions (e.g., in [LW23]). This question is addressed by the authors in [DL23b], by using the polyhedral measure introduced in [DL22b].

Acknowledgements

The authors would like to thank Goran Radunović and Steffen Winter for their helpful questions about the first version of this paper.

References

[BBR14] Krzysztof Barański, Balázs Bárány, and Julia Romanowska. On the dimension of the graph of the classical Weierstrass function. *Advances in Mathematics*, 265:791–800, 2014.

[BD85] Michael F. Barnsley and Stephen G. Demko. Iterated function systems and the global construction of fractals. *Proceedings of the Royal Society of London*, A(399):243–275, 1985.

[Bou04] Nicolas Bourbaki. *Theory of Sets*. Elements of Mathematics (Berlin). Springer-Verlag, Berlin, 2004. Reprint of the 1968 English translation [Hermann, Paris; MR0237342].

[BU37] Abram S. Besicovitch and Harold Douglas Ursell. Sets of Fractional dimensions (v): On Dimensional Numbers of Some Continuous Curves. *J. London Math. Soc.*, 12(1):18–25, 1937.

[Dav18] Claire David. Bypassing dynamical systems: A simple way to get the box-counting dimension of the graph of the Weierstrass function. *Proceedings of the International Geometry Center*, 11(2):1–16, 2018. URL: `https://journals.onaft.edu.ua/index.php/geometry/article/view/1028`.

[Dav19] Claire David. On fractal properties of Weierstrass-type functions. *Proceedings of the International Geometry Center*, 12(2):43–61, 2019. URL: https://journals.onaft.edu.ua/index.php/geometry/article/view/1485.

[Dav22] Claire David. Wandering across the Weierstrass function, while revisiting its properties, in press. In *Analysis of PDE-Morningside Lecture Notes* (edited by Jean-Yves Chemin, Ping Zhang and Fang-Hua Lin), 6, 2022. URL: https://www.intlpress.com/site/pub/pages/books/items/00000504/index.php.

[Dev03] Robert L. Devaney. *An Introduction to Chaotic Dynamical Systems*. Westview Press, 2003.

[DL22a] Claire David and Michel L. Lapidus. Fractal complex dimensions and cohomology of the Weierstrass curve, 2022. URL: https://hal.science/hal-03797595v2.

[DL22b] Claire David and Michel L. Lapidus. Iterated fractal drums ~ Some new perspectives: Polyhedral measures, atomic decompositions and Morse theory, 2022. URL: https://hal.sorbonne-universite.fr/hal-03946104v2.

[DL22c] Claire David and Michel L. Lapidus. Weierstrass fractal drums - II - Towards a fractal cohomology, 2022. URL: https://hal.archives-ouvertes.fr/hal-03758820v3.

[DL23a] Claire David and Michel L. Lapidus. Complex Dimensions of nowhere differentiable Weierstrass-type functions (tentative title), in preparation, 2023.

[DL23b] Claire David and Michel L. Lapidus. Polyhedral neighborhoods vs tubular neighborhoods: New insights for the fractal zeta functions (tentative title), in preparation, 2023.

[ELMR15] Kate E. Ellis, Michel L. Lapidus, Michael C. Mackenzie, and John A. Rock. Partition zeta functions, multifractal spectra, and tapestries of complex dimensions. In M. Frame and N. Cohen, editors, *Benoît Mandelbrot: A Life in Many Dimensions*. The Mandelbrot Memorial, pages 267–322. World Scientific Publishers, Singapore and London, 2015. URL: https://arxiv.org/abs/1007.1467.

[Fal86] Kenneth Falconer. *The Geometry of Fractal Sets*. Cambridge University Press, Cambridge, 1986.

[Har16] Godfrey Harold Hardy. Weierstrass's Non-Differentiable Function. *Transactions of the American Mathematical Society*, 17(3):301–325, 1916. URL: https://www.ams.org/journals/tran/1916-017-03/S0002-9947-1916-1501044-1/S0002-9947-1916-1501044-1.pdf.

[HL93] Tian-You Hu and Ka-Sing Lau. Fractal dimensions and singularities of the Weierstrass type functions. *Transactions of the American Mathematical Society*, 335(2):649–665, 1993.

[HL21] Hafedh Herichi and Michel L. Lapidus. *Quantized Number Theory, Fractal Strings and the Riemann Hypothesis: From Spectral Operators to Phase Transitions and Universality*. World Scientific Publishing, Singapore and London, 2021.

[Hun98] Brian Hunt. The Hausdorff dimension of graphs of Weierstrass functions. *Proceedings of the American Mathematical Society*, 12(1):791–800, 1998.

[Hut81] John E. Hutchinson. Fractals and self similarity. *Indiana University Mathematics Journal*, 30:713–747, 1981.

[Kel17] Gerhard Keller. A simpler proof for the dimension of the graph of the classical Weierstrass function. *Annales de l'Institut Henri Poincaré – Probabilités et Statistiques*, 53(1):169–181, 2017.

[KMPY84] James L. Kaplan, John Mallet-Paret, and James A. Yorke. The Lyapunov dimension of a nowhere differentiable attracting torus. *Ergodic Theory and Dynamical Systems*, 4:261–281, 1984.

[Lap91] Michel L. Lapidus. Fractal drum, inverse spectral problems for elliptic operators and a partial resolution of the Weyl-Berry conjecture. *Transactions of the American Mathematical Society*, 325:465–529, 1991.

[Lap92] Michel L. Lapidus. Spectral and fractal geometry: From the Weyl-Berry conjecture for the vibrations of fractal drums to the Riemann zeta-function. In *Differential Equations and Mathematical Physics (Birmingham, AL, 1990)*, volume 186 of *Math. Sci. Engrg.*, pages 151–181. Academic Press, Boston, MA, 1992.

[Lap93] Michel L. Lapidus. Vibrations of fractal drums, the Riemann hypothesis, waves in fractal media and the Weyl-Berry conjecture. In *Ordinary and Partial Differential Equations, Vol. IV (Dundee, 1992)*, volume 289 of *Pitman Research Notes Mathematical Series*, pages 126–209. Longman Sci. Tech., Harlow, 1993.

[Lap08] Michel L. Lapidus. *In Search of the Riemann Zeros: Strings, Fractal Membranes and Noncommutative Spacetimes*. American Mathematical Society, Providence, RI, 2008.

[Lap19] Michel L. Lapidus. An overview of complex fractal dimensions: From fractal strings to fractal drums, and back. In *Horizons of Fractal Geometry and Complex Dimensions* (R. G. Niemeyer, E. P. J. Pearse, J. A. Rock and T. Samuel, eds.), volume 731 of *Contemporary Mathematics*, pages 143–265. American Mathematical Society, Providence, RI, 2019. URL: `https://arxiv.org/abs/1803.10399`.

[Lap22] Michel L. Lapidus. *From Complex Fractal Dimensions and Quantized Number Theory To Fractal Cohomology: A Tale of Oscillations, Unreality and Fractality,* book in preparation. World Scientific Publishing, Singapore and London, 2022.

[Led92] François Ledrappier. On the dimension of some graphs. in symbolic dynamics and its applications (New Haven, CT, 1991). *Contemp. Math.*, 135:285–293, 1992.

[LLVR09] Michel L. Lapidus, Jacques Lévy Véhel, and John A. Rock. Fractal strings and multifractal zeta functions (special issue dedicated to the memory of Moshe Flato). *Letters in Mathematical Physics*, 88(1), 2009. URL: `https://arxiv.org/abs/math-ph/0610015v3`.

[LM95] Michel L. Lapidus and Helmut Maier. The Riemann hypothesis and inverse spectral problems for fractal strings. *Journal of the London Mathematical Society. Second Series*, 52(1):15–34, 1995.

[LP93] Michel L. Lapidus and Carl Pomerance. The Riemann zeta-function and the one-dimensional Weyl-Berry conjecture for fractal drums. *Proceedings of the London Mathematical Society. Third Series*, 66(1):41–69, 1993.

[LP06] Michel L. Lapidus and Erin P. J. Pearse. A tube formula for the Koch snowflake curve, with applications to complex dimensions. *Journal of the London Mathematical Society. Second Series*, 74(2):397–414, 2006.

[LPW11] Michel L. Lapidus, Erin P. J. Pearse, and Steffen Winter. Pointwise tube formulas for fractal sprays and self-similar tilings with arbitrary generators. *Advances in Mathematics*, 227(4):1349–1398, 2011.

[LR09] Michel L. Lapidus and John A. Rock. Towards zeta functions and complex dimensions of multifractals. *Complex Var. Elliptic Equ.*, 54(6):545–559, 2009.

[LRŽ17a] Michel L. Lapidus, Goran Radunović, and Darko Žubrinić. Distance and tube zeta functions of fractals and arbitrary compact sets. *Advances in Mathematics*, 307:1215–1267, 2017.

[LRŽ17b] Michel L. Lapidus, Goran Radunović, and Darko Žubrinić. *Fractal Zeta Functions and Fractal Drums: Higher-Dimensional Theory of Complex Dimensions*. Springer Monographs in Mathematics. Springer, New York, 2017.

[LRŽ17c] Michel L. Lapidus, Goran Radunović, and Darko Žubrinić. Zeta functions and complex dimensions of relative fractal drums: theory, examples and applications. *Dissertationes Mathematicae*, 526:1–105, 2017.

[LRŽ18] Michel L. Lapidus, Goran Radunović, and Darko Žubrinić. Fractal tube formulas for compact sets and relative fractal drums: Oscillations, complex dimensions and fractality. *Journal of Fractal Geometry*, 5(1):1–119, 2018.

[LvF00] Michel L. Lapidus and Machiel van Frankenhuijsen. *Fractal Geometry and Number Theory: Complex Dimensions of Fractal Strings and Zeros of Zeta Functions*. Birkhäuser Boston, Inc., Boston, MA, 2000.

[LvF06] Michel L. Lapidus and Machiel van Frankenhuijsen. *Fractal Geometry, Complex Dimensions and Zeta Functions: Geometry and Spectra of Fractal Strings*. Springer Monographs in Mathematics. Springer, New York, 2006.

[LvF13] Michel L. Lapidus and Machiel van Frankenhuijsen. *Fractal Geometry, Complex Dimensions and Zeta Functions: Geometry and Spectra of Fractal Strings*. Springer Monographs in Mathematics. Springer, New York, second revised and enlarged edition (of the 2006 edition), 2013.

[LW23] Michel L. Lapidus and Sean Watson. Fractal zeta functions in ahlfors spaces and alfhors-type spaces, in preparation, 2023.

[LY85] François Ledrappier and Lai-Sang Young. The metric entropy of diffeomorphisms. ii. Relations between entropy, exponents and dimension. *Ann. of Math.*, 2(122):540–574, 1985.

[Man77] Benoît B. Mandelbrot. *Fractals: Form, Chance, and Dimension*. W. H. Freeman & Co Ltd, San Francisco, 1977.

[Man83] Benoît B. Mandelbrot. *The Fractal Geometry of Nature*. English translation, revised and enlarged edition (of the 1977 edition). W. H. Freeman & Co, New York, 1983.

[Not98] Laurent Nottale. *La relativité dans tous ses états*. Hachette Littératures; Hachette édition, Paris, 1998.

[Ols01] Lars Ole Ronnow Olsen. Review: Fractal Geometry and Number Theory. Complex Dimensions of Fractal Strings and Zeros of Zeta Functions by M. L. Lapidus and M. van Frankenhuijsen, Birkhäuser. *Bulletin of the London Mathematical Society*, 33:254–255, 2001.

[Ols13a] Lars Ole Ronnow Olsen. Multifractal tubes. In *Further Developments in Fractals and Related Fields*, Trends Math., pages 161–191. Birkhäuser/Springer, New York, 2013.

[Ols13b] Lars Ole Ronnow Olsen. Multifractal tubes: Multifractal zeta-functions, multifractal Steiner formulas and explicit formulas. In *Fractal Geometry and Dynamical Systems in Pure and Applied Mathematics*. I. Fractals in Pure Mathematics, volume 600 of *Contemp. Math.*, pages 291–326. Amer. Math. Soc., Providence, RI, 2013.

[PU89] Feliks Przytycki and Mariusz Urbański. On the Hausdorff dimension of some fractal sets. *Studia Mathematica*, 93(2):155–186, 1989.

[She18] Weixiao Shen. Hausdorff dimension of the graphs of the classical Weierstrass functions. *Mathematische Zeitschrift*, 289:223–266, 2018.

[Tao06] Terence Tao. *Nonlinear dispersive equations*, volume 106 of *CBMS Regional Conference Series in Mathematics*. Published for the Conference Board of the Mathematical Sciences, Washington, DC; by the American Mathematical Society, Providence, RI, 2006. Local and global analysis.

[Tit39] Edward Charles Titschmarsh. *The Theory of Functions*. Oxford University Press, second edition, 1939.

[Wei75] Karl Weierstrass. Über continuirliche Funktionen eines reellen Arguments, die für keinen Werth des letzteren einen bestimmten Differential quotienten besitzen. *Journal für die reine und angewandte Mathematik*, 79:29–31, 1875.

[Zyg02] Antoni Zygmund. *Trigonometric Series. Vols. I, II*. Cambridge Mathematical Library. Cambridge University Press, Cambridge, third edition, 2002. With a foreword by Robert A. Fefferman.